NI 43-101 TECHNICAL REPORT AND MINERAL RESOURCE ESTIMATE

# CHIMO MINE PROJECT, CENTRAL GOLD CORRIDOR

VAL-D'OR, QUÉBEC, CANADA

**Prepared for:**

Cartier Resources Inc.
1740, Chemin Sullivan, Suite 1000
Val-d'Or (Québec, Canada), J9P 7H1

**Prepared by:**

GéoPointCom
895, Rue Lévis
Val-d'Or (Québec, Canada), J9P 4B8

**Qualified Person:**

Christian D'Amours, P.Geo., GéoPointCom

Effective Date: July 2nd, 2019
Signature Date: December 17th, 2019

**DATE AND SIGNATURE PAGE**

NI 43-101 TECHNICAL REPORT AND MINERAL RESOURCE ESTIMATE

# CHIMO MINE PROJECT, CENTRAL GOLD CORRIDOR

VAL-D'OR, QUÉBEC, CANADA

Prepared for:

Cartier Resources Inc.

1740, Chemin Sullivan, Suite 1000

Val-d'Or (Québec, Canada), J9P 7H1

Signed in Val-d'Or, December 17th, 2019

Effective date: July 2nd, 2019

**Signed and sealed original on file**

Christian D'Amours, P.Geo., B.A.Sc. (OGQ No. 226)
GéoPointCom

## CERTIFICATE OF QUALIFIED PERSON – CHRISTIAN D'AMOURS

I, Mr. **Christian D'Amours**, residing at 895, rue Lévis, Val-d'Or, do hereby certify that:

1. This certificate applies to the report entitled "NI 43-101 Technical Report and Mineral Resource Estimate, Chimo Mine Project, Central Gold Corridor, Val-d'Or, Québec, Canada" (the Technical Report) dated December 17th, 2019;
2. I graduated from the University of Québec in Montréal in geology in 1984;
3. I have been practising on an ongoing basis, the profession of geologist since May 1985;
4. From 1985 to 1994, the practice of my profession mainly focused on exploration. From 1994 to 1999, I worked primarily in the field of mining. Since 1999, most of my work has been resource and reserve evaluation and geostatistics. I am president and founder of GéoPointCom;
5. I am a member of the Order of Geologists of Québec (No. 226);
6. I have read the definition of "qualified person" set out in National Instrument 43-101 ("NI 43-101") and certify that by reason of my education, affiliation with a professional association (as defined in NI 43-101) and past relevant work experience, I fulfill the requirements to be a "qualified person" for the purposes of NI 43-101;
7. I visited the property on October 4 and 7, 2019. I resampled some mineralized sections from four different drill holes;
8. I am the author of/and responsible for all sections of the Technical Report;
9. As at December 17th, 2019, I am not aware of any material fact or material change with respect to the subject matter of this Technical Report which is not reflected in this Technical Report or of the omission to disclose any such material fact or material change which could make this report misleading;
10. I am independent of the owners of the lands covered by this Technical Report within the meaning of section 1.5 of National Instrument 43-101 Standards of Disclosure for Mineral Properties ("NI 43-101");
11. I have read the NI 43-101 and Form 43-101F1, and hereby certify that this Technical Report has been prepared in compliance with NI 43-101 and Form 43-101F1;
12. The Technical Report gives a true picture of the state of scientific and technical knowledge as of July 2nd, 2019.

Signed this December 17th, 2019, in Val-d'Or, Québec.

Effective Date: July 2nd, 2019

GÉOLOGUE
CHRISTIAN D'AMOURS
# 226
QUÉBEC

*Signed and sealed original on file*

________________________________________

Christian D'Amours, P.Geo. (OGQ #226)

## TABLE OF CONTENTS

## LIST OF FIGURES

## LIST OF TABLES

# 1 SUMMARY

## 1.1 Introduction

In September 2019, Mr. Gaétan Lavallière of Cartier Resources Inc. (Cartier, the Company or the issuer) commissioned GéoPointCom to estimate the mineral resources in the Central Gold Corridor (or Central Corridor) on the Chimo Mine Property (the Property or the Project). Under this mandate, Christian D'Amours, Geologist and President of GéoPointCom, prepared a maiden mineral resource estimate for the Central Corridor in accordance with National Instrument 43-101 Respecting Standards of Disclosure for Mineral Projects (NI 43-101) and Form 43-101F1. Christian D'Amours is a QP and independent of the issuer, as defined by NI 43-101.

## 1.2 Property Description and Location

The Property is situated in the province of Québec, Canada, and more specifically in the administrative region of Abitibi-Témiscamingue. The Property lies 40 km east-southeast of the city of Val-d'Or and 12 km southeast of the municipality of Louvicourt.

The Property includes 12 mining titles registered in the name of Cartier Resources Inc. IAMGOLD Corporation retains a 1% NSR (Net Smelter Return) royalty. The Property has been mined in the past, and surface facilities have been dismantled. The Property is considered an exploration project that has passed the preliminary stage since gold resources are present, but the project has not reached the advanced exploration stage as no economic assessment has been made to determine its potential for economic viability.

## 1.3 Accessibility, Climate, Local Resources, Infrastructure and Physiography

The Property is easily accessed from the town of Val-d'Or by taking the paved Trans-Canada Highway 117 eastward for about 40 km, then heading east on the gravel Chimo Road for 11 km.

The regional climate is continental and typical of the Canadian Shield at this latitude. Winters are very cold and dry, lasting from October to April, with precipitation in the form of snow. Summers are relatively hot, humid and short, from June to August.

A skilled and experienced workforce in mineral exploration and mining is available in the region.

Underground mine workings comprise 7 km of drifts distributed over 19 main levels that are connected by a 3-compartment shaft of 5.5 m x 1.8 m that extends to a depth of 920 m. About 20 sublevels and raises complete the underground infrastructure. The headframe, concentrator and other surface facilities were dismantled in 2008, but the 25 kV power line is in good condition, and the sandpit is still in place.

## 1.4 Geological Setting and Mineralization

The Property is located in the Southern Volcanic Zone of the Abitibi Subprovince. The northern part of the Property is transected by a possible extension of the Cadillac–Larder Lake Deformation Zone.

No outcrops are present on the Property. It is underlain by volcano-sedimentary rocks of the Trivio Complex. The Trivio Complex is a structural complex enclosing a set of lenticular bands of sedimentary rocks and mafic volcanic rocks, in sheared contact with each other; stratigraphic correlations are not possible.

At the former Chimo mine, mineralized zones and their margins (wallrocks) are characterized by hydrothermal alteration that manifests in different ways depending on the lithology:

- Silicification took place in sedimentary host rocks where iron formations were present. Silicification, typically accompanied by chloritization and biotization, is limited to the immediate wallrock in mineralized areas;

- Carbonatization affects a much larger volume of rock in volcanic or pyroclastic lithologies. Primarily characterized by calcite, sometimes accompanied by chlorite;

- Tourmalinization affects all the zones, but its distribution is very irregular. It can be found locally along the margins of mineralized veins; and

- Sulphidation manifests as pyrrhotite and coarse arsenopyrite in veins, as semi-massive horizons, or as disseminations in quartz veins and selvages. Arsenopyrite replaces pyrite and pyrrhotite.

Mineralization on the Property consists of five main lenses (zones 1 to 3 and 5 to 6).

Based on the nature of the host rock in the Chimo mine, the mineralized zones have been divided into two types of lode deposits: semi-massive sulphide veins associated with iron formations (zones 1 and 2), and lenticular quartz veins associated with altered volcanic rocks mineralized with arsenopyrite (zones 3, 5 and 6).

It is unlikely that these two types of gold mineralization are genetically distinct since they occur together in the Chimo mine. Mineralization is associated with injections of quartz and sulphide minerals into sheared zones at the contacts between lithologies of contrasting competency and chemical composition.

## 1.5 Drilling, Sampling method, Approach and Analysis

From 2016 to 2019, Cartier drilled 109 holes during a 3-phase drilling program for a total of 49,243 m. Deep drill holes with multiple wedges required close monitoring of the deviation. Drill core logging and sample selection were carried out at Cartier's facilities in Val-d'Or. The selected samples were sawed in two. One half was kept for future reference and the other half shipped to a certified independent laboratory. The procedures used at both laboratories during the drilling program are fairly standard and in line with industry practices. Cartier's QA/QC program monitored the quality of the process.

GéoPointCom is of the opinion that the sample preparation, analysis, QA/QC and security protocols used for the project follow generally accepted industry standards and that the data is valid and of sufficient quality to be used for mineral resources estimation.

## 1.6 DATA VERIFICATION

On October 4 and 7, 2019, Christian D'Amours visited the issuer's facilities. The visit included an assessment of field sites (drilling locations and access road), as well as the adequacy of the facilities used to log the drill core.

Christian D'Amours collected 20 samples from four (4) pre-selected drill holes. These samples corroborated the results obtained by Cartier.

To prepare for the resource estimation, the author performed a detailed verification of all holes drilled between 2016 and 2019 (location, deviation, logging and sampling). This due diligence revealed only a few minor irregularities during the final grade calculations. To remove any risk, it was decided that all analytical results from the 2016 to 2019 programs would be re-imported directly from the original certificates and that the calculation of final grade would be standardized.

The nature of the historical drilling information prevented diligent verification of the source data; instead, only a geometric check was possible. The author, therefore, reconciled the current resource estimate with areas that had been mined in the past. Given the excellent reconciliation result (less than 5% difference in tonnage and ounces), the author is of the opinion that while the historical data contains errors, these are minor and do not affect the quality of the estimate.

GéoPointCom believes that the database is sufficiently reliable and accurate to be used for mineral resource estimation.

## 1.7 CENTRAL GOLD CORRIDOR MINERAL RESOURCE ESTIMATE

The resource estimate for the Central Corridor on the Chimo Mine Project was prepared by Christian D'Amours, P.Geo., using all available data as at July 2, 2019.

The Central Corridor consists of seven (7) structures, separated into five (5) different sectors.

The estimation method consists of Ordinary Kriging (OK) applied to a percent block model composed of 10 m x 10 m X 10 m cells. GéoPointCom used Isatis geostatistical software.

GéoPointCom is of the opinion that the current mineral resource estimate can be categorized as indicated and inferred resources based on assay accuracy, search ellipsoid criteria, drill hole spacing and interpolation parameters.

Using a cut-off of 2.50 g/t, the Indicated Resources amount to 3,263,300 tonnes at a grade of 4.40 g/t Au, for a total of 461,280 troy ounces. The Inferred Resources amount to 3,681,600 tonnes at a grade of 3.53 g/t Au, for a total of 417,250 troy ounces (Table 1-1).

GéoPointCom considers the current resource estimate to be reliable and based on quality data, reasonable hypotheses, and parameters that follow CIM Definition Standards and CIM Best Practice Guidelines. The mineral resource estimate reflects the current state of knowledge on the Project.

The mineral resources presented in this Technical Report are not mineral reserves as economic viability has not been demonstrated.

| Indicated Resource | | | | |
|---|---|---|---|---|
| Sector | Structure | Metric Ton (t) | Grade (g/t Au) | Troy ounce (oz) |
| Mine | 5B | 1 766 200 | 4.54 | 257 800 |
| | 5B2 | 8 600 | 3.01 | 840 |
| | 5C | 91 700 | 4.07 | 12 000 |
| | 5M | 387 900 | 4.22 | 52 630 |
| | 5M2 | 34 200 | 5.58 | 6 140 |
| | 5N | 203 900 | 4.78 | 31 340 |
| | **Sub Total** | 2 492 500 | 4.50 | 360 740 |
| Ext | 5B | 101 500 | 3.76 | 12 270 |
| | 5B2 | 0 | 0 | 0 |
| | 5C | 14 900 | 3.64 | 1 740 |
| | 5M | 49 100 | 3.95 | 6 230 |
| | 5M2 | 62 500 | 5.84 | 11 740 |
| | 5N | 0 | 0 | 0 |
| | **Sub Total** | 228 000 | 4.36 | 31 990 |
| East | 5B | 100 800 | 3.49 | 11 310 |
| | 5B2 | 0 | 0 | 0 |
| | 5C | 0 | 0 | 0 |
| | 5M | 23 800 | 3.90 | 2 990 |
| | 5M2 | 0 | 0 | 0 |
| | 5N | 109 100 | 4.02 | 14 110 |
| | **Sub Total** | 233 700 | 3.78 | 28 400 |
| Other | 5B | 46 400 | 3.56 | 5 310 |
| | 5B2 | 0 | 0 | 0 |
| | 5C | 7 900 | 4.32 | 1 100 |
| | 5M | 12 600 | 3.94 | 1 600 |
| | 5M2 | 0 | 0 | 0 |
| | 5N | 24 700 | 3.03 | 2 410 |
| | **Sub Total** | 91 600 | 3.53 | 10 420 |
| Muck | 5B | 87 700 | 4.55 | 12 830 |
| | 5M | 100 | 2.61 | 10 |
| | 5M2 | 0 | 0 | 0 |
| | 5N | 0 | 0 | 0 |
| | **Sub Total** | 87 800 | 4.55 | 12 840 |
| 6N1 | Upper | 113 300 | 4.00 | 14 570 |
| | Lower | 16 300 | 4.44 | 2 330 |
| | **Sout Total** | 129 600 | 4.06 | 16 900 |
| **TOTAL** | | **3 263 300** | **4.40** | **461 280** |

| Inferred Resource | | | | |
|---|---|---|---|---|
| Sector | Structure | Metric Ton (t) | Grade (g/t Au) | Troy ounce (oz) |
| Mine | 5B | 114 400 | 3.48 | 12 800 |
| | 5B2 | 0 | 0 | 0 |
| | 5C | 80 000 | 3.24 | 8 330 |
| | 5M | 55 200 | 3.56 | 6 320 |
| | 5M2 | 1 200 | 3.66 | 140 |
| | 5N | 141 800 | 3.18 | 14 500 |
| | **Sub Total** | 392 600 | 3.33 | 42 090 |
| Ext | 5B | 520 100 | 3.63 | 60 700 |
| | 5B2 | 0 | 0 | 0 |
| | 5C | 107 500 | 3.30 | 11 400 |
| | 5M | 118 700 | 3.27 | 12 480 |
| | 5M2 | 219 700 | 3.11 | 21 970 |
| | 5N | 0 | 0 | 0 |
| | **Sub Total** | 966 000 | 3.43 | 106 550 |
| East | 5B | 620 500 | 3.26 | 65 030 |
| | 5B2 | 0 | 0 | 0 |
| | 5C | 0 | 0 | 0 |
| | 5M | 88 900 | 3.29 | 9 400 |
| | 5M2 | 0 | 0 | 0 |
| | 5N | 458 900 | 4.25 | 62 700 |
| | **Sub Total** | 1 168 200 | 3.65 | 137 140 |
| Other | 5B | 311 800 | 3.29 | 32 980 |
| | 5B2 | 0 | 0 | 0 |
| | 5C | 23 900 | 3.70 | 2 840 |
| | 5M | 94 200 | 3.59 | 10 870 |
| | 5M2 | 0 | 0 | 0 |
| | 5N | 39 000 | 3.40 | 4 260 |
| | **Sub Total** | 468 900 | 3.38 | 50 960 |
| Muck | 5B | 0 | 0 | 0 |
| | 5M | 0 | 0 | 0 |
| | 5M2 | 0 | 0 | 0 |
| | 5N | 0 | 0 | 0 |
| | **Sub Total** | 0 | 0 | 0 |
| 6N1 | Upper | 435 000 | 3.49 | 48 810 |
| | Lower | 250 900 | 3.93 | 31 700 |
| | **Sub Total** | 685 900 | 3.65 | 80 520 |
| **TOTAL** | | **3 681 600** | **3.53** | **417 250** |

Table 1-1: Central Gold Corridor Mineral Resources.

## 1.8 INTERPRETATION AND CONCLUSIONS

GéoPointCom has verified all available data as well as the procedures and processing methods. GéoPointCom believes that the information presented in this report provides a fair and accurate picture of the Property's potential.

The Property is located in the Val-d'Or mining camp, a 50-km drive east of the city of Val-d'Or. Mining infrastructure is still present at the site and could facilitate the transition to a more advanced stage of exploration.

This Technical Report presents the maiden mineral resource estimate for the Central Corridor since CAMBIOR closed the mine in 1997. At a cut-off of 2.50 g/t, the Indicated Resources amount to 3,263,300 tonnes at a grade of 4.40 g/t Au, for a total of 461,280 troy ounces. The Inferred Resources amount to 3,681,600 tonnes at a grade of 3.53 g/t Au, for a total of 417,250 troy ounces. Table 1-2 assesses the sensitivity of the mineral resource estimate to market fluctuations. According to the author, this mineral resource estimate reflects the current state of knowledge on the Project. The mineral resources presented in this Technical Report are not mineral reserves as economic viability has not been demonstrated.

| Indicated Resource | | | | | Inferred Resource | | | |
|---|---|---|---|---|---|---|---|---|
| Cut Off Grade (g/t Au) | Metric Ton (t) | Grade (g/t Au) | Troy Ounce (oz) | | Cut Off Grade (g/t Au) | Metric Ton (t) | Grade (g/t Au) | Troy Ounce (oz) |
| 1.5 | 6 157 300 | 3.24 | 642 060 | | 1.5 | 8 520 400 | 2.62 | 716 570 |
| 2.0 | 4 479 300 | 3.81 | 548 380 | | 2.0 | 5 591 300 | 3.09 | 555 530 |
| **2.5** | **3 263 300** | **4.40** | **461 280** | | **2.5** | **3 681 600** | **3.53** | **417 250** |
| 3.0 | 2 389 100 | 5.01 | 384 540 | | 3.0 | 2 347 800 | 3.97 | 299 800 |
| 3.5 | 1 759 400 | 5.63 | 318 680 | | 3.5 | 1 199 000 | 4.66 | 179 470 |
| 4.0 | 1 255 900 | 6.40 | 258 410 | | 4.0 | 728 300 | 5.25 | 122 950 |

Table 1-2: Sensitivity of the gold resource to cut-off grade.

## 1.9 RECOMMENDATIONS

GéoPointCom recommends pursuing the current resource estimation to include the North and South gold corridors in order to provide a complete estimate of the current state of resources for the three known gold corridors on the Property. The resource estimation for the North and South gold corridors should begin as soon as possible. This work is expected to take approximately 10 to 12 weeks at a total cost of approximately $60,000.

Concurrently, drilling should continue in order to expand resources at depth in the extensions of zones 5B4-5M4-5NE at a distance of 450 m to the east of the underground workings, as well as around the periphery of Zone 6N1, which is located 125 m from the underground infrastructure. The objective of this program would be to add gold mineralization over a vertical distance of 600 m below zones 5B4-5M4-5NE between depths of 700 m and 1,300 m, and to increase the width of zone 6N1 over a vertical distance of 500 m between depths of 600 m and 1,100 m. Drilling began on November 19, 2019, and is expected to be completed in July 2020. To achieve this goal, 11 km of controlled directional precision drilling will be required at an estimated cost of $2.5 million.

## 2 INTRODUCTION

The Chimo Mine Property (the Property or the Project) is a gold exploration project in the Abitibi region of the province of Québec, Canada, about a 50 km drive from the city of Val-d'Or. The property is 100% owned by Cartier Resources Inc. (Cartier, the Company or the issuer).

Cartier is a junior exploration company listed on the Toronto Venture Exchange (TSXV) under the symbol ECR. Its head office and exploration office are at the same address:

1740, chemin Sullivan, Suite 1000
Val-d'Or, J9P 7H1, Québec, Canada
Telephone: 1-877-874-1331

In September 2019, Mr. Gaétan Lavallière, Vice-President of Cartier, commissioned GéoPointCom to estimate the mineral resources in the Central Gold Corridor (or Central Corridor) (Figure 2-1) on the Property. Mr. Gaétan Lavallière is Vice-President of Cartier. Under this mandate, Christian D'Amours, Geologist and President of GéoPointCom, prepared a maiden mineral resource estimate for the Central Corridor in accordance with National Instrument 43-101 Respecting Standards of Disclosures for Mineral Projects (NI 43-101) and Form 43-101F1. Christian D'Amours is a QP and independent of the issuer, as defined by NI 43-101.

GéoPointCom is an independent consulting firm based in Val-d'Or, specializing in geostatistics and resource estimation. GéoPointCom is active almost exclusively in the field of geostatistics and 3D modelling. Since it was founded in 2000, GéoPointCom has carried out more than 160 different projects for 19 independent companies covering 33 mining properties in six different countries. The majority of these mandates consisted of geostatistical studies, 3D modelling, and resource and reserve estimates. In some cases, the mandates included training in the use of the Geotic software series, including GeoticMine, as well as GemCom and DataMine, and the applicability of such software to the specificities of each of the various projects.

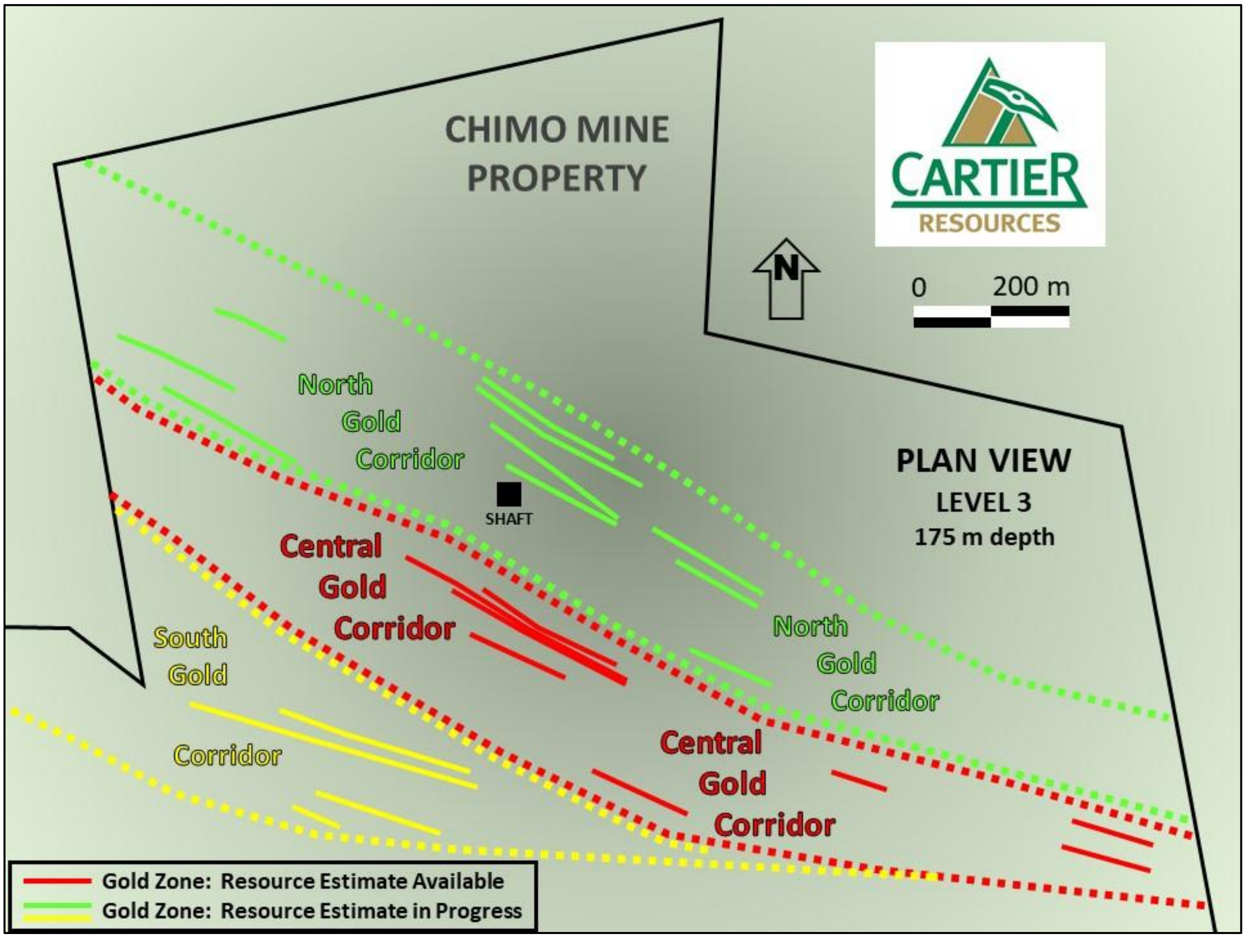


Figure 2-1: Location of the Central Gold Corridor on the Chimo Mine Property.

### 2.1 Report Responsibilities and Qualified Person

The Technical Report was prepared by Christian D'Amours, P.Geo., President of GéoPointCom. Mr. D'Amours is a professional geologist and member of the Order of Geologists of Québec (OGQ No. 226). Mr. D'Amours is acting as a QP independent of the issuer.

The QP does not have, nor has he previously had, any material interest in the issuer or its related entities. The relationship with the issuer is solely a professional association between the issuer and the independent consultant. The Technical Report was prepared in return for fees based upon an agreed commercial rate, and the payment of these fees is in no way contingent on the result of the Technical Report.

### 2.2 Effective Dates

This report follows the issuer's press release of November 5th, 2019, entitled "Cartier awards mandate for NI 43-101 resource estimate on Chimo Mine Project."

The effective date (July 2nd, 2019) of the Technical Report is the date of the most recent technical information (last drilling analyses) considered in the Technical Report. This date also corresponds to the database close-out.

The signing date (December 17th, 2019) is the date the Technical Report was sealed.

## 2.3 Sources of Information

This report is based in part on internal company reports, maps, government reports and public information, as listed in Item 27 "References." Sections taken from other reports are clearly indicated in the report.

The mineral resource estimate was prepared using information from the following:

- Technical discussions with Cartier staff;
- A review of exploration data collected by Cartier;
- Internal and public technical documents provided by Cartier;
- A database of historical and recent drilling;
- The QP's visit to the Property;
- Additional information from public domain sources (SIGEOM, GESTIM, etc.).

The author believes the basic assumptions contained in the above information are factual and accurate, and the interpretations are reasonable. The QP has reviewed the data and has no reason to believe that any material facts have been withheld or concealed in connection with the mineral resource estimate.

## 2.4 Site Visit

Christian D'Amours visited the Property and Cartier's core shack on October 4 and 7, 2019, as covered by the mandate. The visit included an overview of the Property and various procedures, a visual inspection of mineralized drill core, and discussions on the QA/QC protocols in place.

The QP collected samples to corroborate the analytical results obtained by Cartier.

## 2.5 Currency, Units of Measure and Abbreviations

All currency amounts are stated in Canadian dollars ($).

Metric units are used throughout the Technical Report, including metric tons (tonnes, t) and kilograms (kg) for weight, kilometres (km) or metres (m) for distance, hectares (ha) for area, grams per metric ton (g/t) for gold grades and troy ounces (oz) for total contained gold.

A list of the abbreviations, acronyms and symbols used in this Technical Report is provided in Table 2-1.

| Abbreviation or Symbol | Unit or Term |
|---|---|
| AA | Atomic absorption |
| AGB | Abitibi Greenstone Belt |
| Au | Gold |
| BIF | Banded Iron Formation |
| BQ | BQ-caliber drill hole |
| Cartier | Cartier Resources Inc. |
| CIM | Canadian Institute of Mining, Metallurgy and Petroleum |
| CLLDZ | Cadillac–Larder Lake Deformation Zone |
| cm | Centimetre |
| CO2 | Carbon dioxide |
| ° | Degree |
| °C | Celsius degree |
| *et al.* | And others |
| g | Gram |
| g/t | Gram per metric ton |
| Ga | Billion years |
| GESTIM | Gestion des titres miniers (MERN's online claim management system) |
| GPS | Global Positioning System |
| H2O | Water |
| h | Hour |
| ha | Hectare |
| HQ | HQ-caliber drill hole |
| ISO | International Organization for Standardization |
| K | Potassium |
| km | Kilometre |
| $km^2$ | Square kilometre |
| kV | Kilo volt |
| LIMS | Laboratory Information Management System |
| lvl | Level |
| m | Metre |
| Ma | Million years |
| MDDEP | Ministère du Développement durable, de l'Environnement et des Parcs (Centre de contrôle environnemental) |
| MERN | Ministère de l'Energie et des Ressources naturelles du Québec (Québec's Ministry of Energy and Natural Resources) |
| MF | Metal Factor |
| MFFP | Ministère des Forêts, de la Faune et des Parcs (Québec's Ministry of Forests, Wildlife and Parks) |
| MgO | Magnesian oxide |
| mm | Millimetre |
| MPa | Megapascal |
| Na | Sodium |
| Nad | North American datum |
| NI 43-101 | National Instrument 43-101 |
| NQ | NQ-caliber drill hole |
| NSR | Net Smelter Return |
| OGQ | Ordre des Géologues du Québec (Order of Geologists of Québec) |
| oz | Troy ounces |
| % | Percent |
| Pb | Lead |
| PDDZ | Porcupine-Destor Deformation Zone |
| po | Inch |
| ppb | Part per billion |
| QA/QC | Quality Assurance / Quality Control |
| RQD | Rock Quality Designation |
| S | Sulphur |

| Abbreviation or Symbol | Unit or Term |
|---|---|
| SiO2 | Silica |
| SIGEOM | Système d'information géominière (the MERN's online spatial reference geomining information system) |
| t | Metric ton |
| U | Uranium |
| UTM | Universal Transverse Mercator |
| Y | Yttrium |
| yyyy-mm-dd | Year-month-day |
| Zr | Zirconium |

Table 2-1: List of abbreviations, acronyms and symbols.

## 2.6 ACKNOWLEDGEMENTS

The author of the Technical Report sincerely thanks Mr. Ronan Déroff, Senior Geologist, Project Manager and Geomatician at Cartier for modelling the solids using GeoticMine software. Mr. Déroff was supervised by Mr. Christian D'Amours on matters of technical support and the detailed information presented in several sections in the report and during investigations and verifications to ensure robust information. The author also thanks Gaétan Lavallière, Vice-President at Cartier, for his support during this mandate and in particular for all the technical discussions and his collaboration during the visit to the Property.

## 3 RELIANCE ON OTHER EXPERTS

This Technical Report has been prepared by GéoPointCom at the request of the issuer. Christian D'Amours is the QP responsible for reviewing technical documents relevant to the Technical Report, preparing the mineral resource estimate, and recommending a work program if warranted.

The QP relied on the issuer for almost all information, specifically, the information on mining titles, option agreements, royalty agreements, environmental liabilities and permits. GéoPointCom consulted the mining titles and their status as well as any technical data supplied by the issuer and any technical information available from public sources. GéoPointCom is not qualified to express any legal opinion with respect to the property titles, current ownership, environmental permits or possible litigation.

GéoPointCom has relied on data and information provided by Cartier, and on historical reports (refer to Item 27, *References*). GéoPointCom has reviewed and validated a portion of the collection of data provided by the client. GéoPointCom has, therefore, made judgments about the general reliability of the underlying data and, where deemed either inadequate or unreliable, the data were not used or the procedures modified to account for the lack of confidence in that specific information.

# 4 PROPERTY DESCRIPTION AND LOCATION

## 4.1 Location

The Property is located in the province of Québec, Canada, in the administrative region of Abitibi-Témiscamingue (Figure 4-1). It is about 40 km east-southeast of the town of Val-d'Or and about 10 km southeast of the municipality of Louvicourt.

The Property lies within NTS map sheet 32C03 in Vauquelin Township. The approximate coordinates of the centre of the Property are 332000E, 5320000N (UTM projection, NAD 83, Zone 18).


Figure 4-1: General location map

## 4.2 Mineral Tenure

In Québec, the management of mineral resources and the granting of mineral exploration rights are governed by the Mining Act (http://legisquebec.gouv.qc.ca/en/ShowTdm/cs/M-13.1). The Mining Act also specifies the rights to use mineral substances during the mining phase. Finally, it sets out the rights and obligations of title holders in line with the government's mandate to develop Québec's mineral resources (https://mern.gouv.qc.ca/english/publications/online/mines/claim/index.asp).

The status of the mining titles for the Property, provided to the QP by the issuer, can be verified in GESTIM (the claim management of Québec's Ministry of Energy and Natural Resources; https://gestim.mines.gouv.qc.ca/MRN_GestimP_Presentation/ODM02101_login.aspx).

As at October 23, 2019, all mining titles for the Property are registered to Cartier Resources Inc. (titleholder number: 80277). The mining titles consist of twelve (12) contiguous claims, for a total area of 335 hectares (Figure 4-2 and Table 4-1).

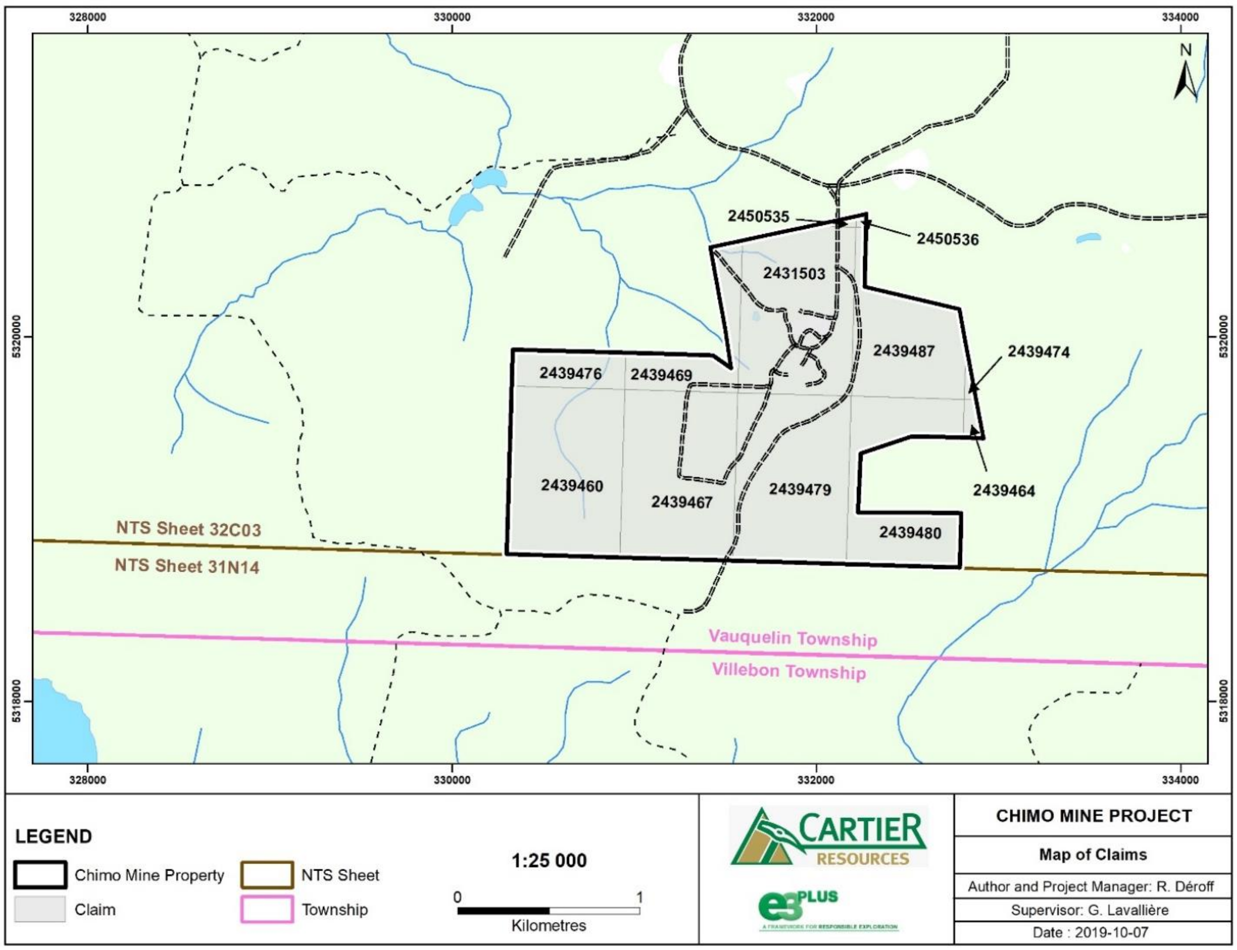


Figure 4-2: Chimo Mine Property claim map

| Title number | Title type | Title status | Area (ha) | Registration date yyyy/mm/dd | Expiration date yyyy/mm/dd | Owner |
|---|---|---|---|---|---|---|
| 2431503 | CDC | Active | 55.8 | 2015-07-23 | 2021-07-22 | Cartier Resources Inc. 100% |
| 2439460 | CDC | Active | 57.6 | 2016-04-22 | 2021-02-28 | Cartier Resources Inc. 100% |
| 2439464 | CDC | Active | 1.9 | 2016-04-22 | 2021-02-28 | Cartier Resources Inc. 100% |
| 2439467 | CDC | Active | 57.6 | 2016-04-22 | 2021-02-28 | Cartier Resources Inc. 100% |
| 2439469 | CDC | Active | 19.1 | 2016-04-22 | 2021-02-28 | Cartier Resources Inc. 100% |
| 2439474 | CDC | Active | 0.9 | 2016-04-22 | 2021-02-28 | Cartier Resources Inc. 100% |
| 2439476 | CDC | Active | 12.3 | 2016-04-22 | 2021-02-28 | Cartier Resources Inc. 100% |
| 2439479 | CDC | Active | 57.6 | 2016-04-22 | 2021-02-28 | Cartier Resources Inc. 100% |
| 2439480 | CDC | Active | 35.4 | 2016-04-22 | 2021-02-28 | Cartier Resources Inc. 100% |
| 2439487 | CDC | Active | 35.2 | 2016-04-22 | 2021-02-28 | Cartier Resources Inc. 100% |
| 2450535 | CDC | Active | 0.7 | 2016-06-22 | 2020-06-21 | Cartier Resources Inc. 100% |
| 2450536 | CDC | Active | 0.4 | 2016-06-22 | 2020-06-21 | Cartier Resources Inc. 100% |

Table 4-1: List of claims.

## 4.3 Royalties, Agreements and Restrictions

Cartier holds a 100% interest in the property for which 1% NSR (Net Smelter Return) royalty has been granted to IAMGOLD Corporation. No rights of first refusal ('' buy-back '') have been granted.

## 4.4 Socio-Environmental Responsibilities

The issuer has a adopted a sustainable development policy that focuses on three main aspects:

- Social: listen to the concerns of stakeholders by carrying out socio-environmental studies; regularly follow up to ensure the social acceptability of activities and to add value to the social environment through structuring actions;
- Environmental: minimize the footprint of Cartier's mineral exploration activities by complying with existing laws and regulations, and remain committed to the e³ Plus principles;
- Preventive Health and Safety: apply Cartier's rigorous preventive health and safety procedure (IPDE: Inspection, Planning, Decision and Execution).

In 2011, Cartier received the AEMQ e³ Plus Award, which recognizes the company's high level of environmental and social responsibility and responsible mineral development.

The tailings pond on the Property, restored by CAMBIOR Inc. ("CAMBIOR"), does not pose any environmental problems. The MERN released CAMBIOR from its mine site restoration obligation in the 2000s as there were no issues related to the final effluent. The site has been restored and no environmental studies have been carried out since. It is classified as safe and the MERN no longer performs monitoring or environmental characterization work (pers. comm. Robert Lacroix, MERN).

In September 2014, an inspection of the Property by the Environmental Control Centre of the MDDEP (Ministry of Sustainable Development, Environment and Parks, now the Ministry of the Environment and the Fight Against Climate Change) confirmed the Property's compliance with the applicable standards.

## 4.5 PERMITS

In Québec, forest management permits are required before cutting down trees when building access roads and drilling sites. These permits are issued by the MFFP (Ministry of Forests, Wildlife and Parks; https://mffp.gouv.qc.ca/). The delay to obtain permits is usually 2 to 4 weeks.

Cartier has obtained all the necessary authorizations to conduct surface drilling on the Property.

## 4.6 OTHER IMPORTANT RISK FACTORS

GéoPointCom is not aware of any other significant factors or risks that could affect access, the holder, the rights or the ability to estimate the mineral resources on the Property.

# 5 ACCESSIBILITY, CLIMATE, LOCAL RESOURCES, INFRASTRUCTURE AND PHYSIOGRAPHY

## 5.1 Accessibility

The Property is easily accessed from the city of Val-d'Or, using the paved Trans-Canada Highway 117 eastward for about 40 km, then heading east on the gravel Chimo Road for 11 km (Figure 5-1). A multitude of secondary gravel roads and forestry trails on the Property make it accessible throughout the year.

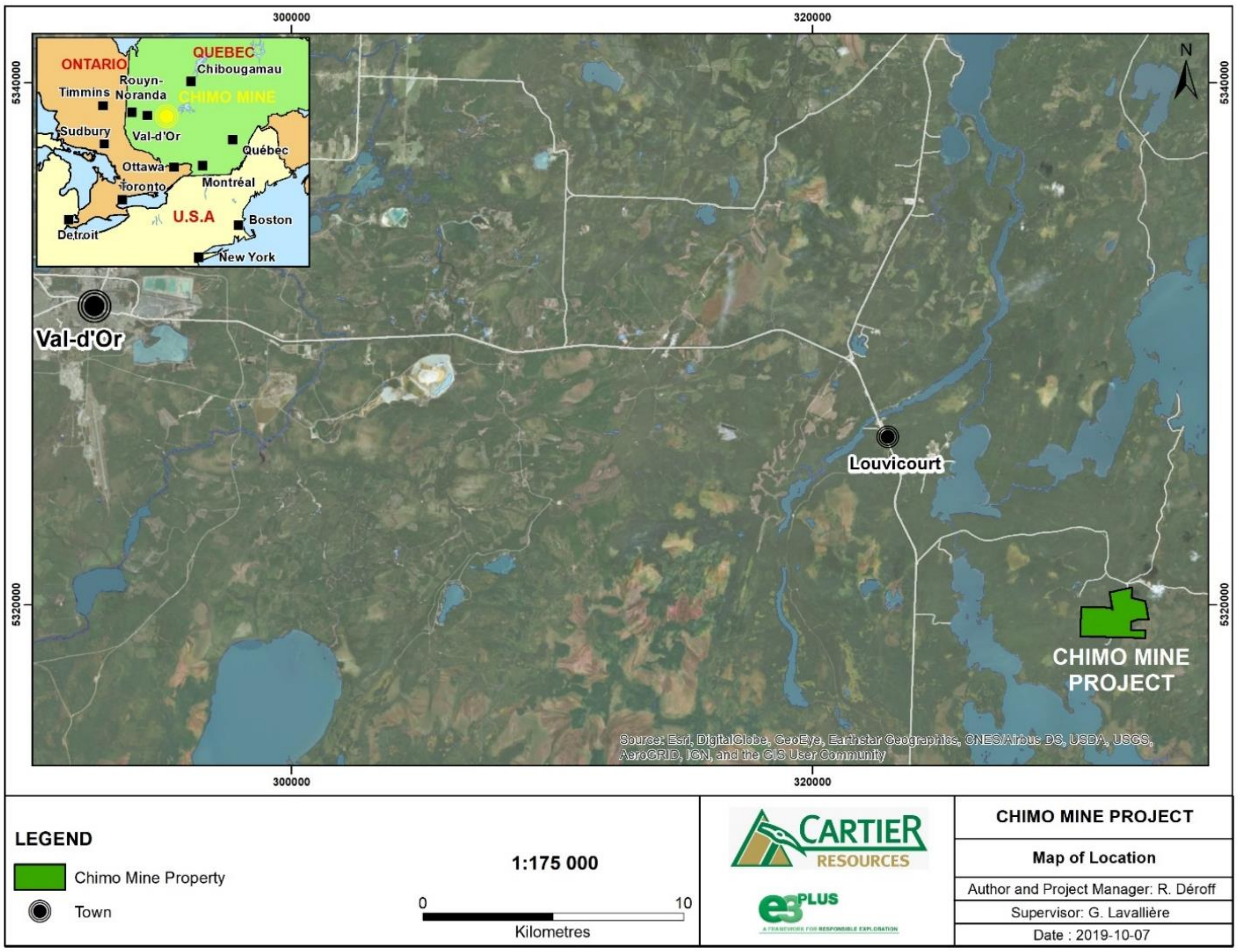


Figure 5-1: Chimo Mine Project location map.

## 5.2 Climate

The regional climate is continental and typical of the Canadian Shield at this latitude. Winters are cold, dry and snowy, lasting from October to April. Summers are relatively hot, humid and short, from June to August.

According to Environment Canada statistics from 1971 to 2000, the region was characterized by an average daily temperature of 1.2°C. July has an average temperature of 17.2°C, while January drops to an average of -17.2°C. Rainfall is 635 mm per year, including 99 mm in July. The amount of snowfall is 300 cm per year, of which 61 cm falls in January (http://climat.meteo.gc.ca/climate_normals/).

Climate conditions do not have a major impact on exploration activities. However, it is preferable to conduct drilling on the few marshy areas on the Property during winter when the ground is frozen.

## 5.3 Local Resources and Infrastructure

The following is taken in part from Richard *et al.* (2019).

### 5.3.1 Local labour

Val-d'Or is part of the regional county municipality of La Vallée-de-l'Or. The population of the latter is approximately 43,000 (2016 Census of Canada) and covers an area of approximately 24,500 $km^2$.

A skilled and experienced workforce in mineral exploration and mining is available in the region. The city also offers a multitude of services and many mining-related companies: analytical laboratories, drilling and surveying companies, consulting and engineering firms, construction and mining contractors, and service and equipment suppliers.

### 5.3.2 Additional services

The Property is situated near six mills in the Val-d'Or region. It is accessible year-round by taking Trans-Canada Highway 117 and then turning onto a gravel logging road 6 km south of Louvicourt and driving another 11 km to the Property. The logging road is in good condition with a wide, recently built solid road base.

Underground mine workings comprise 7 km of drifts distributed over 19 main levels that are connected by a 3-compartment shaft of 5.5 m x 1.8 m that extends to a depth of 920 m. About 20 sublevels and raises complete the underground infrastructure. The spacing between levels 18 and 19 is 75 m, which also corresponds to the length of the long-hole production holes and the vertical dimension of the stopes. This spacing decreases to 65 m between levels 17 and 18 and to 35 m between levels 16 and 17. The other upper levels are spaced 30 m apart and the sublevels are spaced between 10 and 20 m, depending on which zone is being mined. In the fourth quarter of 1996, more than 1,500 t were hoisted per day using the equipment in place at that time (skips, cable, hoist and headframe) (Vallières, 1996).

The headframe, mill and other surface facilities were dismantled in 2008, but the 25 kV power line is in good condition and the sandpit is still in place. The walls of the shaft and its underground infrastructure were in good condition when the mine closed, and the shaft access at surface was carefully sealed with a concrete slab. The tailings pond has been restored and a certificate of release and letter of authorization were issued by the Ministry of Natural Resources and the Ministry of the Environment.

Cartier's office and the fully equipped core shack are located in Val-d'Or and provide easy access and logistics for all exploration work carried out on the Property.

### 5.4 PHYSIOGRAPHY

The topography of the Property is fairly flat. The average altitude is around 360 to 380 m above sea level. The vegetation comprises moss, alder, spruce, aspen, birch, larch, fir, cedars and pine. There are many marshy areas in the region and sandy areas are also present.

Outcrops are rare on the Property. Overburden is often thick, ranging from 20 to 50 m, and consists mainly of boulders, sand and clay.

# 6 HISTORY

The following is taken from a CAMBIOR internal report (Houle, 1995).

The bedrock rarely crops out in the vicinity of the mine. The deposit was discovered by drilling magnetic anomalies. Prospecting had previously revealed gold showings, which stimulated interest in the area.

## 6.1 Quemartic Mines – 1936 to 1938

The area of the future Property and mine site was staked in the fall of 1936 and transferred in September 1937 to Quemartic Mines Ltd, who then transferred it to a subsidiary, Quemartic Mines (Québec) Ltd. While prospecting in 1937 and 1938, visible gold was discovered at two locations in volcanic rocks (Zone 2 and the western part of the mine). Two exploration drill holes totalling 336 m did not encounter mineralization of economic interest and the claims were eventually abandoned.

## 6.2 Chimo Gold Mines – 1943 to 1948 and 1963 to 1967

The land was again staked in 1943 and purchased in 1945 by Chimo Gold Mines Ltd. A magnetometric survey was carried out, and 45 drill holes totalling 5,800 m were drilled between 1945 and 1947. The first drill holes, located near the original discovery, were disappointing, but encouraging results were obtained further south where six gold zones were soon recognized. In 1948, preparations were made to sink the shaft and machinery was transported to the site, but the work was suspended until 1963.

In 1963, a detailed magnetometric survey and an airborne electromagnetic survey were conducted, followed by a 44-hole drilling program (8,390 m) located 300 m east of the known gold zones. Four new areas were discovered (including zones 2 and 3). A vertical 3-compartment shaft was sunk to a depth of 183 m, and drifts were developed at depths of 80, 120 and 175 m from November 1964 to June 1965. Production began on January 1, 1966, and the first gold brick was poured in February 1967. Production was halted in late August 1967 when the known near-surface reserves had been depleted. The ore was transported to the Bevcon Mill, which had been purchased by Chimo Gold Mines.

## 6.3 SOQUEM/LOUVEM – 1978 to 1989

SOQUEM acquired the Property in 1978 and proceeded to carry out magnetic and electromagnetic surveys. A 12-hole drilling program (1,548 m) was carried out in 1978, followed by a second 25-hole program (6,230 m) in 1980. SOQUEM then sold the claims to its subsidiary LOUVEM Mines Inc. (LOUVEM). Between 1981 and 1983, LOUVEM dewatered and rehabilitated the former mine, excavated exploration drifts, and performed 10,750 m of diamond drilling. Start-up work commenced, and the mine entered into production in August 1984. In 1984, 33 holes drilled from surface led to the discovery of a new gold zone (Zone 5), 150 m south of the previously mined areas. Mining work in the old areas was suspended to hasten the development of Zone 5. Production resumed in mid-August 1985. New drilling (29 holes for 5,755 m) was carried out on the extensions of known zones and on geophysical targets, leading to the discovery of Zone 6 in April 1985. Successive drilling programs (1986: 11 holes for 1,878 m; 1987: 14 holes for 1,118 m) were carried out to better define the known zones.

## 6.4 CAMBIOR – 1989 TO 1997

On May 8, 1989, CAMBIOR Inc. (CAMBIOR) acquired 50% of LOUVEM's interest and became the operator. In 1990, CAMBIOR bought the 50% residual interest from LOUVEM. The work carried out from 1989 to 1997 was mainly construction, production and development. The shaft was deepened to 920 m and two additional levels were developed (18 and 19). In addition, the concentrator was relocated from the Lucien Béliveau Mill to the Chimo mine, and a paste backfill plant and administrative office were constructed. Surface exploration on the Property ceased during this period; however, the lateral extensions of Zone 6 were drill-tested from claims on the adjacent Nova Property belonging to CAMBIOR (1989-90: 12 holes, 2,141 m). In 1995, exploration drilling (11 holes for 3,492 m) tested the strike extensions of Zone 5, revealing a possible extension to the zone, 750 m to the east.

## 6.5 EXPLORATION MALARTIC SUD, X-ORE RESOURCES AND BLUE NOTE MINING – 2001 TO 2013

On January 24, 2001, South-Malartic Exploration purchased all of the mineral rights to the Chimo and Nova properties. On April 24, 2007, South-Malartic Exploration changed its name to X-Ore Resources, which was amalgamated with Blue Note Mining on January 15, 2010. The first exploration work since 1997 took place in 2010 and 2011 when Blue Note Mining conducted a 12-hole drilling program (3,427 m) that tested the strike extensions of the main gold zones.

# 7 GEOLOGICAL SETTING AND MINERALIZATION

## 7.1 Regional Geology

The Property is located in the Abitibi Greenstone Belt of the southeastern Abitibi Subprovince, in the Archaean Superior Province.

The following is taken from Beausoleil *et al.* (2019) unless mentioned otherwise.

### 7.1.1 Archean Superior Province

The Archean Superior Province forms the core of the North American continent and is surrounded by provinces of Paleoproterozoic age to the west, north and east, and by the Mesoproterozoic Grenville Province to the southeast (Figure 7-1).


Figure 7-1: Location map of the Abitibi Greenstone Belt within the Superior Province (Monecke *et al.*, 2017).

Tectonic stability has prevailed since approximately 2.6 Ga in large parts of the Superior Province. Proterozoic and younger activity is limited to rifting of the margins, emplacement of numerous mafic dyke swarms (Buchan and Ernst, 2004), compressional reactivation, large-scale rotation at approximately 1.9 Ga, and failed rifting at approximately 1.1 Ga. With the exception of the northwest and northeast Superior margins that were pervasively deformed and metamorphosed at 1.9 to 1.8 Ga, the craton has escaped ductile deformation.

A first-order feature of the Superior Province is its linear subprovinces, or "terranes", of distinctive lithological and structural character, accentuated by subparallel boundary faults (e.g., Card and Ciesielski, 1986). Trends are generally E-W in the south, WNW in the northwest, and NW in the northeast. The term "terrane" is used in the sense of a geological domain with a distinct geological history prior to its amalgamation into the Superior Province during the 2.72 to 2.68 Ga assembly events, and a "superterrane" shows evidence for internal amalgamation of terranes prior to the Neoarchean assembly. "Domains" are defined as distinct regions within a terrane or superterrane.

### 7.1.2 Abitibi Subprovince

The Abitibi Subprovince is located in the southern portion of the Superior Province (Figure 7-2).

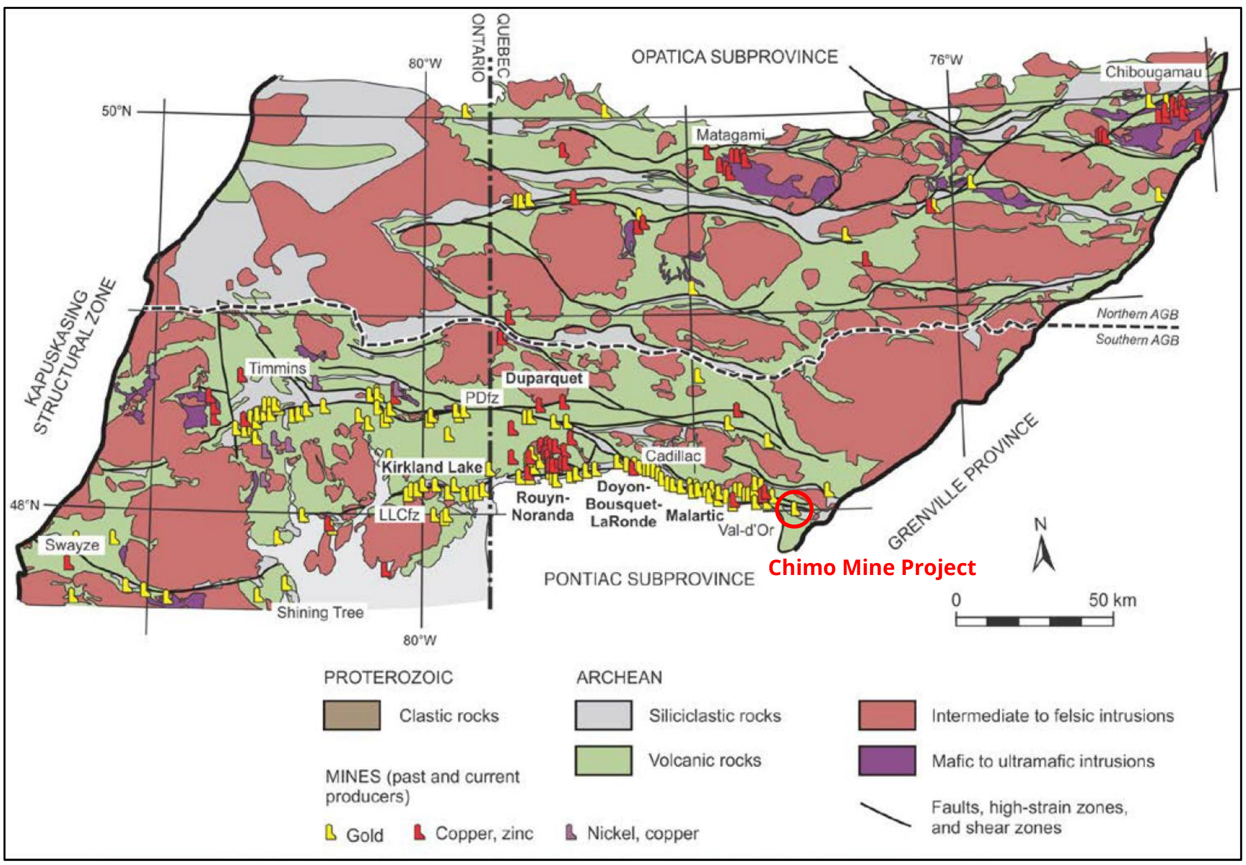


Figure 7-2: Geological map of the Abitibi Greenstone Belt (Monecke *et al.*, 2017).

It is bounded to the west by the Kapuskasing Structural Zone and to the east, by the Grenville Province. To the north, the Abitibi Subprovince is in structural contact with the plutonic Opatica Subprovince. The southern boundary of the Abitibi Greenstone Belt (AGB) is marked by the Cadillac–Larder Lake Deformation Zone (CLLDZ), a major structural break marking the contact with the younger metasedimentary rocks of the Pontiac Subprovince.

The AGB was formed over a period that spans approximately 150 Ma and is composed of east-trending synclines of largely volcanic rocks and intervening domes cored by synvolcanic and/or syntectonic plutonic rocks (gabbro-diorite, tonalite and granite in composition) alternating with east-trending bands of turbiditic wackes (Ayer *et al.*, 2002; Daigneault *et al.*, 2004; Goutier and Melançon, 2007; Monecke *et al.*, 2017). Most of the volcanic and sedimentary strata have a subvertical dip.

Volcanic and sedimentary packages are generally separated by steep east-trending faults. Some of these faults, such as the major CLLDZ and the Porcupine-Destor Deformation Zone, and similar breaks in the northern Abitibi, transect the entire belt and display evidence of overprinting deformation events including early thrusting, and later strike-slip and extension (Daigneault *et al.*, 2004; Benn and Peschler, 2005; Bateman *et al.*, 2008).

The CLLDZ is transcrustal and inherited from the accretion suture between the Pontiac and the AGB. The fault is important not only for its metallogenic wealth but also for its geodynamic models and juxtaposition of varied lithologic assemblages along its subsidiary faults. As the E-W and ESE-WNW segments of the fault cross through the AGB, they reflect a deep asymmetry, a feature that influenced the styles and episodes of gold mineralization.

In addition, the AGB is cut by numerous late-tectonic plutons ranging in composition from gabbro to granite with lesser dykes or plugs of syenite, lamprophyre and carbonatite. The greenstone belt is affected by a widespread greenschist facies metamorphism (Jolly, 1978; Dimroth *et al.*, 1983; Powell *et al.*, 1993; Benn *et al.*, 1994; Faure, 2015). The grade of metamorphism increases to amphibolite at the fringes of some plutons and approaching the Pontiac and Opatica subprovinces or the Proterozoic Grenville Province.

According to Monecke *et al.* (2017) and references therein, the AGB is subdivided into eight discrete stratigraphic episodes or assemblages, depending on the authors (Figure 7-3), based on groupings of U-Pb zircon ages. Submarine volcanism mostly occurred between 2795 and 2695 Ma and was followed by sedimentation in large deep basins and then by large-scale thin-skin folding and thrusting. New U-Pb zircon ages and recent mapping by the Ontario Geological Survey and Géologie Québec clearly shows similarity in the timing of volcanic episodes and ages of plutonic activity between the northern and southern AGB.

Two ages of unconformable sedimentary basins are recognized: early, widely and laterally extensive distributed Porcupine-style basins of fine-grained clastic rocks (turbidites), followed by Timiskaming-style basins of coarser aerial clastic and minor volcanic rocks, which are largely proximal to major faults where strike-slip movements occurred (Thurston and Chivers, 1990; Mueller *et al.*, 1992; Ayer *et al.*, 2002; Goutier and Melançon, 2007).

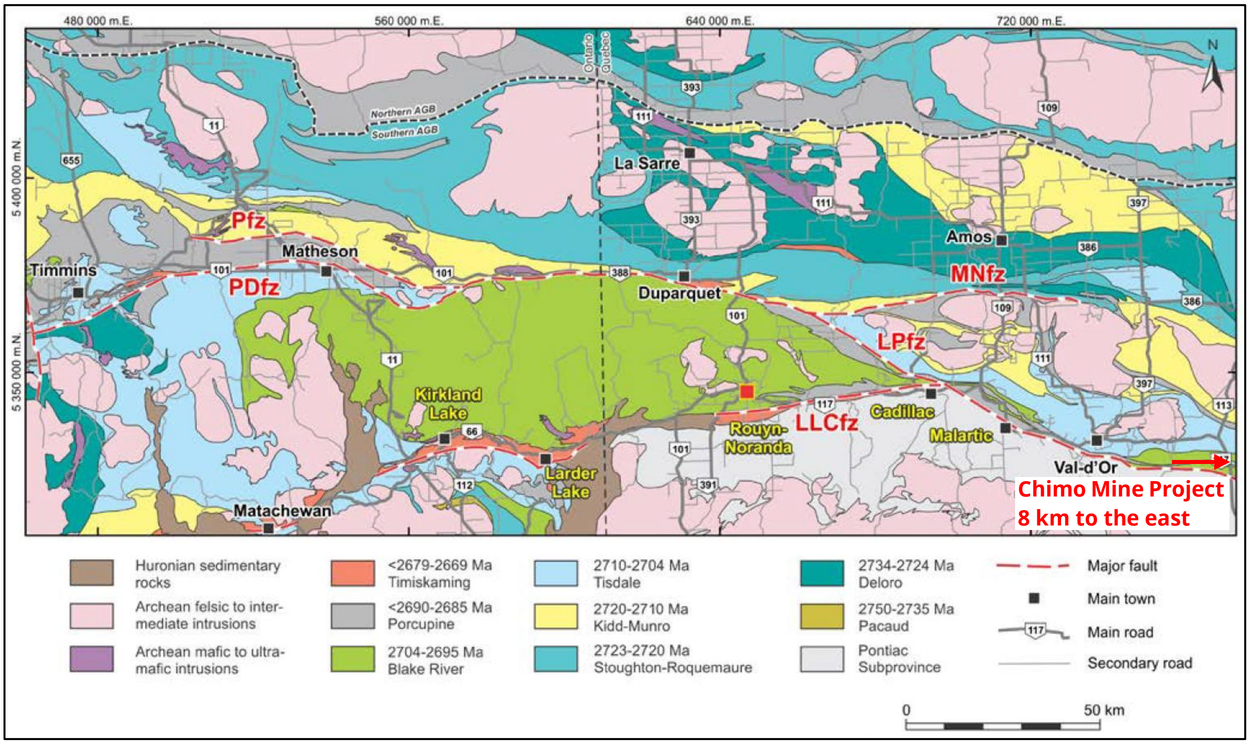


Figure 7-3: Geological map of the southern Abitibi Greenstone Belt (Monecke *et al.*, 2017).

The episodes are listed below from oldest to youngest:

- Pacaud Assemblage (2750-2735 Ma);
- Deloro Assemblage (2734-2724 Ma);
- Stoughton-Roquemaure Assemblage (2723-2720 Ma);
- Kidd-Munro Assemblage (2720-2710 Ma);
- Tisdale Assemblage (2710-2704 Ma);
- Blake River Assemblage (2704-2695 Ma);
- Porcupine Assemblage (<2690-2685 Ma); and
- Timiskaming Assemblage (<2679-2669 Ma).

Three large intrusions are found within the local stratigraphy: 1) the Bourlamaque batholith (Campiglio, 1977), a coarse-grained synvolcanic quartz-diorite intrusive (2700 ±1 Ma) of transitional affinity, which is interpreted to be the magma chamber that fed the Val-d'Or Formation volcanism; 2) the Bevcon pluton, a similar but higher level and more differentiated medium- to fine-grained tonalite of transitional affinity; and 3) the East Sullivan stock, a post-kinematic (2684 ±1 Ma) alkaline composite monzonitic stock (Taner, 1996). Numerous calc-alkaline granodioritic-tonalitic intrusives and subconcordant to discordant sill-like intrusions of subvolcanic to post-kinematic origin and a suite of early- to post-kinematic feldspar/quartz-feldspar/porphyry dykes occur throughout the region.

The Chimo Mine Property is close to the contact of the CLLDZ, which hosts numerous gold deposits and mines that have produced several million ounces of gold. The Kirkland Lake, Rouyn-Noranda, Cadillac, Malartic and Val-d'Or mining camps are all found along this deformation zone.

## 7.2 Local Geology

The following descriptions were taken in part from Sauvé *et al.* (1988), Rocheleau *et al.* (1997) and Moorhead *et al.* (2000).

The Property is located in the Southern Volcanic Zone of the Abitibi Subprovince. The northern part of the Property is transected by a structure that may represent a branch of the CLLDZ.

No outcrops are present on the Property (Figure 7-4). According to Racine (1989) and Rocheleau *et al.* (1997), the Property is underlain by volcano-sedimentary rocks of the Trivio Complex. The Trivio Complex is a structural complex enclosing lenticular bands of sedimentary rocks and mafic volcanic rocks in sheared contact with each other; stratigraphic correlations are not possible.

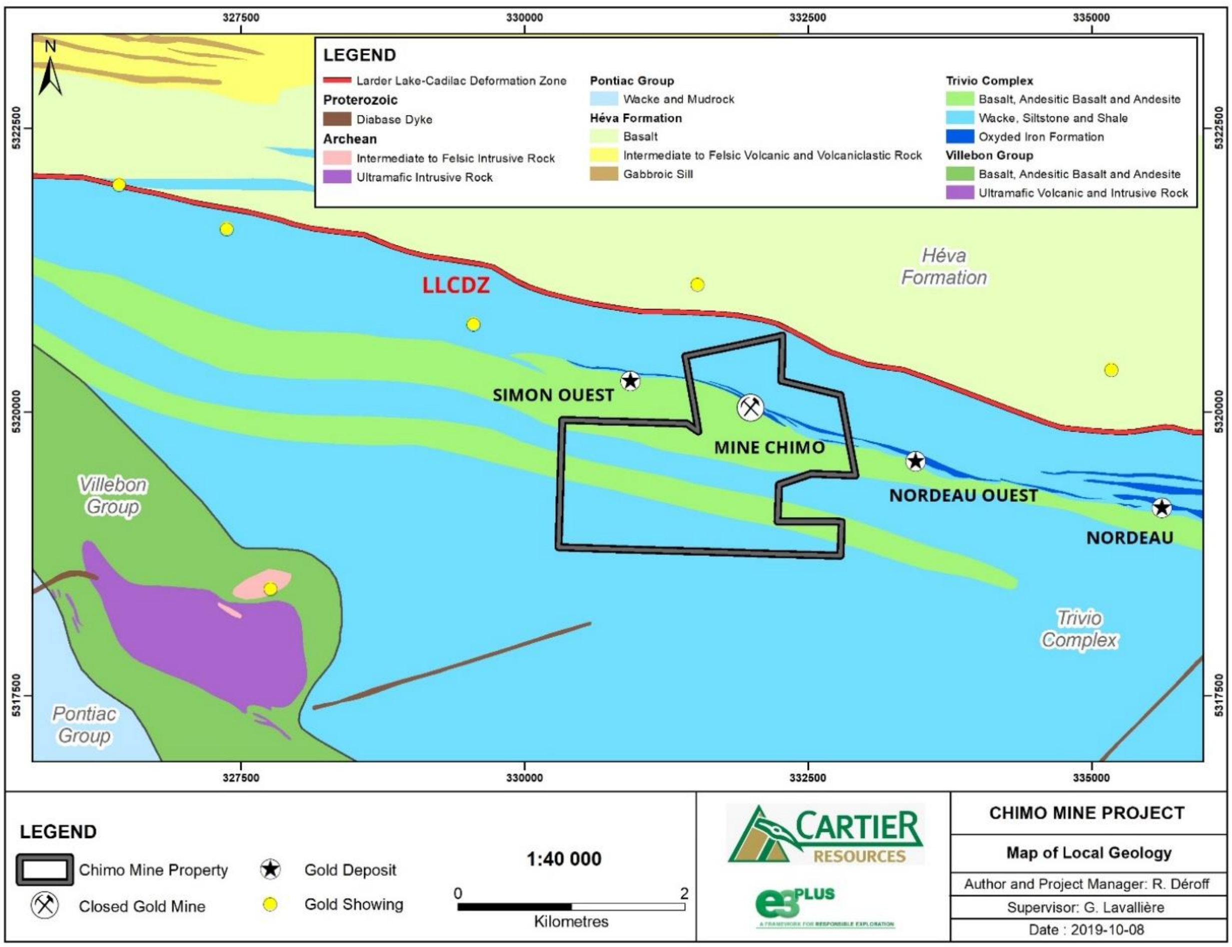


Figure 7-4: Map of the local geology of the Chimo Mine Property.

Sedimentary rocks form a rhythmic sequence of proximal turbidites, composed of fine quartzofeldspathic sandstone and siltstone, interbedded with magnetite iron formation, coarse feldspathic sandstone and minor polymictic conglomerate.

Volcanic rocks form two main belts (northern and southern) and consist mainly of basaltic and andesitic flows with massive, pillowed and more rarely brecciated facies (Racine 1989; Rocheleau *et al.*, 1997). Layers of volcanoclastic and exhalative rocks interdigitate with sedimentary rocks, indicating that volcanism was active during sedimentation.

### 7.2.1 Sedimentary bands

The most common sedimentary facies is a rhythmic sequence of beds of fine quartzofeldspathic sandstone and siltstone of varying thickness, 5 to 10 cm on average, often showing normal grading, alternating with thin interbeds of shale 1 to 5 cm thick. A thin layer of parallel laminae is observed at the top of some beds. In thin section, the sandstone is composed of rounded fragments of feldspar and quartz. Lithic fragments are rare and, when present, appear restricted to coarser-grained beds. The abundant matrix (30-40%) is completely recrystallized as quartz, muscovite, biotite and chlorite.

A magnetite iron formation can be traced on magnetic maps produced by the federal government and in drill holes over a distance of more than 16 km, from the former Chimo mine to the Lac Matchi-Manitou area (Rocheleau *et al.*, 1988). Magnetite beds are interstratified with sandy pelitic beds displaying graded bedding, and they form a folded band ranging in width from 3 to 70 m in the Chimo mine area. The iron formations are characterized by alternating magnetite-rich millimetric to centimetric laminations, white cherty laminations, and green beds of iron silicates with or without magnetite. Under the microscope, magnetite occurs as small irregular grains 0.05 mm in diameter or as poikiloblastic grains 0.3 mm across. Quartz forms a mosaic of 0.05 mm grains and is likely recrystallized chert (Sauvé *et al.*, 1987). Iron silicates include grunerite, ferrohornblende, chlorite and some biotite. Slightly manganiferous almandine garnet was documented in the southern iron formation in the Chimo mine (Sauvé *et al.*, 1987).

A secondary sandy facies consists of coarse feldspathic and conglomeratic (2 to 4 mm) sandstone, chloritized and quartz-poor (<5%). On outcrop, the beds have an average thickness of 15 to 30 cm. The boundaries between the beds are not very sharp. These sandstones are generally massive with no sedimentary structures. Thin interbeds of shale break the monotony of this sequence. In thin section, the coarse sandstone is made up of fragments of plagioclase (albite) in a matrix similar to that of the sandstone described above. The matrix is recrystalized as chlorite, biotite and quartz, and also contains 3 to 7% carbonate minerals (calcite).

The polymictic conglomerate, characterized by pebbles, cobbles and boulders, is generally strongly deformed and occurs as lenticular beds of variable thickness, either massive or showing graded bedding. The proportions of fragments to matrix are particularly difficult to determine due to the high degree of deformation. However, in less deformed areas, the matrix appears abundant enough to support the fragments. The fragments are composed mainly of volcanic rocks, mainly felsic tuffs and crystal tuffs, intrusive rocks of tonalitic composition, and lesser quantities of pebbles of black chert and mafia volcanic rocks. More rarely, it is possible to identify pebbles of felsic volcanic rocks, sedimentary rocks and fuchsite. The matrix is either sandy or silty and of the same composition as the fine quartzofeldspathic sandstone and siltstone facies. These lenticular conglomerate layers are interpreted as filled submarine channels.

### 7.2.2 Volcanic bands

The mafic and intermediate lavas, mainly basalts and andesites, show massive, pillowed and more rarely brecciated facies. Massive lavas are generally aphanitic, although locally coarse (1 to 2 mm). The pillow lavas are vesicular in places, and the pillows are highly variable in size with very little associated hyaloclastic material. Brecciated lavas are infrequent and generally restricted to thin lenticular horizons. These are usually flow breccias containing fragments of lava rock, relatively abundant (0 to 60%) and small (1 to 5 cm), in a hyaloclastic matrix. Pyroclastics consist of feldspar-rich mafic tuffs: ash tuffs, crystal tuffs, lapilli tuffs and agglomerates. In the vicinity of the Chimo mine, some levels are particularly rich in graphite. In thin section, the observed mineralogy is similar for all volcanic rocks: the mineral assemblage and textures are essentially metamorphic, the rocks being completely recrystallized. The major constituents are quartz, chlorite, actinolite and epidote (zoisite and clinozoisite). A small amount of biotite and opaque minerals (magnetite, ilmenite and pyrite) are present, along with traces of sphene, leucoxene and tourmaline.

## 7.3 Lithogeochemistry

The following text is taken in part from Moorhead *et al.* (2000).

Mafic lava analyses reveal some samples with high levels of MgO (10.0%, 13.4% and 17.1%), consistent with magnesian basalt compositions (Rocheleau *et al.*, 1997). Basalts and andesites have Zr/Y ratios ranging from 2 to 6, grouped into two trends: the first, with a Zr/Y ratio of 2.5, would be tholeiitic, and the second, less abundant, with a Zr/Y ratio of 5.5 would be transitional. Volcanoclastic rocks have more felsic compositions ($SiO_2$ between 53 and 73%), usually dacitic (Rocheleau *et al.*, 1997). They have Zr/Y ratios ranging from 2 to 12.

According to Racine (1989), the northern volcanic belt of the Trivio Complex is composed mainly of tholeiitic basalts, while the volcanics in the southern band are tholeiitic andesites. Lavas have Zr/Y ratios ranging from 2.2 to 5.5; the vast majority of the analyzed lava samples have ratios less than 4, clearly indicating their tholeiitic affinity. The lavas of the two belts form the same linear trend on a Zr-Y diagram, indicating that they are probably comagmatic (Racine, 1989).

## 7.4 Hydrothermal Alteration

The following text is taken in part from Plouffe (1990).

At the former Chimo mine, mineralized zones and their margins (wallrocks) are characterized by hydrothermal alteration that manifests in different ways depending on the lithology:

- Silicification took place in sedimentary host rocks where iron formations were present. Silicification, typically accompanied by chloritization and biotization, is limited to the immediate wallrock in mineralized areas;
- Carbonatization affects a much larger volume of rock in volcanic or pyroclastic lithologies. Primarily characterized by calcite, chlorite may also be present;
- Tourmalinization affects all the zones, but its distribution is very irregular. It can be found locally along the margins of mineralized veins; and

- Sulphidation manifests as pyrrhotite and coarse arsenopyrite in veins, as semi-massive horizons, or as disseminations in quartz veins and along vein walls. Arsenopyrite replaces pyrite and pyrrhotite.

## 7.5 MINERALIZATION

The Chimo mine produced 379,012 ounces of gold (MERN DV 85-05 to DV-97-01) from three producers between 1964 and 1997. The following is taken in part from Sauvé *et al.* (1988) and Plouffe (1990). Mineralization on the Property consists of five main lenses (zones 1 to 3 and 5 to 6; Figures 7-5 and 7-6).

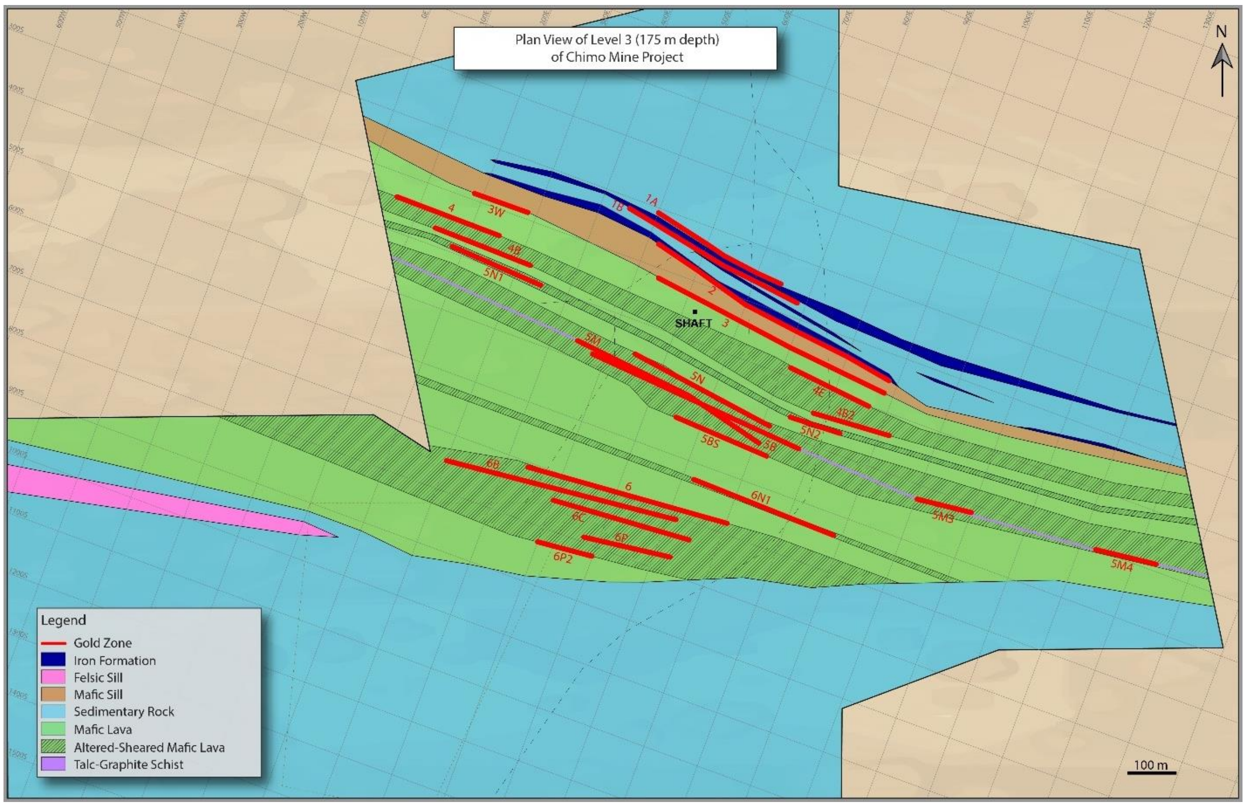


Figure 7-5: Plan view of level 3 (depth of 175 m) showing the mineralized areas of the Chimo Mine Property (before the reinterpretation of 2019).

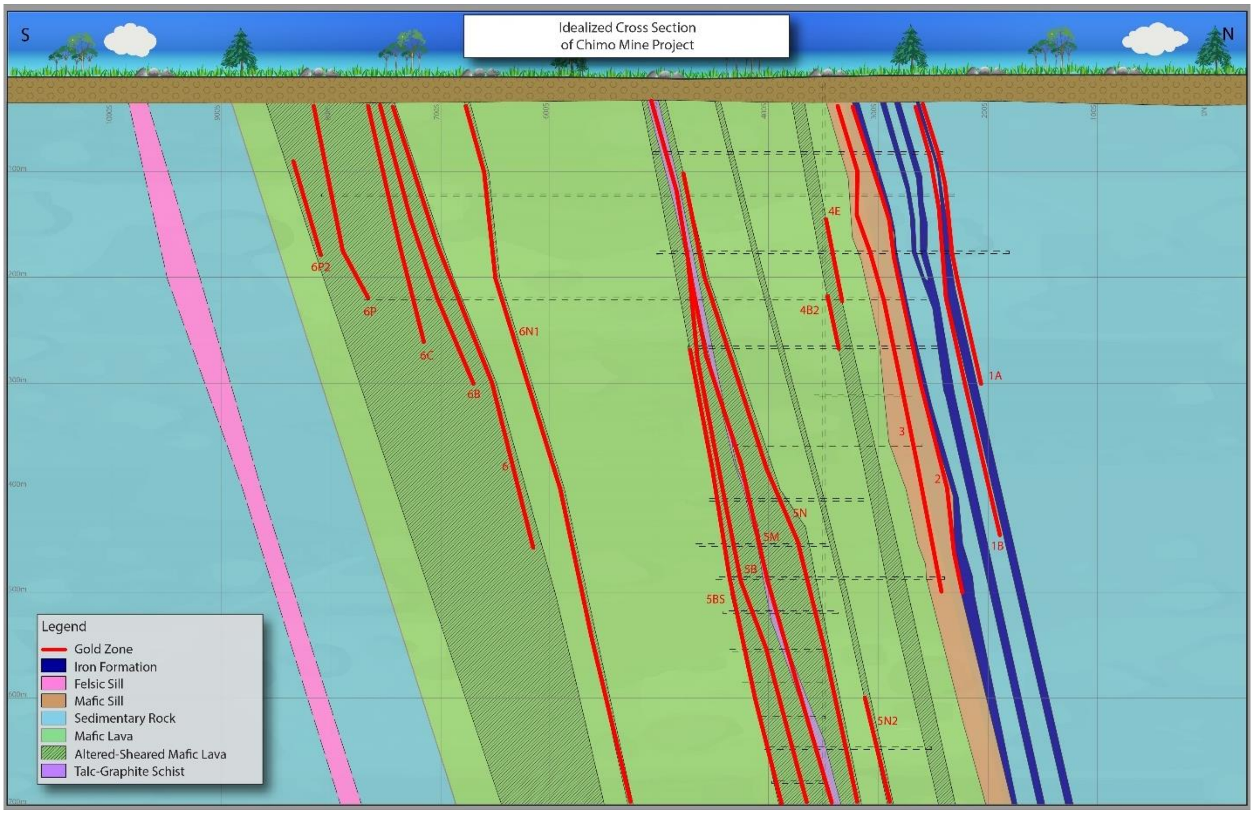


Figure 7-6: Idealized cross-section (looking west) of the mineralized zones on the Chimo Mine Property (before the reinterpretation of 2019).

Zone 1 generally follows the northernmost iron formation. Mineralization consists mainly of a juxtaposition of centimetric to decimetric veinlets of coarse arsenopyrite. Semi-massive layers of pyrrhotite with minor pyrite are sometimes present, but these latter sulphide minerals are almost barren if not accompanied by arsenopyrite. Lenses or veins of white quartz are found along the margins of uneconomic sulphidized areas. Arsenopyrite veins are sometimes deformed into small tight folds and occasionally intersect the bedding at a low angle.

Zone 2 roughly follows the contact between the southernmost iron level and a mafic intrusion. Sulphide minerals are found in a brownish-coloured area rich in biotite. Pyrrhotite and coarse arsenopyrite define thick ribbons parallel to schistosity. The margins of mineralized areas consist of finely ribboned pyrrhotite or disseminated arsenopyrite. Bluish quartz forms irregular lenses and veins and contains visible gold, but few sulphides.

Zone 3 is located along the southern contact of the schistose and carbonatized mafic intrusion. Mineralization consists, on average, of 3 to 5% disseminated sulphides and multiple veins of bluish quartz showing good continuity. The veins show ribboning that may include layers of wallrock containing disseminated sulphides. Sulphides consist mainly of fine arsenopyrite with lesser pyrrhotite and small amounts of pyrite and chalcopyrite. Quartz veins contain a lot of visible gold, especially near their borders, but few sulphides.

Zone 5 lies within a schistose and carbonatized greyish lava and includes thin units of graphitic schist. The sheared zone may have followed a thin layer of tuff, but deformation and alteration extended into the surrounding volcanics. In the upper parts of level 5, the main type of mineralization is a large concordant lens of black quartz intersected by numerous graphitic veins. Sulphide content is low, but visible gold is present. At each end, the lens may terminate abruptly against graphitic schist. Elsewhere, the lens splits into parallel quartz veins that locally intersect with each other or intersect schistosity. These multiple digitations or veins give the impression that the wide lens formed gradually by accretion in a dilating zone. The rock encasing the lens of graphitic quartz contains many quartz veins and veinlets that contain only small amounts of arsenopyrite, although greater concentrations are found along the selvages. These veins of quartz and arsenopyrite do not contain graphite. They yield good gold grades but are narrow and lenticular. In the lower parts of level 5, the graphitic quartz lens disappears and gives way to graphite-free quartz veins with borders of disseminated arsenopyrite.

Zone 6 is similar in many ways to Zone 5. It consists of several subparallel *en echelon* gold-bearing lenses. These lenses are composed of sheared and carbonatized rock of volcanic and pyroclastic origin, injected with multiple lenticular quartz veins. Disseminated arsenopyrite, pyrrhotite and pyrite occur within the veins and along the vein walls. Free gold is found in quartz veins and as scattered fine grains in the selvages, or as inclusions in arsenopyrite. Layers of graphitic schist occur in the eastern part of the zone.

Gold appears to be the last metal phase in the mineralized zones of the former Chimo mine. It is preferentially associated with arsenopyrite and some of the quartz veins.

The layers of semi-massive coarse arsenopyrite have consistently elevated gold grades; however, when arsenopyrite is disseminated, the grade is much lower. Massive pyrrhotite and pyrite have negligible gold grades when arsenopyrite is absent.

Quartz veins bordered by disseminated arsenopyrite have good gold grades. Visible gold is present within the veins and along the vein walls. Veins devoid of arsenopyrite have negligible gold grades, with the exception of the graphitic quartz veins that contain visible gold.

Based on the nature of the host rock in the Chimo mine, the mineralized zones have been divided into two types of lode deposits: semi-massive sulphide veins associated with iron formations (zones 1 and 2), and lenticular quartz veins associated with altered volcanic rocks mineralized with arsenopyrite (zones 3, 5 and 6).

It is unlikely that these two types of gold mineralization are genetically distinct since they occur together in the Chimo mine. Mineralization is associated with injections of quartz and sulphide minerals into sheared zones at the contacts between lithologies of contrasting competency and chemical composition.

These contacts promoted the development of deformation and micro-porosity in ductile rock and fracturing and brecciation in more competent rock, and thus the circulation of hydrothermal fluids.

## 7.6 METAMORPHISM

The following text is taken in part from Moorhead *et al.* (2000).

In the Trivio Complex, an assemblage of garnet-hornblende-calcite-quartz±biotite is associated with WNW-ESE faults delimiting contrasting blocks (volcanics and sediments) and marks areas with a strong gradient. The northern zone contains metasomatic lenses rich in pyrrhotite, with low gold and copper grades. These lenses are oriented N260° to N280°, with dips from 62° to 75° to the north. Their thickness ranges from 0.5 to 3.0 m. The southern zone extends along the axis of the former Chimo mine and the Nordeau showing, and it corresponds to the contact between volcanic rock and an iron formation. In this area with economic gold concentrations, the garnet-hornblende-calcite-quartz assemblage is accompanied by pyrrhotite, arsenopyrite, chalcopyrite and pyrite.

Berclaz (1993) conducted a mineralogical and geochemical study of the amphibolite- and garnet-rich metasomatized rocks in the volcanic belts of the Trivio Complex. He determined that the volcanic and sedimentary rocks were recrystallized into massive amphibolite and garnetiferous aluminous schist in the high-temperature area of a hydrothermal system with a high geothermal gradient, and is attributed to a hydrothermal episode that took place before the main Kenorean phase of deformation and metamorphism. Pressure-temperature conditions for this high-temperature metasomatic episode are estimated at 600-700 MPa and 500-580°C (Berclaz 1993). This event is characterized by calcic, ferric and aluminous hydrothermal metamorphism, including almandine garnet, calcic amphibole, calcic plagioclase, biotite, chlorite and pyrrhotite (Berclaz 1993).

## 7.7 Structure

The following text is taken in part from Rocheleau *et al.* (1997) and Moorhead *et al.* (2000).

The Trivio Complex forms a structural discontinuity and represents an area of strong deformation that transects less deformed areas. This lithotectonic domain is characterized by the presence of anastomosing deformation corridors (shear zones and/or brittle faults) of variable widths (metric, decametric and even hectometric), which restrict the structural blocks to hectometric and kilometric size. Deformation intensity (flattening and stretching of geological materials) is relatively low in the centre of the structural blocks but increases significantly as it approaches the deformation corridors where rocks are completely mylonitized. The change from less deformed rocks into mylonites is either gradual (over tens of metres) or sharp (over a few metres).

Regardless of the width of the deformation corridors, all the structural elements (folds, schistosities, lineations, etc.) increase in intensity in the mylonitic zones and are transposed, in some cases forming tectonic layering. The rock changes into chlorite-carbonate schist or amphibolite. Schistosity and shear planes, usually E-W with a steep dip to the north or south, are defined by the alignment of phyllosilicates, mainly biotite and chlorite, and amphiboles. As shown by Racine (1989) for the CLLDZ, schistosity sometimes forms at a low angle to the shear, revealing a dextral component of strike-slip movement at surface. Stretching lineations are generally well developed and always steep, plunging to the east or west.

Within the less deformed structural blocks of these tectonic zones, regional E-W folds can be traced for several kilometres. These folds were mapped in the sedimentary and volcanic rocks of the Trivio Complex.

Two main features reflecting changes in Archean deformation have been documented on the Property:

- Regional pre-deformation phase: characterized by early, isoclinal, very localized folds. The S1 schistosity is difficult to recognize due to overprinting by the regional D2 deformation. Observed only locally in sedimentary rocks and pyroclastics, never in lavas, S1 forms an angle of 10° to 15° with the S2 schistosity (Racine, 1989).

- Regional deformation phase: responsible for the E-W-oriented tectonic grain, major F2 folds and dominant S2 schistosity. Interpreted as flow cleavage, it represents a much stronger structural event than the previous phase of Archean deformation. It is characterized by very tight, isoclinal, generally E-W trending mesoscopic folds, with a variable plunge of 30° to 70° generally towards the NE. Shears, subparallel to the axial planes of the mesoscopic folds, are considered contemporaneous with this phase of deformation. S2 schistosity is subparallel to the axial planes of most mesoscopic F2 folds, and also to the E-W shears and the planes of flattening affecting geological features (pillows, vesicles, clasts and crystals). Microscopically, this foliation is expressed as the preferential alignment of all minerals in the rock, particularly minerals such as chlorite, sericite, biotite and some amphiboles.

### 7.8 Stratigraphic Relationships

The following text is taken in part from Moorhead *et al.* (2000).

No U-Pb isotopic dating has been performed on the sedimentary rocks of the Trivio Complex. However, the complex is comparable to other predominantly sedimentary lithotectonic domains in the southern part of the Abitibi Subprovince, to the west of the Property. Detrital zircons from these sequences have been dated by the U-Pb method, yielding maximum ages. These sedimentary sequences include the Kewagama Group (<2687 Ma; Davis, 1991), the Cadillac Group (<2688 Ma; Davis, 1991) and the Pontiac Group (<2688 Ma; Davis, 1991). Further west, the Trivio Complex is in mapping continuity with the Pontiac Group. The age of the Trivio sediments should be comparable to that of the Pontiac.

The volcanic rocks of the Trivio Complex form lenticular bands within a structural complex dominated by sedimentary rocks. Where they have been documented, contacts between volcanics and the encasing sedimentary rocks are sheared (Rocheleau *et al.*, 1997). There does not appear to be any stratigraphic relationship between sedimentary and volcanic rocks. If the Trivio volcanic rocks are allochthonous vis-à-vis the sedimentary rocks, they may have originated in the adjacent volcanic sequences and been imbricated by the thrust faults affecting the Trivio sedimentary assemblage. Mafic volcanics are composed mainly of basalts and andesites of tholeiitic affinity and, to a lesser extent, basalts and andesites of transitional affinity. These tholeiitic lavas are similar to those in the lower part of the Val-d'Or Formation or the Jacola Formation. The presence of magnesian basalts, locally intercalated with bands of Trivio mafic lava (Rocheleau *et al.*, 1997), supports the hypothesis that a portion of the tholeiitic mafic lavas may correlate with the Jacola Formation. Basalts and andesites with transitional affinities are similar to the mafic lavas of the Val-d'Or Formation. Intermediate to felsic volcaniclastics have transitional to calcalkaline affinities and may correlate with the intermediate to felsic volcaniclastics of the Val-d'Or Formation.

In summary, it is plausible that the lenticular bands of volcanic rocks in the Trivio Complex represent sections of the Val-d'Or Formation or, to a lesser extent, the Jacola Formation, which has been thrust southward and imbricated into the Trivio Complex sedimentary assemblage during compressional deformation.

To the west of Lac Trivio, the sheared basaltic and ultramafic lavas of the Piché Group encompass the CLLDZ, at the contact between the sedimentary Cadillac and Pontiac groups. If the same hypothesis used for the lava horizons in the Trivio Complex is applied to the Piché Group, the latter's mafic and ultramafic lavas would represent structural slices of ultramafic-mafic volcanic units from the Val-d'Or Formation, and possibly the Jacola, Dubuisson or La Motte-Vassan formations, thrust southwards and imbricated into the deformed sedimentary units.

## 8 DEPOSIT TYPES

The following description is taken from Langton *et al.* (2019) unless specified otherwise.

Archean orogenic gold deposits are generally defined as structurally controlled vein or shear margin deposits emplaced epigenetically in all lithologies occurring in Archean volcano-plutonic belts (Groves *et al.*, 1998). These gold concentrations are the result of relatively homogeneous hydrothermal fluid flows of variable origin, including metamorphic devolatilization, felsic plutonism and mantle fluids (Hagemann and Cassidy, 2000).

Orogenic gold deposits are emplaced along active convergent margins during compressive tectonic regimes (Groves *et al.*, 1998). This type of setting promotes the flow of hydrothermal fluids along major dislocation zones, which serve as structural traps for gold that precipitates out of solution. The importance of these structures is very clear in the Abitibi, where the vast majority of mines are located within 5 km of major structural discontinuities; however, relatively few deposits are situated at the heart of the main conduits (Eisenlohr *et al.*, 1989, Groves *et al.*, 1998; Robert, 1990), but are preferentially deposited along second- and third-order structures of the regional fracture/shear network, in close proximity to the large-scale compressive structures.

Structural control is predominant at both the mesoscopic and macroscopic scales of mineralization. The brittle to ductile nature of the structural controls is expressed in a wide variety of styles, including (a) brittle faults in ductile shear zones indicating low to high-angle reverse movement, strike-slip or oblique movement; (b) networks of fractures, stockworks or brecciated zones in competent rocks; (c) foliated zones; and, (d) fold hinges in ductile turbidite and iron formation sequences (Groves *et al.*, 1998).

Orogenic gold deposits exhibit strong hydrothermal alteration with lateral zoning composed of mineral assemblage indicative of proximal to distal alteration. These assemblages composed generally of carbonates (ankerite, dolomite and/or calcite) and sulphides (mainly pyrite, pyrrhotite and arsenopyrite), vary with the type of host rock and crustal depth. Alkaline metasomatism is characterized by sericitization or albitization, or by the formation of fuchsite, biotite, alkaline feldspars and/or by chloritization of mafic minerals. Sulphidation reaches a peak in iron formations and in iron-rich host rocks. Greenschist facies alteration of host rocks implies the addition of significant quantities of $CO_2$, S, K, $H_2O$, $SiO_2$, ±Na and light lithophile elements (Groves *et al.*, 1998).

The Property has geological potential for two main types of orogenic gold deposits: Type I) greenstone-hosted quartz-carbonate vein type (Dubé and Gosselin, 2007); and Type II) BIF-hosted gold mineralization type (Robert *et al.*, 2007).

### 8.1 GOLD DEPOSITS ASSOCIATED WITH QUARTZ-CARBONATE VEINS (TYPE I)

Type I gold deposits comprise structurally controlled gold mineralization in altered high-strain ("shear") zones infilled with quartz or quartz and carbonate veins, parallel with the shear zones, which are most likely to be within the volcanic units. Associated disseminated sulphides include arsenopyrite, pyrite and minor chalcopyrite. Graphitic horizons are common.

The following description is modified from Dubé and Gosselin (2007).

Greenstone-hosted quartz-carbonate vein deposits typically occur in deformed greenstone belts of all ages, especially those with variolitic tholeiitic basalts and ultramafic komatiitic flows that are intruded by intermediate to felsic porphyry intrusions, and sometimes with swarms of albitite or lamprophyre dykes. These deposits are distributed along major compressional to trans-tensional crustal-scale fault zones in deformed greenstone terrains, commonly marking the convergent margins between major lithological boundaries, such as volcano-plutonic and sedimentary domains. The large greenstone-hosted quartz-carbonate vein deposits are commonly spatially associated with fluvio-alluvial conglomerate distributed along major crustal fault zones. This association suggests an empirical time and space relationship between large-scale deposits and regional unconformities.

The greenstone-hosted quartz-carbonate vein deposits are structurally controlled complex epigenetic deposits characterized by simple to complex networks of gold-bearing, laminated quartz-carbonate fault-fill veins. These veins are hosted by moderately to steeply dipping compressional brittle-ductile shear zones and faults with locally associated shallow-dipping extensional veins and hydrothermal breccias. The deposits are hosted by greenschist to locally amphibolite-facies metamorphic rocks of dominantly mafic composition and formed at intermediate depth (5-10 km).

## 8.2 Gold Deposits Associated with Iron Formations (Type II)

Type II gold deposits are hosted in, or spatially associated with, banded iron formations (BIF). Gold mineralization is generally located in silicified lodes with disseminated to semi-massive sulphides (arsenopyrite, pyrrhotite and pyrite) spatially related to the BIF. Secondary quartz veining is commonly associated with this type of mineralization.

The following description is modified from Robert *et al.,* 2007.

The deposits consist mainly of sulphidic replacements of Fe-rich layers in magnetite or silicate-BIF, containing variably-developed quartz veins and veinlets. The intensely mineralized central parts of some deposits consist of nearly continuous wallrock replacements that can obscure their epigenetic character and can lead to ambiguities about the timing of mineralization.

BIF-hosted deposits occur in greenstone belts that are either volcanic dominated or sediment dominated, where they are located stratigraphically near regional volcanic-sedimentary transitions. These deposits may also occur near the edges of large clastic sedimentary basins, in the absence of significant mafic volcanic rocks. Magnetite-BIF is the dominant host in greenschist grade rocks, whereas silicate-BIF prevail in rocks of mid-amphibolite grade or higher.

At the local scale, BIF-hosted deposits are commonly associated with the hinge areas of folds, and with intersections of shear zones and faults. As a consequence, the deposits are commonly stratabound and plunge parallel to their host fold hinge, or to the line of intersection of controlling shear zones with the BIF unit. In greenstone belts, many BIF-hosted deposits also contain concentrations of intermediate to felsic porphyry stocks and dykes.

The best intersections from the various recent and historical drilling campaigns on the Property consistently occur at or near the contacts of the iron formation; however, the mineralized zones are not present along the entire BIF/country rock contact, but rather appear to cross-cut stratigraphy. It is envisioned that a mineralized hydrothermal "front" cross-cut stratigraphy, depositing gold-bearing sulphides at the iron formation horizons. As it is generally accepted that the fluids that precipitated auriferous, shear-zone associated quartz veins in the Larder Lake-Cadillac Deformation Zone were not locally derived, and it is assumed that the close association between iron formation and gold mineralization along the mineralized horizon that transects the Property is the result of a chemical interaction at the iron-rich horizons rather than the existence of primary auriferous iron formation.

The two described gold deposit types, which belong to the Greenstone Vein and Slate Belt "clans" are shown in Figure 8-1 at their inferred crustal level of formation. Although sulphides are associated with the gold mineralization on the Property, the discovery of significant base metal deposits on the Property is not likely, as its geological environment appears to be relatively distal to any paleo-volcanic centre.

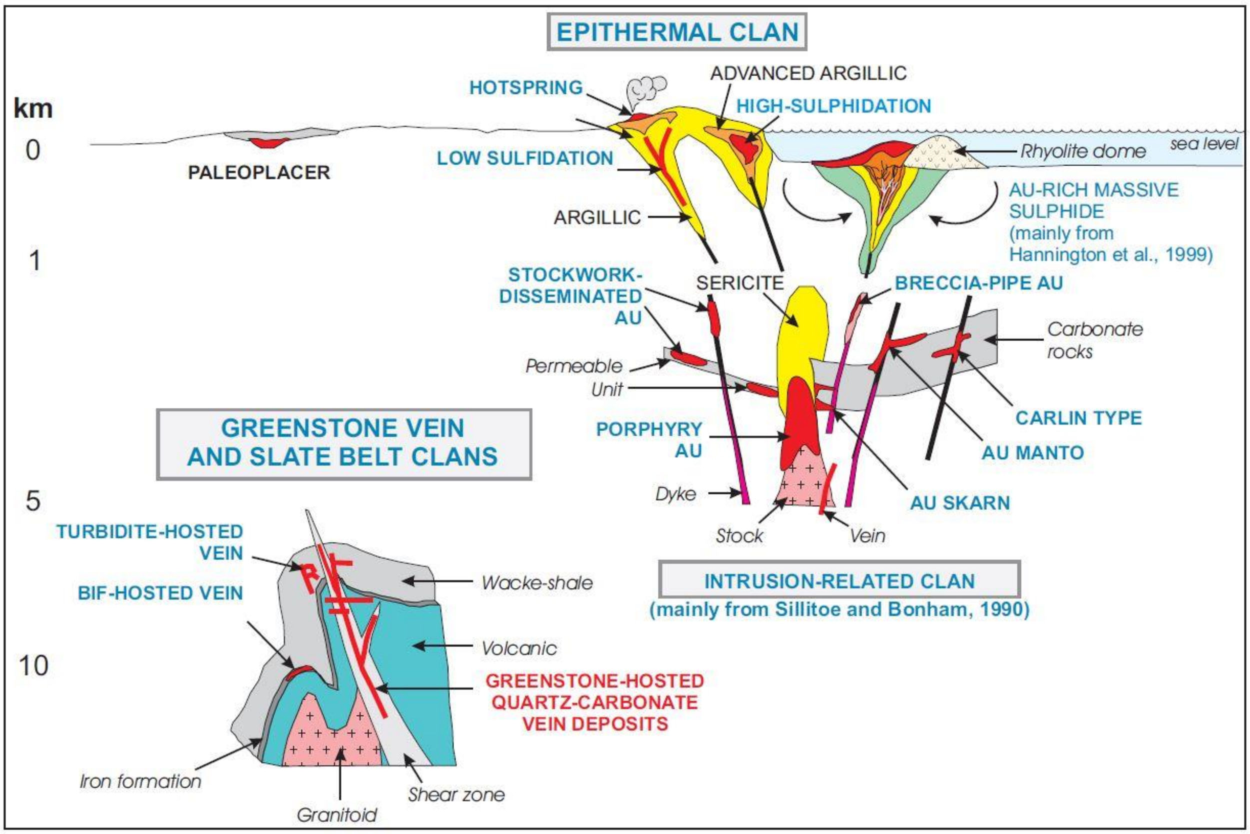


Figure 8-1: Schematic illustration of different types of gold deposits (Dubé *et al.*, 2007).

### 8.3 GOLD MINERALIZATION EAST OF THE VAL-D'OR DISTRICT

The following text is taken in part from Rocheleau *et al.* (1997) and Moorhead *et al.* (2000).

The area to the east of the Val-d'Or district (about 20 km from Val-d'Or) is host to a multitude of mineralized showings, deposits of gold and massive sulphides, and former mines (Louvicourt, LOUVEM, Béliveau, Sigma 2, Monique, Beaufor and Chimo).

The gold deposits have a number of common parameters: epigenetic-type mineralization, dominant structural control, and the physical and chemical behaviour of the host rock affected by variable degrees of extensive metasomatism. Although all stratigraphic units in the region carry gold, there is a frequent association with synvolcanic or at least pre-orogenic intrusions (quartz-feldspar porphyries, dioritic sills and dykes, and the granodioritic Bevcon pluton).

The structural aspect seems common to all deposits: mineralized zones are associated with shears, faults, tension fractures and/or tectonic breccias. Ductile-brittle and brittle deformation appear to be the dominant controls on gold mineralization, as is the case with many other Abitibi Greenstone Belt deposits (Colvine *et al.*, 1988).

The gold potential of metasomatized E-W shear zones has been clearly established in the region (Gaudreau *et al.*, 1986; Rocheleau *et al.*, 1987). These shear zones, in addition to acting as a conduit for hydrothermal fluids, are at the contact between rocks of different competencies and compositions, thus promoting fracturing and gold precipitation. Mineralization is generally found in E-W quartz or quartz-carbonate veins and lenses, generally subparallel to shear zones and the regional S2 schistosity. The walls of the shear zones are sometimes fractured and transformed into mineralized tectonic breccias. In some places, tension fractures (Riedel shears) developed at an angle of 15° to 75° with the shear C planes and are then infilled with subvertical mineralized veins. Another type of mineralized vein, decimetric in size, is also found in generally subhorizontal to shallow dipping tension fractures.

Hydrothermal metamorphism is very evident in the Chimo mine area along the CLLDZ. The information gathered in this area sheds light on the physico-chemical conditions involved in the formation of some epigenetic deposits where mineralizing fluids circulated in high geothermal gradient settings.

## 9 EXPLORATION

In February 2019, Cartier began compiling, interpreting and modelling the mineralized structures on the Property. 3D modelling was carried out using GeoticMine software under the supervision of GéoPointCom. This work improved the geological understanding of the Property. Cartier identified three gold corridors containing 16 gold structures (Table 9-1, Figures 9-1 and 9-2).

| | Gold Corridor | Gold Structure | |
|---|---|---|---|
| | | Number | Name |
| | North | 5 | 1A, 1B, 2, 3 and 4B |
| | Central | 7 | 5B, 5B2, 5C, 5M, 5M2, 5N and 6N1 |
| | South | 4 | 6, 6B, 6P and 6P2 |
| **Total** | **3** | **16** | |

Table 9-1: Summary of the gold corridors and structures on the Chimo Mine Property.

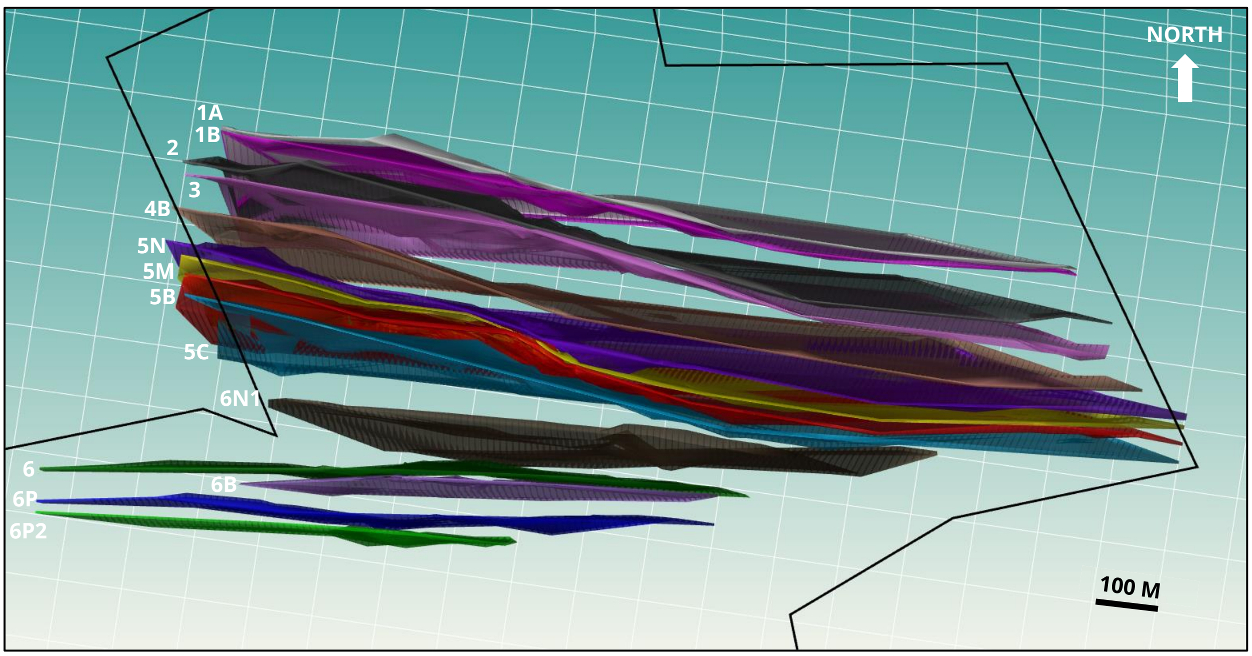


Figure 9-1: Plan view of gold corridors and structures (2019 interpretation).

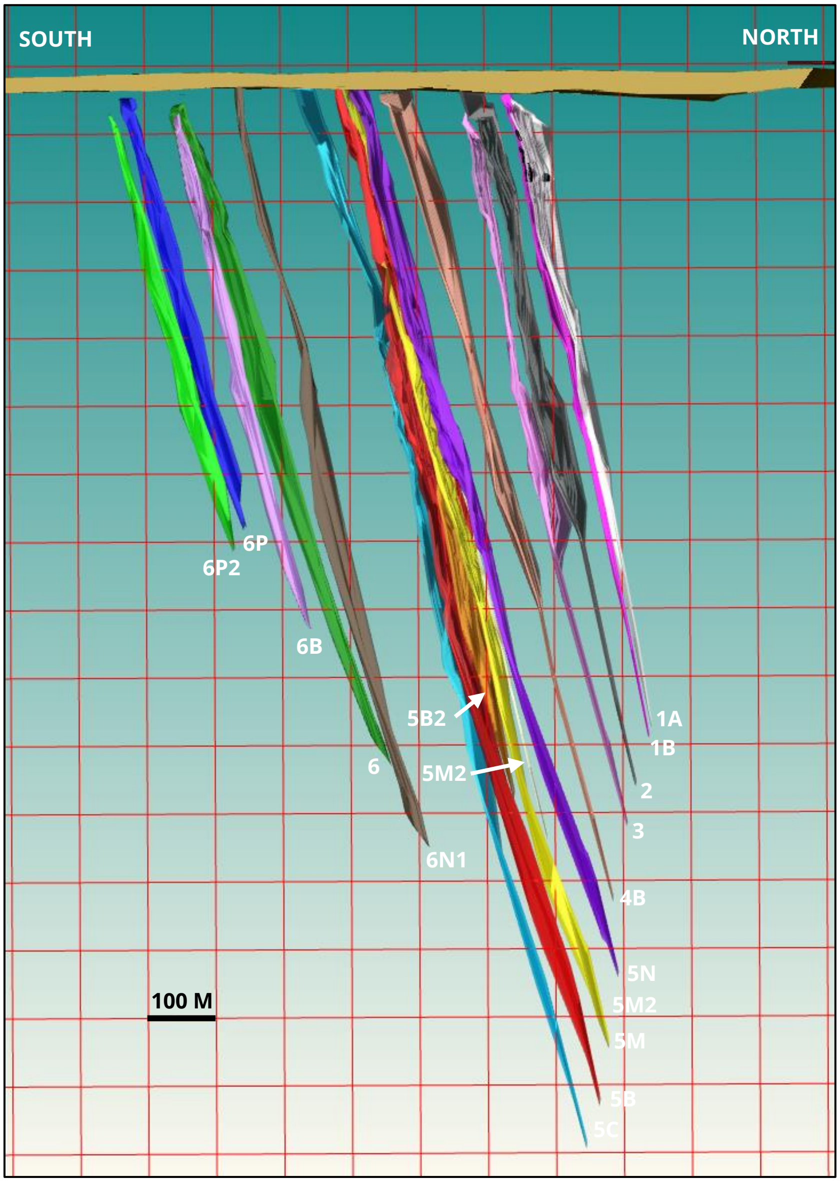


Figure 9-2: Idealized cross section (looking west) of gold corridors and structures (interpretation 2019).

Gold structures were interpreted based on structural, geological and analytical criteria (gold grade):

- Interfaces of wacke/iron formation, wacke/basalt or iron formation/basalt;
- Graphitic marker horizon;
- Sulphides (mainly arsenopyrite);
- Veins and veinlets of smokey and/or milky quartz;
- Alteration (biotite-carbonate);
- Shearing and deformation.

All information related to the 3D model can be found in Item 14.

# 10 DRILLING

## 10.1 Drilling Methodology

### 10.1.1 Drill hole location and positioning

Drilling on the Property has identified a network of fractures oriented roughly N200°/70°, traceable to varying degrees, as well as 16 gold-bearing structures oriented N295°/75° (Figures 9-1 and 9-2) and grouped into three gold corridors (North, Central and South) (Figure 2-1). The N295°/75° gold structures are relatively easy to trace and model across the property using accurate stratigraphic markers. All 25 gold zones on the Property (Figure 2-1) are located along the axes representing the intersections of these two deformation systems. The geometry of the exploration targets is pencil-shaped and plunge -65° toward N320°. These gold zones are semicontinuous over a length of 1.5 km along the intersection axis, as is seen in Zone 5B.

Drilling programs are planned to intersect geometric extensions of gold zones along the intersection axes of the two deformation systems. Information from longitudinal sections (looking north), cross sections (looking west) and plan views is used to increase the accuracy of the intersection angles (as perpendicular as possible to strike and dip). All geomatics operations during the planning stage and when monitoring the drilling every 3, 6 or 9 m were carried out by Cartier using Devisoft software and the Geotic software suite (GeoticLog, GeoticGraph, GeoticCAD and GeoticMine) from the firm Geotic in Val-d’Or.

Drill collars are positioned using three comparable readings taken with a Garmin 60CSx GPSmap (coordinate system: UTM, NAD 83, Zone 18) and then marked with a wooden stake flagged with orange fluorescent tape inscribed with the drill hole number as well as the intended direction and plunge of the hole. A TN 14 Gyrocompass from Reflex Instruments is used to align the drill rig. The gyroscope in this apparatus detects geographical north through its sensitivity to the rotation of the Earth and is therefore not affected by the interference caused by the highly magnetic ground and the drift effect.

Access to some drill sites is afforded by an existing but old network of forestry trails and roads. These were restored to a useable condition to minimize the environmental impact and maximize employee safety. For other sites, new access roads were built. The trees, shrubs and alders growing on the sites and access roads were all shredded by the contractor F. Alarie of Val-d'Or and then used as ground cover.

Since October 2016, when Cartier first started drilling, all HQ, NQ and BQ calibre drilling has been carried out using YS2000 hydraulic rigs supplied by the Orbit Garant Drilling of Val-d’Or; the rigs are enclosed and skid-mounted. The rig and ancillary equipment were transported by a D6 track-type tractor (bulldozer). Water was supplied to the rig by either a submersible pump fed by water from ventilation raises or existing pipes, or a pumping station drawing from streams near the drill site. The rigs operated on two 12-hour shifts, 7 days a week, continuously until the end of the 23-month program. Two hexagonal core barrels and a 36-inch reaming shell were used for almost all the drilling.

Daily production, including demobilization between drill sites, is variable and depends on the type of rock to be drilled, but is generally around 35 m per 12-hour period. The type of target on the Property (the intersection of two planes) requires a high degree of precision. The maximum allowable error was 5 m per 1,500 m.

When the drilling program ended, Cartier closed the drill sites by conducting inspections and collecting any waste left behind after the rig was demobilized. All anchor casings are left in place and secured with bolted steel caps to prevent debris from falling inside, with the exception of abandoned holes. Aluminum tags with the engraved hole number are fixed to the base of the casing as well as to the top of the 2 m rod connected to the steel cap. Drill sites visible from gravel roads are seeded so they can quickly return to their natural state.

#### 10.1.2 Drill hole deviation

Once the drill hole has passed through the overburden, the first measurement is taken 9 m after the bedrock contact, using the EZ-GYRO (Reflex Instruments). If the value corresponds to the desired azimuth and plunge, drilling can continue. However, if this value is considered too far off (azimuth and/or plunge), the hole is pulled out and restarted until the measurement in the bedrock is satisfactory.

Then, deviation tests are carried out every 6 to 9 m down the hole, depending on whether one or two core barrels are used. The closer distances allow anomalies (bad values, incorrect readings, or excessive deviations) to be quickly detected, and corrections applied (reaming shell shortened or lengthened, hexagonal core barrel added or removed, etc.).

Despite all these protocols, it is possible that the hole may not return to the intended trajectory. In such cases, it may be necessary to use Devico's DeviDrill technology, which corrects the hole plunge or azimuth, in order to quickly reposition the hole along its planned trajectory. The maximum recommended deviation is a curve, known as a "DogLeg," of 11° per 3 m (Table 10-1). The correction can be made to the azimuth only, the plunge only, or the azimuth and plunge combined. This technique can be used over a maximum recommended distance of about 30 m to avoid too much pressure, stress or wear on the drill rods, which could lead to cracks, breaks or the loss of the hole. When the DeviDrill is deemed necessary, 3 m tests are carried out to quickly obtain deviation readings and determine the next actions to be taken. Continued coring during the guidance process ensures a complete geological survey. The process leaves nothing in the hole except a bent elbow that can accommodate the drill rods.

| Drill hole plunge (°) | DeviDrill intervention | Azimuth correction (°) | Plunge correction (°) | DeviDrill intervention | Azimuth correction (°) | Plunge correction (°) | DogLeg (°) |
|---|---|---|---|---|---|---|---|
| -45 to -50 | / 3 m | 1.5 | 0.5 | / 30 m | 15.0 | 5.0 | 11 |
| -55 | / 3 m | 1.7 | 0.5 | / 30 m | 17.0 | 5.0 | 11 |
| -60 | / 3 m | 2.0 | 0.5 | / 30 m | 20.0 | 5.0 | 11 |
| -65 | / 3 m | 2.3 | 0.5 | / 30 m | 23.0 | 5.0 | 11 |
| -70 | / 3 m | 2.9 | 0.5 | / 30 m | 29.0 | 5.0 | 11 |
| -75 | / 3 m | 4.0 | 0.5 | / 30 m | 40.0 | 5.0 | 11 |

Table 10-1: Example of curvature during DeviDrill intervention.

At the start of each day or when a DeviDrill intervention is underway, the project geologist collects the readings from the drilling foreman. The deviation data, once filtered and validated, is added to the GeoticLog database. The Cartier's geomatician can generate the drill hole trace and, if necessary, stop the hole to reposition it.

### 10.1.3 Drill core logging

The core is recovered by the wireline technique. It is then removed from the salvage casing by the driller helper and placed in wooden boxes. A wooden block is placed at the end of each 3 m run, or closer if a DeviDrill correction is underway. Once the boxes are filled (the length of core in a box varies depending on the size of the box), they are sealed with metal staples.

Every morning or when the target is intersected, the foreman brings the core boxes to the Cartier core shack in Val-d'Or. If the geologist halts the drilling, he or she brings the boxes to the core shack.

A Cartier employee halts drilling once the hole has passed through the target, with a high level of confidence, by approximately 25 m.

A detailed log of the drill core is documented by experienced and qualified geologists, who are members in good standing of the Order of Geologists of Québec (OGQ). The description of lithological units, as well as alteration, structures, veins and mineralization, are recorded by geologists in the GeoticLog software.

The core boxes are arranged on tables for core logging, in rows of five at a time, for a maximum of 30 boxes. The numbering of the boxes, as well as the markings on the blocks that had been inserted by the driller helper, are checked by geologists to detect any errors in numbering or footage. Then the core is aligned and fitted to eliminate gaps. The footage interval of each box is recorded in the log. Lastly, the core is wetted, and a single photograph is taken of each row of four to five core boxes.

### 10.1.4 RQD measurements and recovery percentage

RQD and the percentage of core recovery are measured in mineralized zones and their wall rocks (over a 5-m core length on each side of the mineralized zone).

RQD (rock quality designation) is a geotechnical parameter that measures the degree of core fracturing. The parameter is expressed as a percentage and represents the competency of the rock. RQD is calculated by measuring each section 10 cm or longer. These sections are summed within each interval of 3 m, the distance between two blocks of wood (i.e., a drilled interval). Thus, an RQD close to 100% means that the rock is very competent with few fractures, whereas an RQD approaching 0% represents a very incompetent and highly fractured rock or even a fault zone.

Core recovery is also calculated as a percentage. Recovery of 100% means that 3 m of core has been placed into the box between the two blocks of wood representing a 3-m run.

### 10.1.5 Core storage

The technician attaches an aluminum dymo-embossed tag to the front of each box with core of interest (characteristic mineralized areas and/or stratigraphy typical of the sector). The technician enters the drill hole number, box number and from-to interval contained in the box. Once the drilling program is over, all boxes of barren core (no significant gold values) or core of no interest to the current drilling objective are placed on securely wrapped and tied wooden pallets and stored outdoors on the premises of MNG Services (near the Val-d'Or airport) temporarily. MNG is free to discard these core boxes at any time and retain the pallets for future use.

Boxes containing core of interest (numbered boxes with aluminum tags) are stacked on other pallets, wrapped, tied and placed in medium- to long-term storage inside the MNG facility. Cartier staff writes (with a permanent black marker) the drill hole ID and/or the pallet number on the pallet in order to quickly track it down if needed for review. The best gold-bearing sections are kept inside Cartier's core shack for quick and easy access as needed (investor visits, assessment by potential third parties, or other work).

## 10.2 Cartier Drilling Program

### 10.2.1 Technical data

Following the acquisition of the Property on August 1, 2013, Cartier initiated the first drilling program on November 1, 2016. Since then, the Company has drilled 109 holes totalling 49,243 m and collected 18,985 samples (Table 10-2 and Figure 10-1). The drilling work was divided into three phases to test the deep geometric extensions of the Property's three gold corridors. The objective was to expand the known gold zones and enhance the discovery potential for new gold zones.

| Phase | Year | Number of holes | Total length (m) | Number of samples collected for gold analysis (excluding QA/QC) | Gold corridor |
|---|---|---|---|---|---|
| 1 | 2016-18 | 72 | 34,332 | 13,776 | North, Central and South |
| 2 | 2018-19 | 33 | 13,248 | 4,502 | North, Central and South |
| 3 | 2019 | 4 | 1,663 | 707 | Central |
| **Total** | **2016-19** | **109** | **49,241** | **18,986** | |

Table 10-2: Summary of drilling by Cartier.

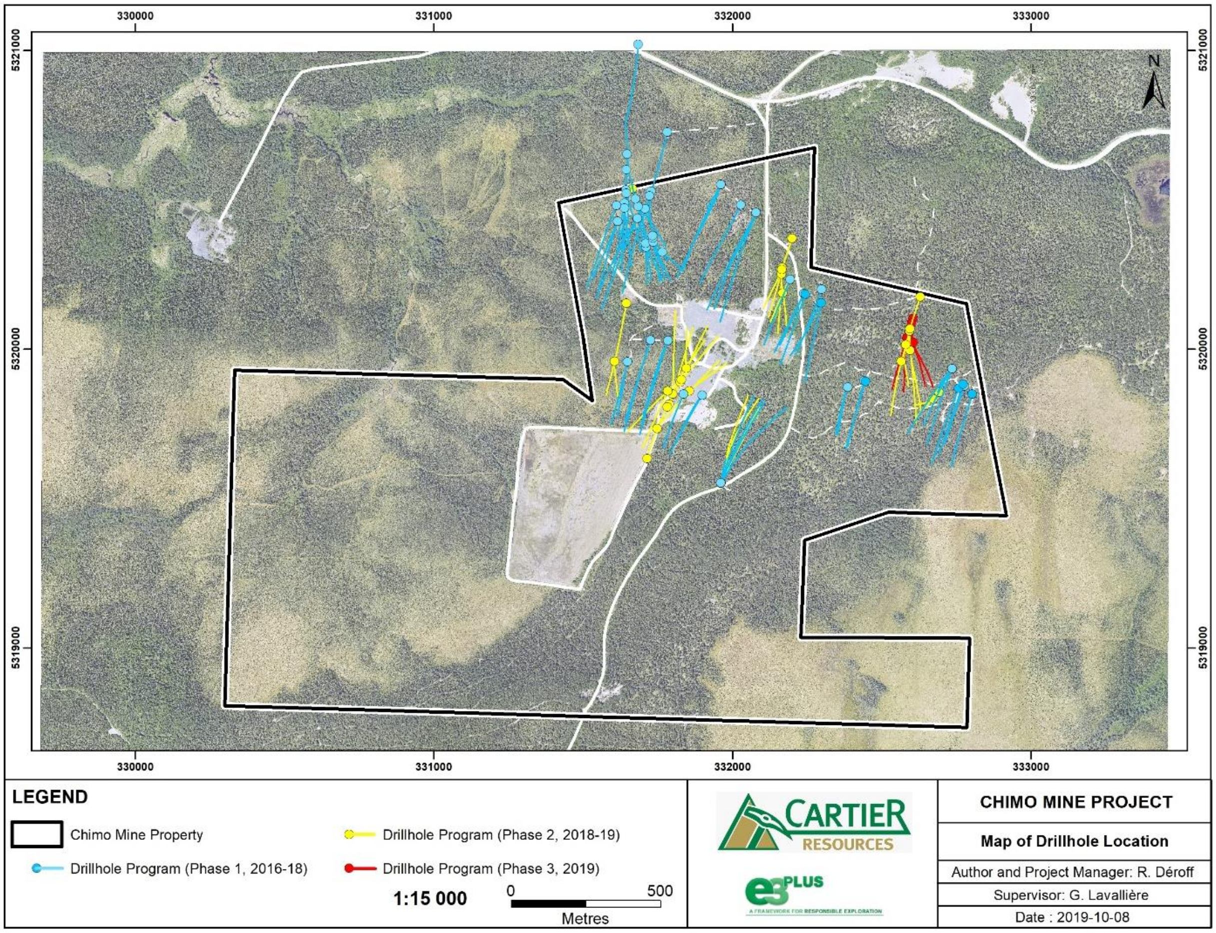


Figure 10-1: Surface map of drill holes on the Chimo Mine Property.

Phase I, which was completed between November 1, 2016, and August 21, 2018, consisted of 72 drill holes totalling 34,332 m (Table 10-3). The goal of this program was twofold. The first objective was to delineate the geometric extensions of zones 2, 2B, 2W, 3, 3W, 3E, 4B and 4B2, between depths of 200 and 700 m (structures 2, 3 and 4B of the North Corridor), zones 5B3, 5B4, 5M3, 5M4, 5NE and 6N1, between depths of 200 and 500 m (structures 5B, 5M, 5N and 6N1 of the Central Corridor) and finally zones 6, 6B, 6P and 6P2, between depths of 300 and 600 m (structures 6, 6B, 6P and 6P2 of the South Corridor). The second objective was to test the geometric extensions of zones 5B, 5B2, 5C, 5M, 5M2 and 5N (structures 5B, 5B2, 5C, 5M, 5M2 and 5N of the Central Corridor) below the old Chimo mine, between depths of 900 and 1,500 m. Combined, holes CH17-46 and CH17-47 amount to 10,113 m.

| Drill hole ID | UTM E (m) | UTM N (m) | Elevation (m) | Azimuth (°) | Plunge (°) | Total length (m) | Start date yyyy/mm/dd | End date yyyy/mm/dd |
|---|---|---|---|---|---|---|---|---|
| CH16-01 | 332245 | 5320185 | 368 | 198 | -60 | 447 | 2016/11/08 | 2016/11/13 |
| CH16-02 | 332198 | 5320156 | 366 | 191 | -61 | 489 | 2016/11/02 | 2016/11/08 |
| CH16-03 | 332447 | 5319893 | 365 | 200 | -52 | 354 | 2016/11/25 | 2016/11/28 |
| CH16-04 | 332758 | 5319870 | 358 | 200 | -51 | 411 | 2016/11/21 | 2016/11/25 |
| CH16-05 | 332774 | 5319884 | 358 | 200 | -59 | 438 | 2016/11/17 | 2016/11/21 |
| CH16-06 | 332804 | 5319851 | 354 | 197 | -50 | 378 | 2016/11/13 | 2016/11/17 |

| Drill hole ID | UTM E (m) | UTM N (m) | Elevation (m) | Azimuth (°) | Plunge (°) | Total length (m) | Start date yyyy/mm/dd | End date yyyy/mm/dd |
|---|---|---|---|---|---|---|---|---|
| CH17-07 | 332387 | 5319874 | 365 | 200 | -75 | 417 | 2017/07/11 | 2017/07/31 |
| CH17-08 | 332442 | 5319894 | 365 | 195 | -64 | 468 | 2017/07/16 | 2017/07/30 |
| CH17-09 | 332387 | 5319874 | 365 | 204 | -77 | 480 | 2017/07/31 | 2017/08/17 |
| CH17-10 | 332736 | 5319936 | 365 | 200 | -59 | 471 | 2017/08/10 | 2017/08/16 |
| CH17-11 | 332736 | 5319936 | 365 | 214 | -67 | 222 | 2017/08/27 | 2017/09/04 |
| CH17-11A | 332736 | 5319936 | 365 | 218 | -65 | 540 | 2017/09/04 | 2017/09/12 |
| CH17-12 | 332736 | 5319936 | 365 | 211 | -74 | 576 | 2017/08/16 | 2017/08/27 |
| CH17-13 | 332777 | 5319878 | 358 | 199 | -70 | 488 | 2017/09/12 | 2017/09/23 |
| CH17-15 | 332194 | 5320234 | 370 | 204 | -74 | 580 | 2017/11/02 | 2017/11/11 |
| CH17-16 | 332240 | 5320187 | 368 | 206 | -69 | 477 | 2017/10/18 | 2017/10/25 |
| CH17-17 | 332240 | 5320187 | 368 | 206 | -74 | 552 | 2017/10/25 | 201711/02 |
| CH17-18 | 332294 | 5320155 | 366 | 206 | -70 | 526 | 2017/09/24 | 2017/10/05 |
| CH17-19 | 332300 | 5320201 | 367 | 202 | -73 | 621 | 2017/10/05 | 2017/10/18 |
| CH17-26 | 332029 | 5320483 | 348 | 211 | -73 | 48 | 2017/12/14 | 2017/12/15 |
| CH17-26A | 332029 | 5320483 | 348 | 211 | -73 | 747 | 2017/12/15 | 2018/01/11 |
| CH17-27 | 332080 | 5320458 | 353 | 201 | -66 | 708 | 2017/11/22 | 2017/12/01 |
| CH17-28 | 332080 | 5320458 | 353 | 205 | -70 | 774 | 2017/11/11 | 2017/11/22 |
| CH17-29 | 332080 | 5320458 | 353 | 204 | -74 | 851 | 2017/12/01 | 2017/12/13 |
| CH17-46 | 331782 | 5320727 | 343 | 192 | -73 | 1186 | 2017/10/20 | 2017/11/17 |
| CH17-46A | 331708 | 5320471 | -298 | 197 | -59 | 552 | 2018/01/13 | 2018/01/31 |
| CH17-46AE | 331711 | 5320342 | -548 | 174 | -66 | 189 | 2018/02/01 | 2018/02/07 |
| CH17-46AE1 | 331710 | 5320355 | -521 | 170 | -63 | 287 | 2018/02/08 | 2018/02/18 |
| CH17-46B | 331728 | 5320529 | -182 | 197 | -65 | 797 | 2018/03/05 | 2018/04/08 |
| CH17-46B1 | 331723 | 5320514 | -214 | 197 | -63 | 258 | 2018/02/18 | 2018/03/01 |
| CH17-46BE | 331736 | 5320359 | -574 | 172 | -71 | 360 | 2018/04/10 | 2018/04/30 |
| CH17-46BE1 | 331734 | 5320373 | -531 | 172 | -72 | 357 | 2018/05/02 | 2018/05/17 |
| CH17-46C | 331734 | 5320381 | -509 | 172 | -72 | 582 | 2018/05/20 | 2018/06/21 |
| CH17-46CW | 331766 | 5320326 | -673 | 135 | -74 | 120 | 2018/06/24 | 2018/07/20 |
| CH17-47 | 331685 | 5321021 | 343 | 182 | -73 | 1551 | 2017/11/20 | 2018/01/23 |
| CH17-47E | 331640 | 5320489 | -753 | 182 | -48 | 282 | 2018/01/30 | 2018/02/12 |
| CH17-47W | 331639 | 5320473 | -770 | 178 | -46 | 271 | 2018/02/12 | 2018/02/27 |
| CH17-47A | 331646 | 5320602 | -608 | 183 | -56 | 570 | 2018/03/01 | 2018/04/02 |
| CH17-47AE | 331644 | 5320534 | -714 | 175 | -63 | 423 | 2018/04/21 | 2018/05/05 |
| CH17-47AW | 331645 | 5320523 | -736 | 175 | -62 | 358 | 2018/04/04 | 2018/04/19 |
| CH17-47B | 331648 | 5320653 | -524 | 177 | -62 | 808 | 2018/05/09 | 2018/06/12 |
| CH17-47BE | 331683 | 5320483 | -928 | 158 | -66 | 332 | 2018/06/14 | 2018/07/13 |
| CH17-47BW | 331685 | 5320478 | -939 | 162 | -65 | 332 | 2018/07/13 | 2018/07/30 |
| CH17-47C | 331676 | 5320504 | -876 | 158 | -68 | 498 | 2018/08/01 | 2018/08/21 |
| CH18-14 | 331962 | 5319553 | 368 | 20 | -50 | 439 | 2018/05/04 | 2018/05/10 |
| CH18-20 | 331962 | 5319553 | 368 | 30 | -55 | 543 | 2018/04/07 | 2018/05/04 |
| CH18-21 | 331962 | 5319553 | 368 | 20 | -61 | 183 | 2018/04/15 | 2018/04/18 |
| CH18-21A | 331962 | 5319553 | 368 | 20 | -55 | 493 | 2018/04/18 | 2018/04/24 |
| CH18-22 | 331962 | 5319553 | 368 | 15 | -58 | 48 | 2018/04/24 | 2018/04/25 |
| CH18-22A | 331962 | 5319553 | 368 | 15 | -58 | 42 | 2018/04/25 | 2018/04/25 |
| CH18-22B | 331962 | 5319553 | 368 | 15 | -58 | 566 | 2018/04/25 | 2018/05/02 |
| CH18-23 | 331962 | 5320552 | 346 | 204 | -75 | 272 | 2018/02/07 | 2018/02/11 |

| Drill hole ID | UTM E (m) | UTM N (m) | Elevation (m) | Azimuth (°) | Plunge (°) | Total length (m) | Start date yyyy/mm/dd | End date yyyy/mm/dd |
|---|---|---|---|---|---|---|---|---|
| CH18-24 | 331962 | 5320552 | 348 | 204 | -80 | 801 | 2018/01/25 | 2018/02/07 |
| CH18-25 | 331962 | 5320552 | 348 | 197 | -73 | 660 | 2018/01/11 | 2018/01/25 |
| CH18-30 | 331899 | 5319847 | 357 | 208 | -65 | 430 | 2018/03/19 | 2018/03/24 |
| CH18-31 | 331837 | 5319851 | 352 | 203 | -76 | 456 | 2018/03/25 | 2018/04/06 |
| CH18-32 | 331899 | 5319847 | 357 | 217 | -77 | 522 | 2018/03/24 | 2018/03/31 |
| CH18-34 | 331649 | 5319959 | 344 | 195 | -74 | 543 | 2018/02/16 | 2018/02/23 |
| CH18-35 | 331649 | 5319959 | 344 | 195 | -81 | 612 | 2018/02/23 | 2018/03/02 |
| CH18-36 | 331727 | 5320031 | 344 | 201 | -63 | 89 | 2018/01/25 | 2018/01/26 |
| CH18-36A | 331727 | 5320031 | 344 | 201 | -64 | 549 | 2018/01/26 | 2018/02/04 |
| CH18-37 | 331727 | 5320031 | 344 | 201 | -73 | 630 | 2018/02/05 | 2018/02/15 |
| CH18-37A | 331727 | 5320031 | 344 | 201 | -73 | 15 | 2018/02/03 | 2018/02/04 |
| CH18-37B | 331727 | 5320031 | 344 | 201 | -73 | 20 | 2018/02/04 | 2018/02/04 |
| CH18-38 | 331785 | 5320030 | 343 | 199 | -66 | 594 | 2018/01/06 | 2018/01/14 |
| CH18-39 | 331785 | 5320030 | 343 | 205 | -73 | 639 | 2018/01/14 | 2018/01/24 |
| CH18-40 | 331613 | 5320482 | 342 | 200 | -76 | 666 | 2018/03/07 | 2018/03/16 |
| CH18-41 | 331616 | 5320429 | 342 | 198 | -67 | 489 | 2018/03/09 | 2018/03/16 |
| CH18-42 | 331616 | 5320429 | 342 | 201 | -73 | 539 | 2018/03/02 | 2018/03/09 |
| CH18-43 | 331682 | 5320439 | 342 | 195 | -64 | 557 | 2018/02/11 | 2018/02/20 |
| CH18-44 | 331682 | 5320439 | 342 | 208 | -74 | 591 | 2018/02/21 | 2018/03/07 |
| CH18-45 | 331962 | 5319553 | 368 | 6 | -59 | 168 | 2018/05/10 | 2018/05/12 |
| **Total (72)** | | | | | | **34,332** | | |

Table 10-3: List of Phase I drill holes on the Chimo Mine Property.

Phase II, which took place between July 26, 2018, and February 26, 2019, consisted of 33 drill holes totalling 13,248 m (Table 10-4). The objective, as before, was to expand the geometry of zones 2B and 3E between depths of 400 and 600 m (structures 2 and 3 of the North Corridor), zones 5B4, 5M4, 5NE and 6N1 between depths of 600 and 1,100 m (structures 5B, 5M, 5N and 6N1 of the Central Corridor), and Zone 6P2 between depths of 300 and 700 m (structure 6P2 of the South Corridor).

| Drill hole ID | UTM E (m) | UTM N (m) | Elevation (m) | Azimuth (°) | Plunge (°) | Total length (m) | Start date yyyy/mm/dd | End date yyyy/mm/dd |
|---|---|---|---|---|---|---|---|---|
| CH17-12A | 332691 | 5319855 | 80 | 204 | -68 | 499 | 2018/11/29 | 2018/12/09 |
| CH17-12AW | 332673 | 5319833 | -27 | 225 | -79 | 246 | 2018/12/09 | 2018/12/17 |
| CH17-47D | 331667 | 5320537 | -789 | 167 | -66 | 126 | 2018/08/22 | 2018/09/09 |
| CH18-33 | 331962 | 5319553 | 368 | 22 | -42 | 233 | 2018/07/26 | 2018/07/29 |
| CH18-33A | 331962 | 5319553 | 368 | 22 | -44 | 363 | 2018/07/31 | 2018/08/05 |
| CH18-48 | 331716 | 5319634 | 349 | 10 | -74 | 1241 | 2018/08/22 | 2018/09/21 |
| CH18-48E | 331826 | 5319890 | -424 | 27 | -60 | 379 | 2018/09/21 | 2018/10/03 |
| CH18-48W | 331830 | 5319898 | -440 | 21 | -60 | 340 | 2018/10/05 | 2018/10/17 |
| CH18-48W1 | 331846 | 5319936 | -512 | 21 | -60 | 42 | 2018/10/17 | 2018/10/20 |
| CH18-48W2 | 331783 | 5319807 | -252 | 30 | -69 | 637 | 2018/10/20 | 2018/11/05 |
| CH18-48A | 331788 | 5319816 | -277 | 24 | -67 | 438 | 2018/11/05 | 2018/11/20 |
| CH18-48AE | 331801 | 5319851 | -344 | 16 | -53 | 316 | 2018/11/20 | 2018/12/05 |
| CH18-48B | 331748 | 5319735 | -34 | 20 | -70 | 531 | 2018/12/06 | 2019/01/12 |
| CH18-48BE | 331857 | 5319861 | -300 | 42 | -53 | 236 | 2019/01/12 | 2019/01/20 |

| Drill hole ID | UTM E (m) | UTM N (m) | Elevation (m) | Azimuth (°) | Plunge (°) | Total length (m) | Start date yyyy/mm/dd | End date yyyy/mm/dd |
|---|---|---|---|---|---|---|---|---|
| CH18-49 | 332736 | 5319936 | 365 | 225 | -82 | 87 | 2018/11/25 | 2018/11/28 |
| CH18-52 | 332630 | 5320176 | 375 | 198 | -79 | 1043 | 2018/09/11 | 2018/10/01 |
| CH18-52E | 332566 | 5319960 | -302 | 192 | -62 | 45 | 2018/10/01 | 2018/10/04 |
| CH18-52E1 | 332581 | 5320015 | -187 | 194 | -65 | 268 | 2018/10/05 | 2018/10/24 |
| CH18-52A | 332594 | 5320062 | -77 | 193 | -70 | 113 | 2018/10/24 | 2018/10/31 |
| CH18-52A1 | 332596 | 5320070 | -54 | 194 | -71 | 507 | 2018/11/01 | 2018/11/16 |
| CH18-52A1E | 332596 | 5319997 | -181 | 172 | -51 | 275 | 2018/11/16 | 2018/11/24 |
| CH18-56 | 331962 | 5319553 | 368 | 9 | -53 | 545 | 2018/08/05 | 2018/08/13 |
| CH18-57 | 331962 | 5319553 | 368 | 10 | -54 | 483 | 2018/08/13 | 2018/08/21 |
| CH19-50 | 332194 | 5320234 | 370 | 208 | -79 | 512 | 2019/01/07 | 2019/01/17 |
| CH19-50E | 332168 | 5320188 | 140 | 202 | -74 | 261 | 2019/01/17 | 2019/01/23 |
| CH19-51 | 332200 | 5320371 | 370 | 197 | -75 | 651 | 2019/01/24 | 2019/02/04 |
| CH19-51W | 332166 | 5320267 | 47 | 194 | -63 | 276 | 2019/02/05 | 2019/02/11 |
| CH19-51A | 332168 | 5320275 | 63 | 194 | -63 | 360 | 2019/02/11 | 2019/02/19 |
| CH19-51AE | 332165 | 5320253 | 21 | 181 | -59 | 289 | 2019/02/19 | 2019/02/26 |
| CH19-53 | 331784 | 5319861 | 346 | 206 | -59 | 378 | 2019/01/21 | 2019/01/25 |
| CH19-59 | 331784 | 5319861 | 346 | 223 | -66 | 425 | 2019/01/26 | 2019/02/01 |
| CH19-61 | 331645 | 5320154 | 346 | 190 | -75 | 853 | 2019/02/01 | 2019/02/16 |
| CH19-61E | 331606 | 5319959 | -219 | 192 | -65 | 250 | 2019/02/17 | 2019/02/24 |
| **Total (33)** | | | | | | **13,248** | | |

Table 10-4: List of Phase II drill holes on the Chimo Mine Property.

Phase III was conducted from February 28 to May 22, 2019, and consisted of 4 drill holes totalling 1,663 m (Table 10-5). The objective of the program was to test the lateral geometric extensions of zones 5B4, 5M4 and 5NE, at a depth of 750 m (structures 5B, 5M and 5N of the Central Corridor).

| Drill hole ID | UTM E (m) | UTM N (m) | Elevation (m) | Azimuth (°) | Plunge (°) | Total length (m) | Start date yyyy/mm/dd | End date yyyy/mm/dd |
|---|---|---|---|---|---|---|---|---|
| CH18-52B | 332605 | 5320103 | 51 | 195 | -73 | 493 | 2019/02/28 | 2019/03/17 |
| CH18-52BE | 332591 | 5320051 | -105 | 194 | -67 | 316 | 2019/03/18 | 2019/03/28 |
| CH18-52C | 332600 | 5320087 | 0 | 195 | -69 | 512 | 2019/03/28 | 2019/04/17 |
| CH18-52CE | 332607 | 5320023 | -168 | 167 | -67 | 342 | 2019/04/18 | 2019/05/22 |
| **Total (4)** | | | | | | **1,663** | | |

Table 10-5: List of Phase III drill holes on the Chimo Mine Property.

### 10.2.2 Analytical data

The 109 drill holes yielded 18,986 samples for gold assaying. The best gold values are grouped by gold corridor. At this stage of the drilling work, the Central Corridor containing zones 5B, 5M, 5B4, 5NE and 6N1 (structures 5B, 5M, 5N and 6N1) appears to have the best potential for delineating significant gold resources and the most promising for discovering new zones (Figures 10-2, 10-3).

The lengths of the mineralized intersections are expressed as downhole core lengths (apparent thickness). The estimated average true thickness averages about 65% of the apparent thickness.

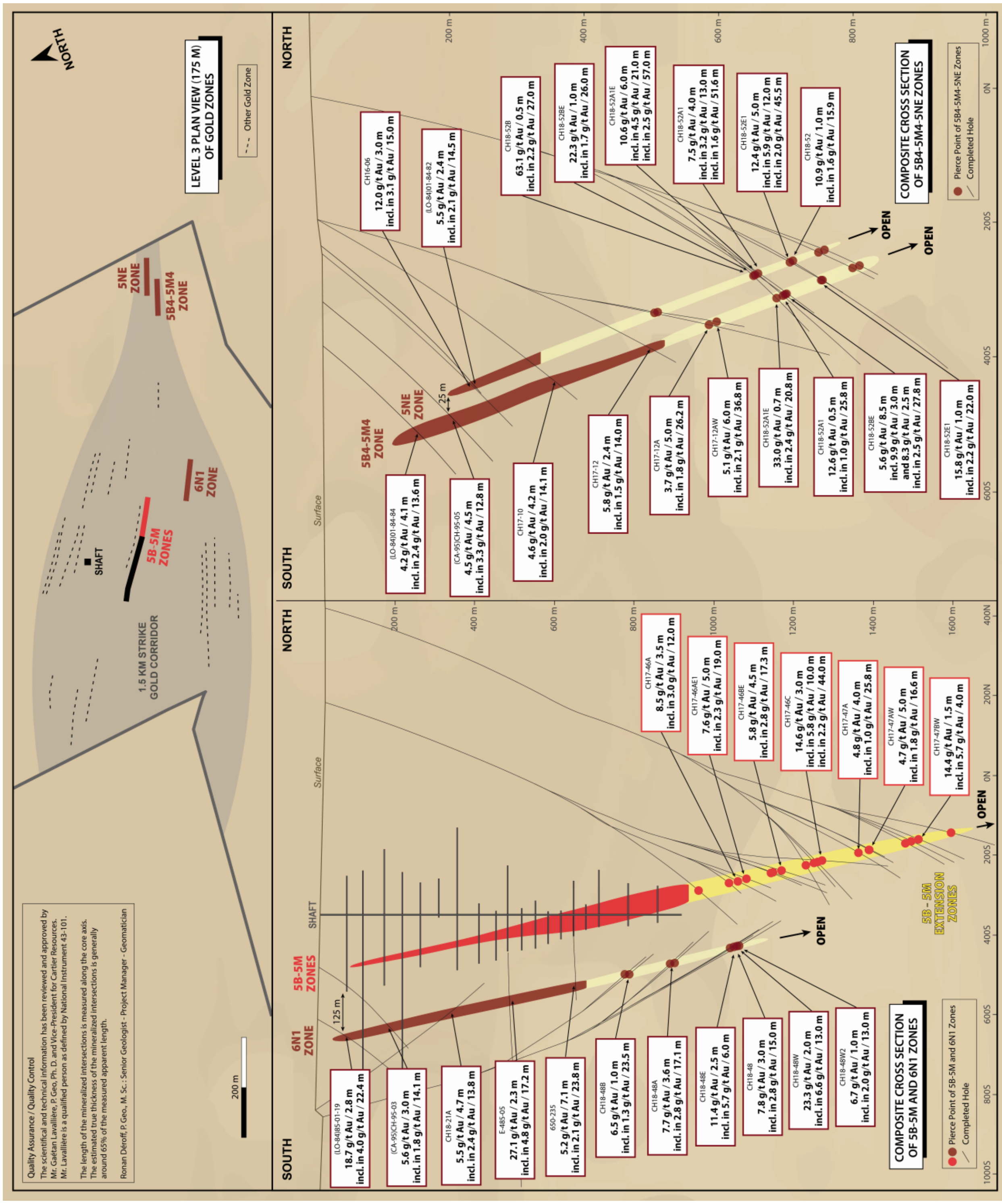


Figure 10-2: Cross section (looking west) of the main gold areas in the Central Corridor.

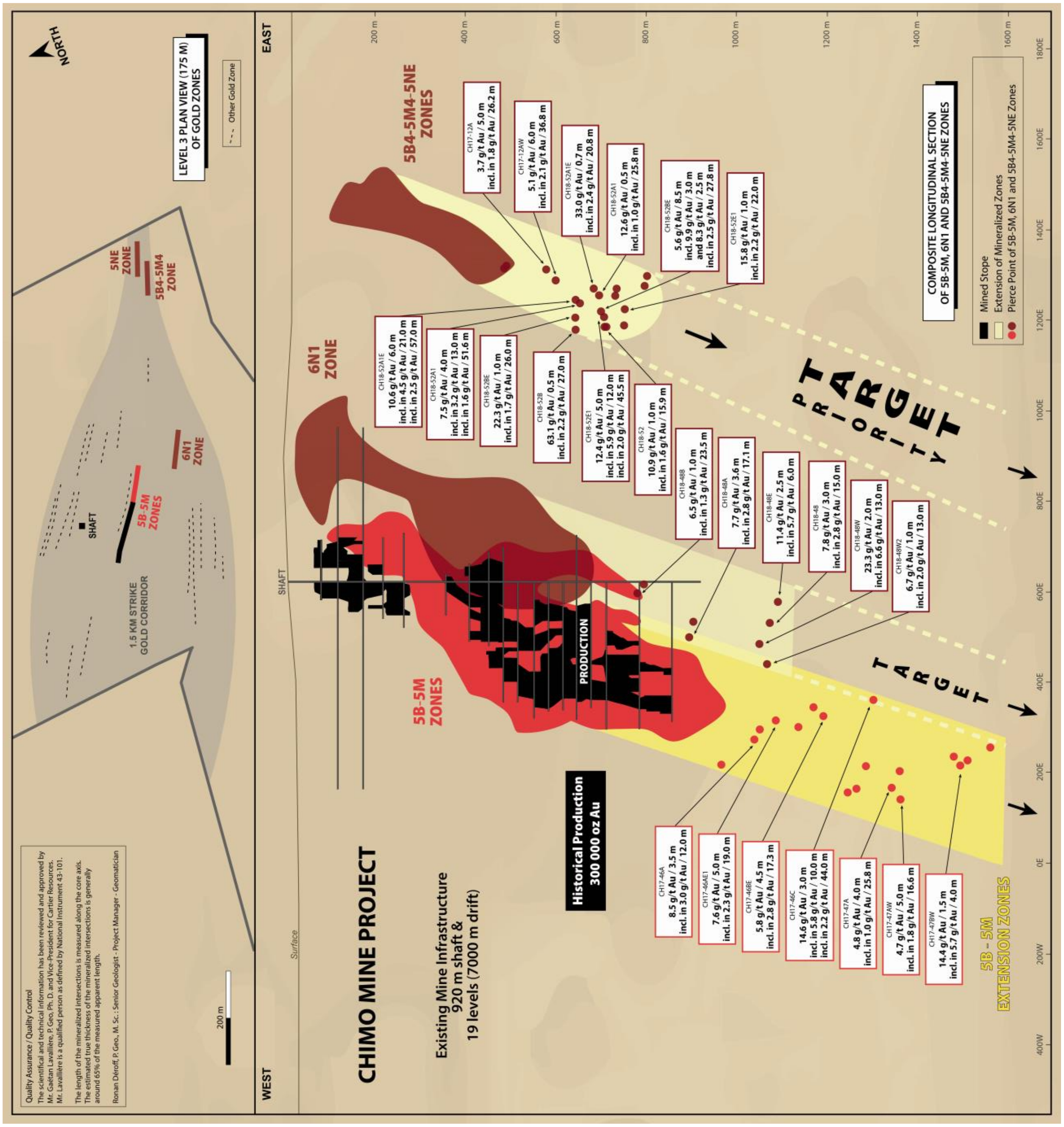


Figure 10-3: Longitudinal section (looking north) of the main gold areas in the Central Corridor.

#### 10.2.2.1 North Gold Corridor

The intersected gold zones of interest are 2B, 3, 3E, and 4B2.

Zone 2B (structure 2)

- 9.4 g/t Au / 6.5 m including 25.2 g/t Au / 2.0 m (CH17-16);
- 8.2 g/t Au / 7.0 m including 25.5 g/t Au / 2.0 m (CH16-01);
- 2.1 g/t Au / 9.8 m including 7.5 g/t Au / 2.0 m (CH17-15).

Zone 3 (structure 3)

- 6.5 g/t Au / 4.0 m including 24.8 g/t Au / 1.0 m (CH17-29).

Zone 3E (structure 3)

- 5.0 g/t Au / 5.1 m including 13.9 g/t Au / 0.7 m (CH19-51AE);
- 5.0 g/t Au / 5.0 m including 11.8 g/t Au / 1.0 m (CH19-50);
- 11.8 g/t Au / 2.0 (CH16-02);
- 2.9 g/t Au / 6.8 m including 7.1 g/t Au / 1.0 m (CH19-51A);
- 3.2 g/t Au / 5.0 m including 11.8 g/t Au / 1.0 m (CH19-51W).

Zone 4B2 (structure 4B)

- 88.6 g/t Au / 1.0 m (CH16-02).

#### 10.2.2.2 Central Gold Zone

The intersected gold zones of interest are 5B, 5B4, 5C, 5M, 5M2, 5N, 5NE and 6N1.

Zone 5B (structure 5B)

- 2.2 g/t Au / 44.0 m including 14.6 g/t Au / 3.0 m (CH17-46C);
- 2.8 g/t Au / 17.3 m including 30.8 g/t Au / 0.6 m (CH17-46BE);
- 1.4 g/t Au / 17.4 m (CH17-46BE1);
- 4.0 g/t Au / 6.0 m including 14.4 g/t Au / 1.5 m (CH17-47BW);
- 1.5 g/t Au / 14.2 m (CH17-46A).

Zone 5B4 (structure 5B)

- 2.1 g/t Au / 36.8 m including 5.5 g/t Au / 5.0 m (CH17-12AW);
- 2.4 g/t Au / 20.8 m including 33.0 g/t Au / 0.7 m (CH18-52A1E);
- 2.2 g/t Au / 22.0 m including 15.8 g/t Au / 1.0 m (CH18-52E1);
- 1.7 g/t Au / 27.6 m including 4.9 g/t Au / 2.0 m (CH17-12A);
- 2.0 g/t Au / 14.1 m including 7.3 g/t Au / 2.2 m (CH17-10);
- 1.0 g/t Au / 25.8 m including 12.6 g/t Au / 0.5 m (CH18-52A);
- 1.5 g/t Au / 14.0 m including 21.0 g/t Au / 0.5 m (CH17-12).

Zone 5C (structure 5C)

- 2.7 g/t Au / 6.0 m including 13.6 g/t Au / 1.0 m (CH17-47E).

Zone 5M (structure 5M)

- 2.5 g/t Au / 17.0 m including 12.2 g/t Au / 2.5 m (CH17-46AE1);
- 1.9 g/t Au / 13.0 m including 3.8 g/t Au / 3.0 m (CH17-29);
- 1.3 g/t Au / 17.4 m including 8.9 g/t Au / 1.0 m (CH17-46B).

Zone 5M2 (structure 5M2)

- 3.9 g/t Au / 8.0 m including 14.6 g/t Au / 2.0 m (CH17-46A);
- 3.2 g/t Au / 8.8 m including 7.2 g/t Au / 2.0 m (CH17-47AW);
- 2.4 g/t Au / 10.0 m including 5.6 g/t Au / 3.0 m (CH17-47A);

- 2.5 g/t Au / 6.3 m including 10.4 g/t Au / 1.0 m (CH17-47BW).

Zone 5N (structure 5N)

- 4.7 g/t Au / 5.1 m including 17.7 g/t Au / 0.5 m (CH17-27).

Zone 5NE (structure 5N)

- 2.5 g/t Au / 57.0 m including 10.6 g/t Au / 6.0 m (CH18-52A1E);
- 2.0 g/t Au / 45.5 m including 12.4 g/t Au / 5.0 m (CH18-52E1);
- 1.6 g/t Au / 51.6 m including 7.5 g/t Au / 4.0 m (CH18-52A1);
- 3.2 g/t Au / 15.0 m including 12.5 g/t Au / 3.0 m (CH16-06);
- 1.6 g/t Au / 15.9 m including 10.9 g/t Au / 1.0 m (CH18-52);
- 0.9 g/t Au / 22.0 m (CH17-12A);
- 0.8 g/t Au / 22.5 m (CH17-12AW).

Zone 6N1 (structure 6N1)

- 6.6 g/t Au / 13.0 m including 23.3 g/t Au / 2.0 m (CH18-48W);
- 2.5 g/t Au / 20.1 m including 7.7 g/t Au / 3.6 m (CH18-48A);
- 2.8 g/t Au / 15.0 m including 7.8 g/t Au / 3.0 m (CH18-48);
- 5.7 g/t Au / 6.0 m including 11.4 g/t Au / 2.5 m (CH18-48E);
- 2.4 g/t Au / 13.9 m including 5.5 g/t Au / 4.7 m (CH18-21A);
- 1.2 g/t Au / 25.5 m including 6.5 g/t Au / 1.0 m (CH18-48B);
- 2.0 g/t Au / 13.9 m including 5.6 g/t Au / 3.0 m (CH18-20);
- 2.0 g/t Au / 13.0 m including 6.7 g/t Au / 1.0 m (CH18-48W2);
- 1.0 g/t Au / 20.0 m including 14.0 g/t Au / 0.5 m (CH19-61).

#### 10.2.2.3 South Gold Corridor

The intersected gold zones of interest are 6, 6B, 6P and 6P2.

Zone 6 (structure 6)

- 1.2 g/t Au / 20.9 m (CH19-59);
- 1.3 g/t Au / 13.5 m including 9.2 g/t Au / 1.5 m (CH18-48);
- 2.1 g/t Au / 8.5 m including 8.8 g/t Au / 2.0 m (CH18-57).

Zone 6B (structure 6B)

- 1.4 g/t Au / 17.0 m including 6.7 g/t Au / 1.0 m (CH19-61E);
- 1.4 g/t Au / 15.0 m including 26.7 g/t Au / 0.5 m (CH19-61);
- 1.0 g/t Au / 17.6 m (CH18-32).

Zone 6P (structure 6P)

- 2.5 g/t Au / 13.3 m including 27.7 g/t Au / 1.0 m (CH18-48W2);
- 5.8 g/t Au / 3.0 m (CH18-35).

Zone 6P2 (structure 6P2)

- 1.3 g/t Au / 23.0 m including 6.0 g/t Au / 3.0 m (CH18-36A);

- 1.0 g/t Au / 22.8 m (CH18-37);
- 1.0 g/t Au / 18.0 m including 8.7 g/t Au / 0.5 m (CH18-39).

# 11 SAMPLE PREPARATION, ANALYSES AND SECURITY

## 11.1 Sampling Procedures, Security and Storage

### 11.1.1 Sampling

Once the core has been logged by the geologist in charge, it is marked with a red grease pencil for metal assaying (gold content). As a general rule, only mineralized zones are sampled, and to be as representative as possible, the sample intervals respect lithological and/or alteration contacts.

The sample length in mineralized zones and wall rocks is 0.5 to 1.0 m (about 66% of the samples collected by Cartier) and 1.5 m outside the mineralized zones (about 34%). Sample intervals are recorded in the drill log, and in the GeoticLog software, as well as in the sample tag notebook. Each page of the notebook is divided into three sections (tags). The first section is for the sampled interval, project name, drill hole number, date and type of analysis required. The second section records the sampled interval and the type of analysis required. Lastly, the third section of the notebook records only the type of analysis required. The first section stays in the notebook, while the other two are detached and placed in the core box at the beginning of each sample. When sawing the sample, the second section is stapled in the bottom of the box and acts as a reference or control, while the third section is placed in the sample bag to be sent to the laboratory.

For lithogeochemical sampling (major elements and trace elements), the core is marked with a blue grease pencil. The length of lithogeochemical samples is always 0.2 m. The rest of the procedure is exactly the same as the metal assay sampling procedure.

Cartier closely monitors the test results sent from the laboratory for evidence of contamination or error in the analytical process. Barren samples (blanks) and certified reference materials (standards) are added to the sample shipments. For each shipment of one hundred (100) samples, no less than five (5) blanks and five (5) standards are included with the core samples.

For verification purposes, Cartier's blanks consist of barren river stone samples purchased from a nursery, as well as certified standards provided by Analytical Solutions Ltd (ASL), a laboratory specializing in the field, whose gold content is very precisely known. These standards arrive in bags, prepared and sealed by ASL, weighing 60 g each.

### 11.1.2 Supervision of protocol conformity monitoring

After the geologist marks the samples, the core boxes are sent to the core sawing room. Sawing is carried out by qualified technicians or day labourers under the supervision of the geologist responsible for the core logging, who is also responsible for overseeing for ensuring that the protocols are followed.

The core is broken into portions that will fit into the rock saw operated by a pneumatic pump. The whole core is then sawn down the long axis along the red line previously been marked by a geologist. The technician is careful not to dislodge the sample label (tag) placed by the geologist at the beginning of each sample. Once the core is completely sawn, one half, along with the third section of the sample tag (the one with only the type of analysis required), is placed in a clear plastic bag on which the technician wrote the sample number beforehand with a permanent marker. The sample number corresponds to the one written on the sample tag by the geologist. The other half of the sawed core is left in the box and can be used as a reference (witness core) if a review is necessary. The second section of the tag is stapled in the bottom of the box and thus marks the beginning of each sample.

The technician then seals the plastic bag with staples, and once seven (7) samples have been sawed, they are placed in a polypropylene bag on which the company name, sample intervals and number of samples are indicated with a permanent black marker.

A shipping form is filled out by the project geologist, providing information on sample numbers, the number of samples, the type of analysis required and the turnaround time (in working days).

For the 2016 Phase I drilling program, a carrier picked up the samples and delivered them to the Accurassay laboratory in Rouyn-Noranda. Samples from the Phase II and III programs (2017-2019) were delivered by the technician to the Techni-Lab (Actlabs) laboratory in Val-d'Or for preparation, and the pulps were then sent to their laboratory in Ste-Germaine-Boulé for analysis.

When the samples are received at one of the laboratories, a laboratory employee verifies the compliance of the shipment and sends the Cartier project geologist a LIMS (Laboratory Information Management System) file that contains a confirmation of the order and the analytical requirements.

### 11.1.3 Storage

Once the results of the tests are received and the final certificate has been signed by the chemist, all pulps sent back by the laboratory are automatically brought to an eco-centre in accordance with municipal regulations on waste disposal. Analytical rejects are also discarded, except those for samples from mineralized (gold-bearing) zones. These rejects are placed on wooden pallets, numbered with a permanent black marker, wrapped, tied and stored indoors at MNG Services for the duration of the project.

## 11.2 Laboratory Preparation Methods and Analytical Procedures

### 11.2.1 Laboratory accreditation and certification

As explained in section 11.1.2, samples from the Phase I drilling program were sent to the Accurassay laboratory in Rouyn-Noranda for sample preparation and analysis, whereas Phase II and III samples were sent to the Techni-Lab (Actlabs) facilities in Val-d'Or for sample preparation and then to Techni-Lab (Actlabs) in Ste-Germaine-Boulé for analysis.

Accurassay and Techni-Lab (Actlabs), both independent of the issuer, are ISO/IEC 17025: 2005 accredited for geochemical analysis. This certification requires proof of quality control covering all aspects of the organization.

All samples are processed through a tracking system (LIMS), which is an integral part of rigorous quality control monitoring. This system uses scannable barcodes to identify each sample received. This allows any given sample to be tracked throughout the preparation and analysis process, which also avoids errors when sample numbers have been manually entered into an Excel file or on the bags.

In 2017, AGAT Laboratories acquired the Accurassay laboratory in Rouyn-Noranda.

### 11.2.2 Accurassay laboratory

The received samples are first dried and then crushed to 85% passing a 10 mesh or less (1.7 mm). A portion of this sample, 250 g, is then pulverized to 85% passing a 200 mesh (74 microns). Only 50 g of this 250 g will be used for the analysis itself (code ALP1). The remaining 200 g are returned as pulp to Cartier's office, along with the reject from the original sample.

The equipment used to crush and pulverize the sample is cleaned with a brush, and a sample of sterile silica is pulverized after each batch of 84 samples or after each highly mineralized sample. Sample preparation stations are also equipped with dust recovery systems to reduce dust levels and the risk of contamination.

A batch of 84 samples includes 72 of Cartier's samples and 12 Accurassay reference materials (blanks, standards and duplicates) as part of the laboratory's internal quality control. If a reference material has an erroneous value or exceeds accepted control limits, an error report is immediately generated. This allows the person in charge to immediately identify the specific batch of analyses related to the problem and correct the situation.

Gold analysis is performed on a 50 g pulp using the fire assay method (ALFA2 code) and measuring the concentration by atomic absorption (AA). Samples with a value between 1.0 and 5.0 g/t Au are re-analyzed by atomic absorption (ALFA2 code) and those with a value greater than 5.0 g/t Au are reanalyzed with a gravity finish (ALFA7 code). For samples containing visible gold, 1,000 g of rock is directly analyzed by the metallic sieve method (code ALPM1). Finally, all samples with a gold content of 1.0 g/t or more are analyzed at least twice.

### 11.2.3 Techni-Lab (Actlabs) laboratory

The received samples are first dried and then crushed. At this stage, more than 80% of the sample has a size of -8 mesh or less (2.36 mm). A 500-g portion of this sample is then pulverized to 90% passing a -200 mesh (0.07 mm). Only 50 g of this 500 g will be used for the analysis itself (code RX-1: 500). The remaining 450 g were returned as pulp to Cartier's office, along with the reject from the original sample.

The equipment used to crush and pulverize the sample is cleaned with a brush, and a sample of sterile silica is pulverized after each batch of 24 samples or after each highly mineralized sample. Sample preparation stations are also equipped with dust recovery systems to reduce dust levels and the risk of contamination.

A batch of 24 samples includes 20 of Cartier's samples and 4 reference materials from Techni-Lab (blanks, standards and duplicates) as part of the laboratory's internal quality control. If a reference material has an erroneous value or exceeds accepted control limits, an error report is immediately generated. This allows the person in charge to immediately identify the specific batch of analyses related to the problem and correct the situation.

Gold analysis is performed on a 50 g pulp using the fire assay method code 1A2-50) and measuring the concentrations by AA. Samples with a value between 1.0 and 5.0 g/t Au are re-analyzed by AA (code 1A2-50), and those with a value greater than 5.0 g/t Au are reanalyzed with a gravity finish (code 1A3-50). For samples containing visible gold, 1,000 g of rock is directly analyzed by the metallic sieve method (code 1A4). Finally, all samples with a gold content of 1.0 g/t or more are analyzed at least twice.

## 11.3 Quality Assurance and Quality Control (QA/QC)

At this stage of the work, Cartier's QA/QC program includes the insertion of one (1) blank and (1) standard for every 20 samples sent to the laboratory. There is no systematic insertion of duplicates, but the analytical protocol ensures that all samples that assay 1.0 g/t or more are re-analyzed at least once and, depending on the result, up to four times. In some cases, the geologist may request a re-analysis if deemed appropriate. In fact, 18% of all duplicate assays show at least one assay of less than 1.0 g/t. In 2017, Cartier selected 31 samples for verification at a second laboratory (AGAT) using rejects. According to the current database, no QA/QC samples were added until 2016. From 2016 to 2019, Cartier analyzed 1,056 blanks, 1,051 CRM standards, 1,506 duplicate pairs on pulps, and 31 duplicate pairs on rejects. As a result, 19% of all samples analyzed during this period were for QA/QC purposes.

According to Cartier's protocol, each certificate of analysis is carefully checked as soon as it is received. The acceptability limit for a blank is three times the detection limit (i.e., 15 ppb Au for Accurassay and 24 ppb Au for Techni-Lab). If a blank returns a value beyond this threshold, the entire batch containing the blank is re-analyzed at no cost to Cartier. However, if a high value precedes the failed blank or if the following analyses do not contain high values a greater tolerance is permitted and the batch does not necessarily require re-analysis. Cartier has a similar protocol for monitoring standards. The acceptability limit is three times the standard deviation. If a standard returns a value beyond this threshold, the entire batch containing the failed standard is re-analyzed at no cost to Cartier. However, if samples that precede or follow the failed standard have not returned an anomalous gold value, re-analysis is not required.

In the data from 2016 to 2019, Cartier identified some anomalies in both blanks and standards, but in each case, the geologist did not consider it appropriate to request re-assays after considering the results before and after the failed QA/QC sample.

By the end of 2016, the high failure rate of standards prompted Cartier to request a meeting with Accurassay managers. Following this meeting, Cartier concluded that a personnel problem was at the root of these analytical errors. This lack of rigour led Cartier to terminate the analytical contract with Accurassay immediately. Following a call for tenders in 2017, Techni-Lab (Actlabs) was selected to prepare and analyze samples for future drilling programs on the Property.

### 11.3.1 Blanks

GéoPointCom has carefully reviewed the analytical results for the 1,056 blanks added by Cartier over the past four years. The acceptability limit was arbitrarily set at five times the detection limit. The best way to visualize these results is by plotting them on a Shewart chart where the X-axis represents the date of the certificates and the Y-axis is the gold content (Figures 11-1 to 11-4). It is often best to use a different chart for each year as laboratory conditions may change from year to year.

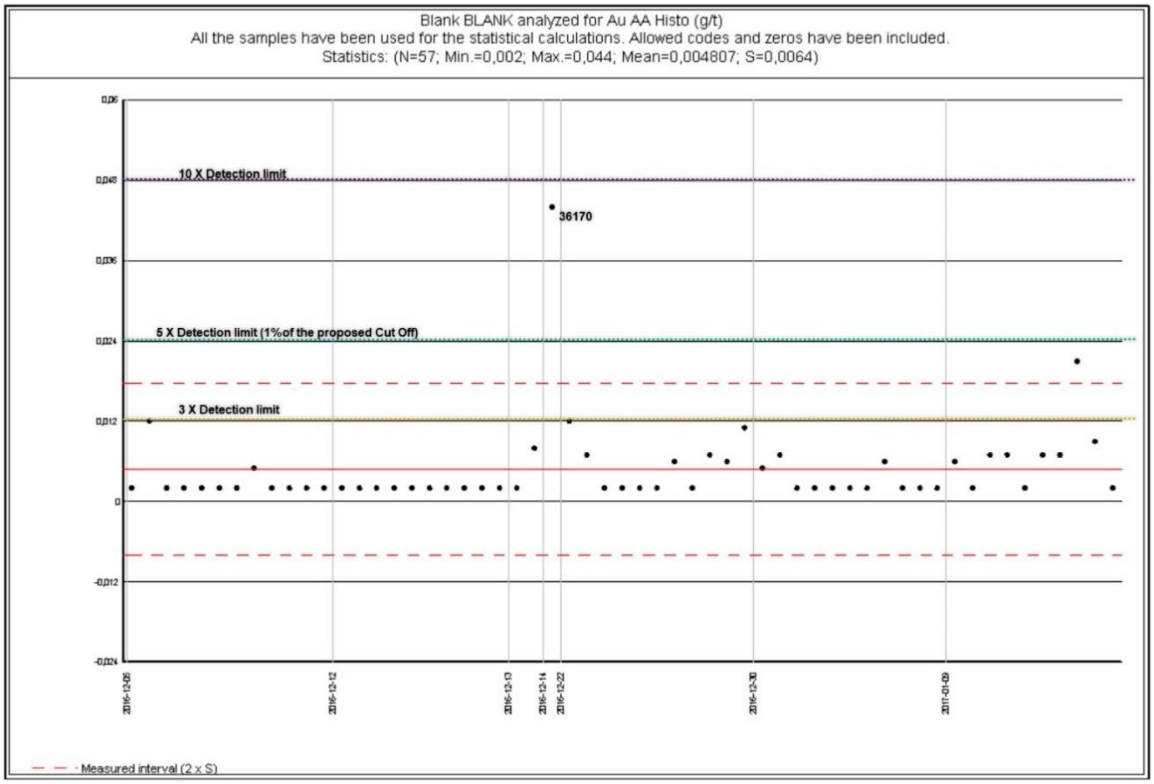


Figure 11-1: Shewart control chart showing gold content in blank material from the 2016 diamond drill holes.

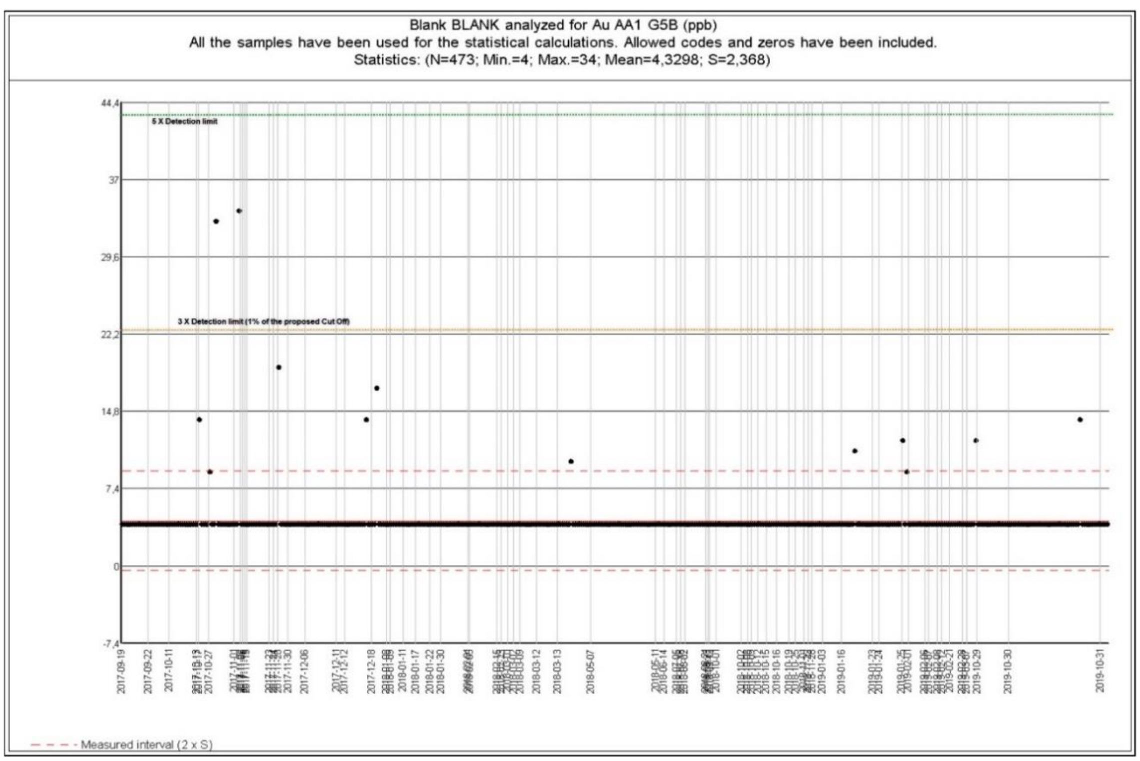


Figure 11-2: Shewart control chart showing gold content in blank material from the 2017 diamond drill holes.

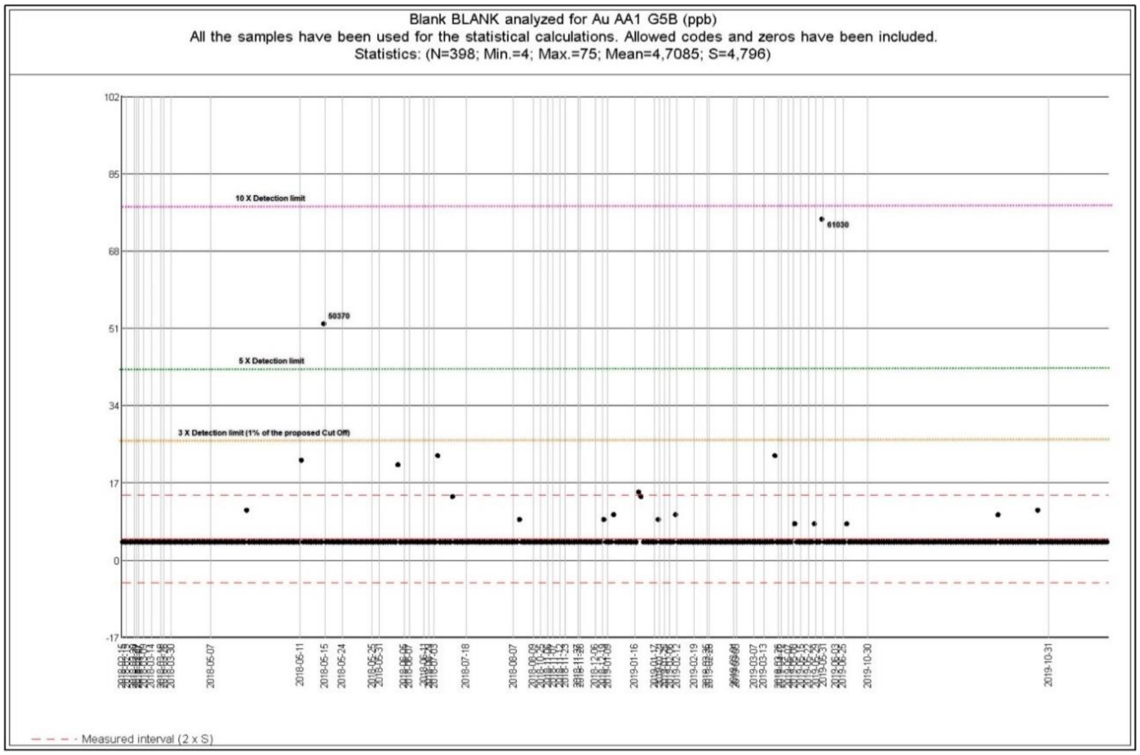


Figure 11-3: Shewart control chart showing gold content in blank material from the 2018 diamond drill holes.

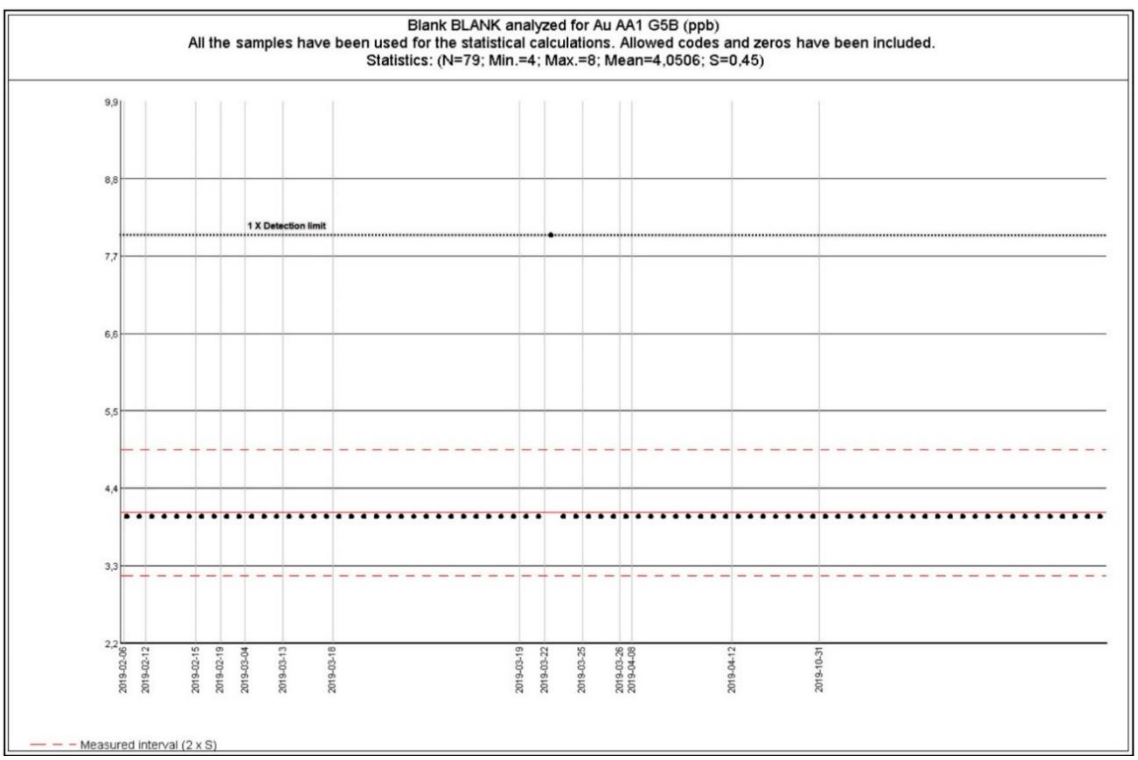


Figure 11-4: Shewart control chart showing gold content in blank material from the 2019 diamond drill holes.

In 2016, sample 36170 (Figure 11-1) was inserted among samples from a mineralized zone. A deficiency in the cleaning procedure can reasonably be claimed. In 2018 (Figure 11-3), however, it is difficult to explain the anomaly of the 50370 sample; a cleaning problem may explain sample 61030 on the same graph as it was included in a batch of samples from a high-grade zone. Given the low number of failures, less than 0.3%, GéoPointCom believes that the cleaning procedures of both laboratories are appropriate and well adapted to the needs of the Project.

### 11.3.2 Standards

GéoPointCom has reviewed in detail the results of analyses for the 1,051 standards added by Cartier over the past four years. Table 11-14 presents the overall results with a 95% confidence level. Standard 62d is the only standard that Accurassay has been able to estimate with a degree of accuracy. Standard 216 was used at both laboratories. Standard 257 is the only standard that Techni-Lab has been unable to estimate with satisfactory accuracy. Standard 257 (Figure 11-13) consists of an oxide matrix. This standard is not designed to be used on samples from a sulphide setting. GéoPointCom recommends that this standard no longer be used to validate the analyses of this Project.

Similar to the blanks, the best way to interpret the results for standards is to plot them in chronological order on Shewart graphs. For a normal distribution, 95% of the samples should be within the range of two standard deviations (±2SD). In other words, for a normal distribution, 5% of the samples will fall outside the ±2SD limit. A review of the ±2SD anomalies reveals that applying this rule would mean 1 in 20 samples should be re-analyzed, which is considered far too strict. Following the same logic, only 3 samples out of 1,000 will have an error greater than ±3SD. For this reason, in general, GéoPointCom considers the following cases questionable and anomalous:

- 1 plotted point at ±3SD;
- 2 consecutive points on the same side of the ±2SD limit;
- 6 consecutive points on the same side of the ±1SD limit;
- 9 consecutive points on the same side of the mean.

Table 11-1 and Figures 11-5 to 11-10 present the results obtained from each of the laboratories and the standards used.

| Laboratory | CRM number | Theoritical average (g/t) | Theoritical Standart Deviation (g/t) | Assayed average (g/t) | Assayed Standart Deviation (g/t) | Number of assay | Pass or Fail (95% confidence) |
|---|---|---|---|---|---|---|---|
| Accurassay | 15d | 1.559 | 0.042 | 1.386 | 0.17 | 18 | Fail |
| Accurassay | 201 | 0.514 | 0.017 | 0.445 | 0.054 | 20 | Fail |
| Accurassay | 209 | 1.58 | 0.044 | 1.455 | 0.166 | 8 | Fail |
| Accurassay | 216 | 6.66 | 0.155 | 6.105 | 0.993 | 8 | Fail |
| Accurassay | 251 | 0.504 | 0.015 | 0.451 | 0.09 | 8 | Fail |
| Accurassay | 62d | 10.5 | 0.33 | 10.058 | 2.118 | 11 | Pass |
| Techni-Lab | 215 | 3.54 | 0.097 | 3.574 | 0.138 | 74 | Pass |
| Techni-Lab | 216 | 6.66 | 0.155 | 6.715 | 0.194 | 253 * | Pass |
| Techni-Lab | 221 | 1.062 | 0.036 | 1.101 | 0.599 | 327 | Pass |
| Techni-Lab | 229 | 12.11 | 0.206 | 12.155 | 0.289 | 262 | Pass |
| Techni-Lab | 257 | 14.18 | 0.264 | 13.675 | 0.947 | 61 | Fail |
| * One sample ignored. | | | | | | | |

Table 11-1: Overall performance for 10 standards used between 2016 and 2019.

The first six figures show the Accurassay results. It must be noted that for each of the six standards used, more than 50% of the points are outside -3SD, which in itself is virtually impossible. On closer inspection, systematic patterns emerge. Figures 11-5 and 11-6 cover the same period. Both start with seven (7) samples relatively close to average, followed by six (6) samples at more than -3SD. The correspondence is disturbing. Similarly, Figures 11-7, 11-8 and 11-9 also cover the same period. Again, the distribution of the three standards displays exactly the same profile. This is likely a temporal drift that can be caused by unstable temperatures or human error. This analysis shows that nearly 30% of the samples analyzed in this period could be underestimated by a factor of 20% to 25%.

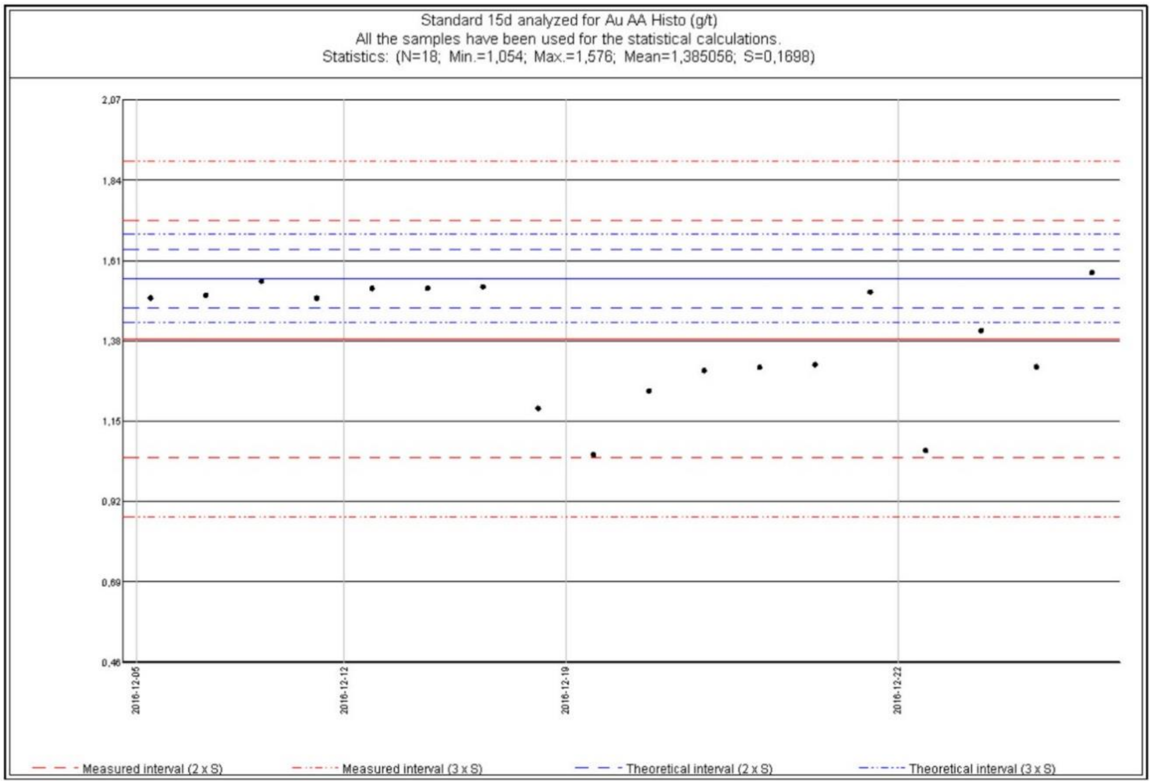


Figure 11-5: Shewart control chart showing gold content in standard 15d assayed at Accurassay.

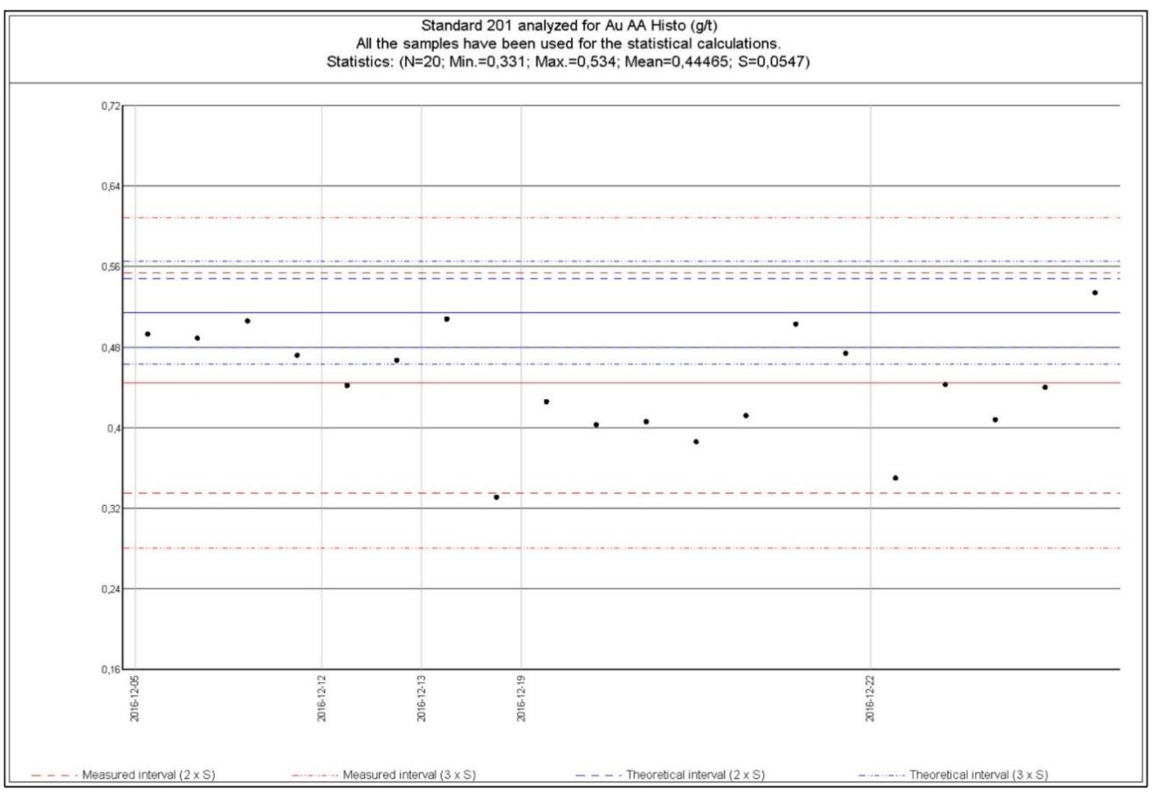


Figure 11-6: Shewart control chart showing gold content in standard 201 assayed at Accurassay.

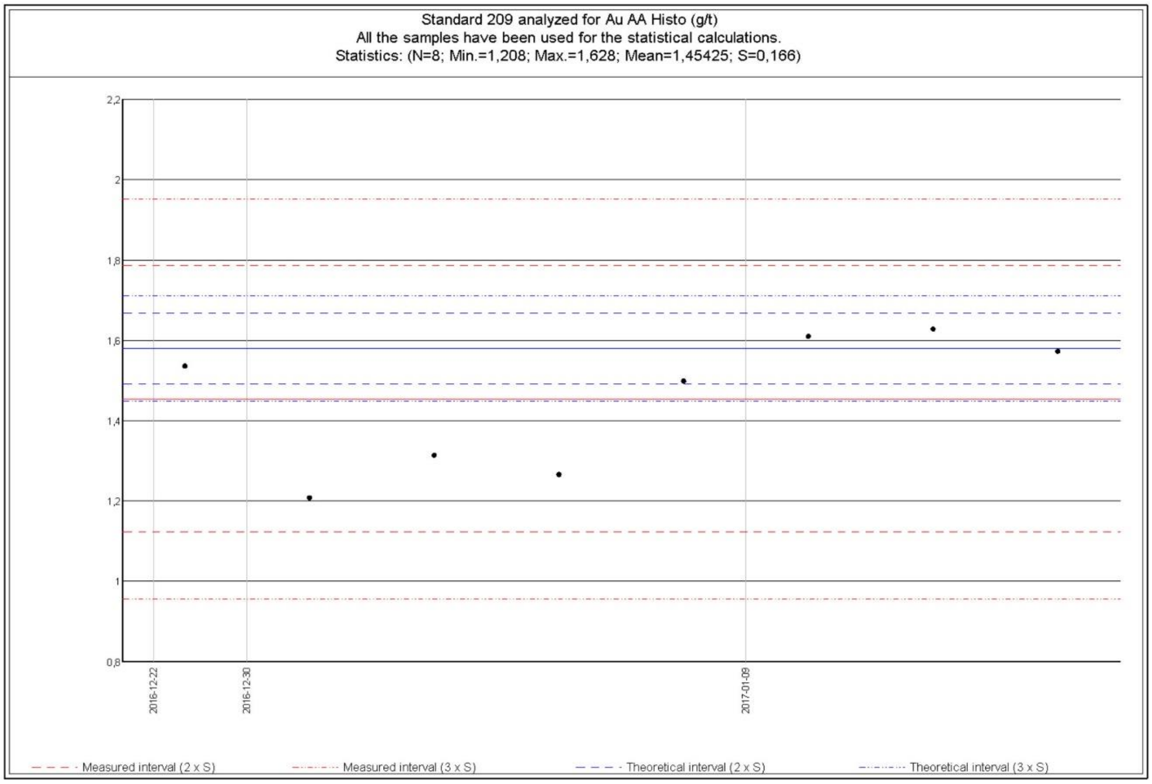


Figure 11-7: Shewart control chart showing gold content in standard 209 assayed at Accurassay.

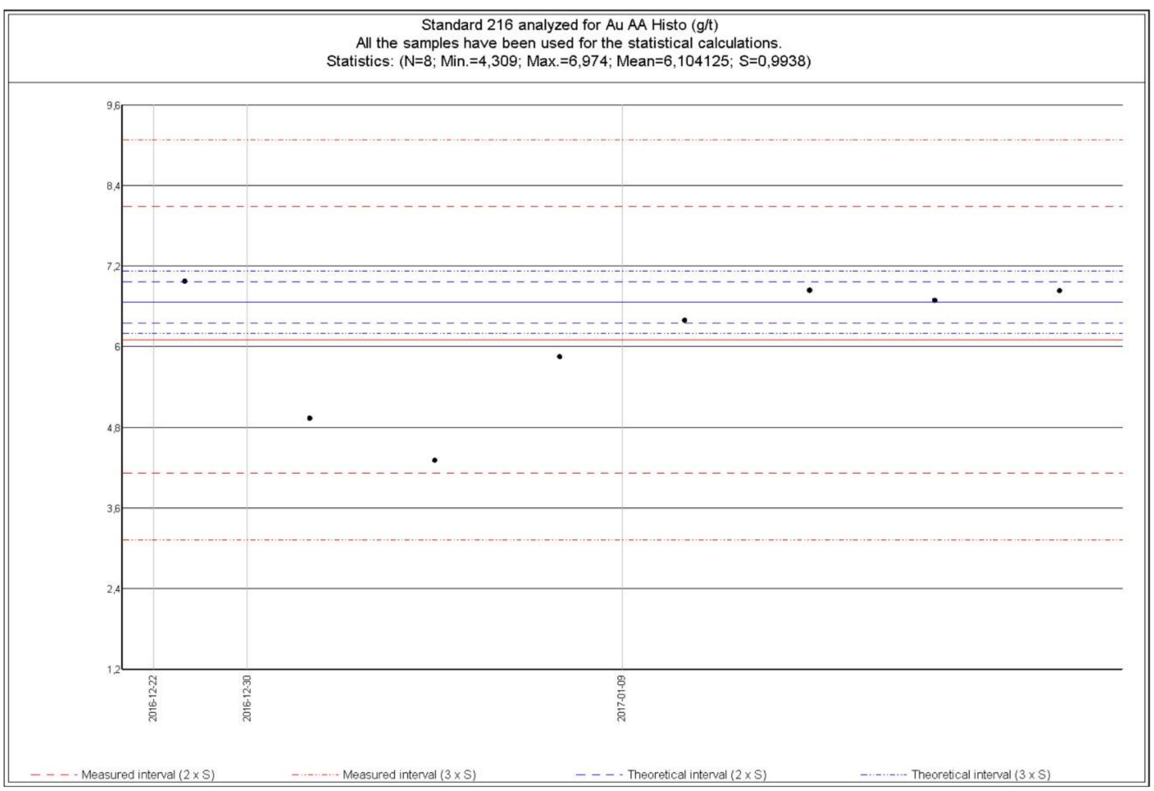


Figure 11-8: Shewart control chart showing gold content in standard 216 assayed at Accurassay.

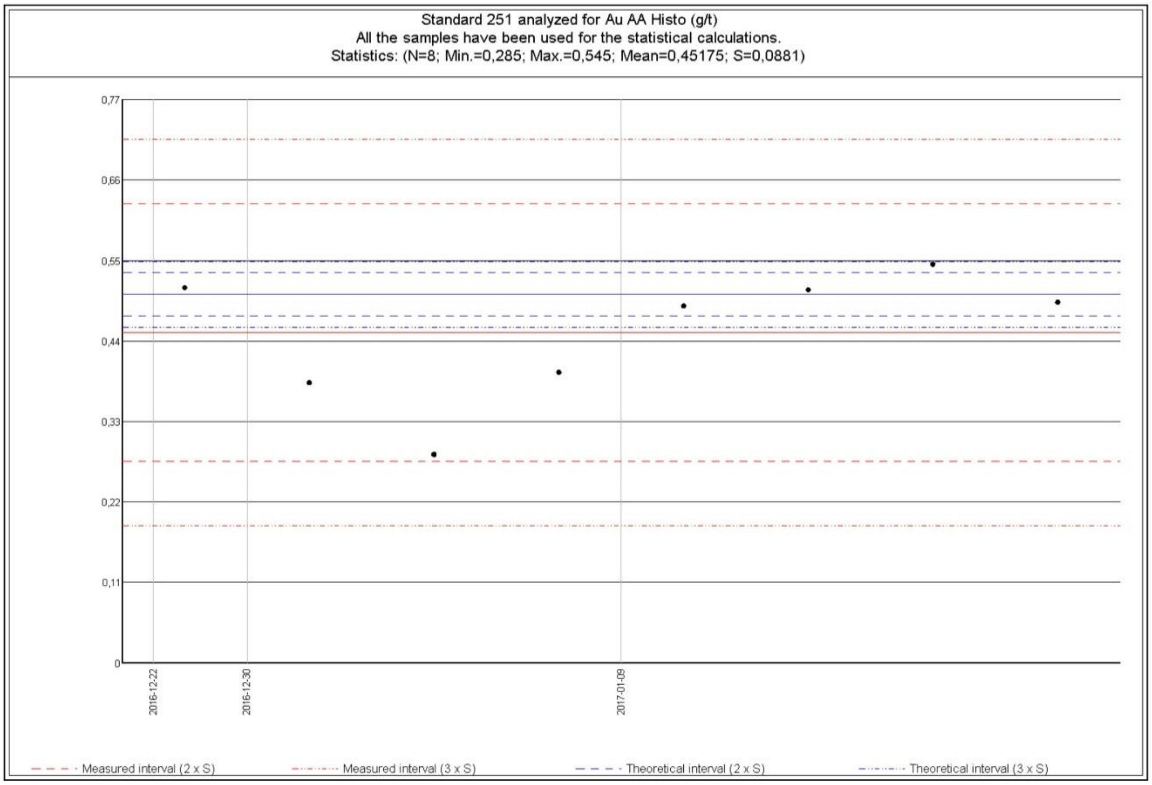


Figure 11-9: Shewart control chart showing gold content in standard 251 assayed at Accurassay.

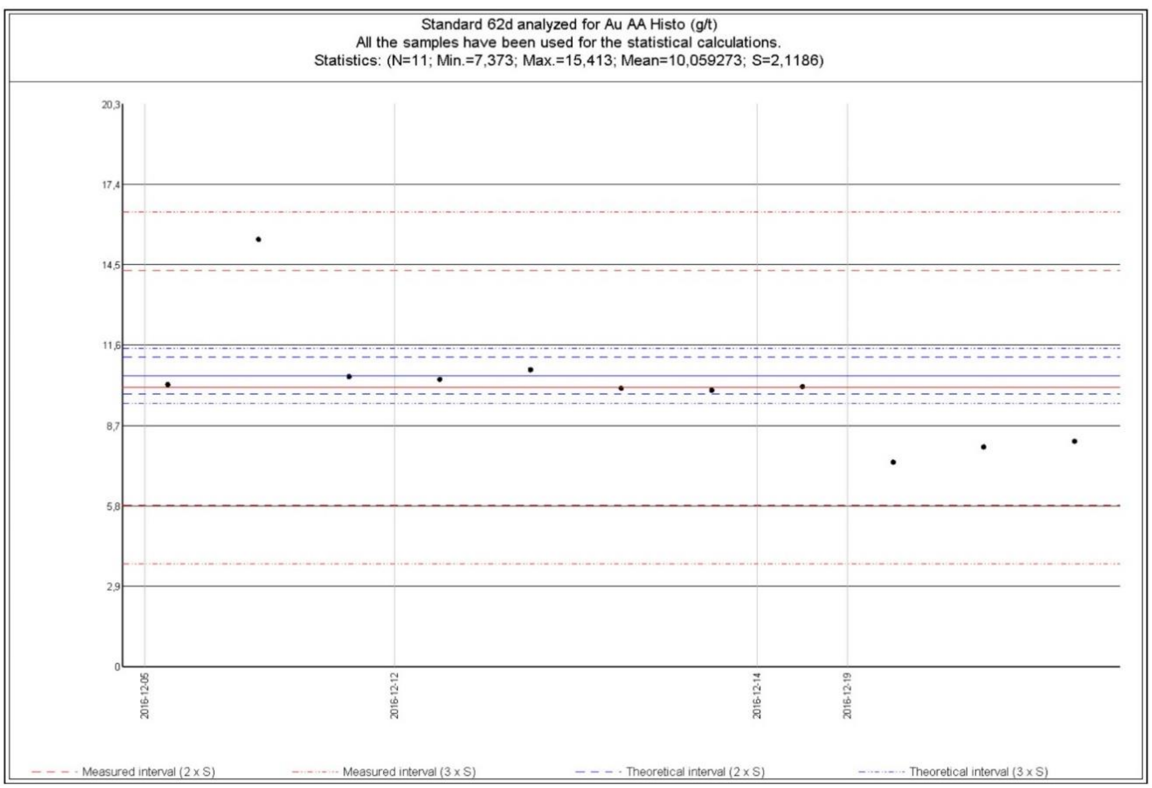


Figure 11-10: Shewart control chart showing gold content in standard 62d assayed at Accurassay.

The next five figures (11-11 to 11-15) show the results from Techni-Lab. Using the criteria cited at the beginning of this section, the author identified more than a dozen cases (bold sample numbers and dots circled in purple) representing potential problems. Overlapping dates from one standard to another made it difficult to discern systematic errors. However, the period from early March to early June 2019 seems problematic (Figures 11-12, 11-13 and 11-14).

The laboratory's difficulty in replicating the results of standard 257 (Figure 11-15) is related to the nature of its matrix. It is a standard developed for use in settings where mineralization is associated with an oxide facies. GéoPointCom recommends that Cartier no longer use this standard.

In summary, despite a few dubious values, the Techni-Lab results from 2017 to 2019 demonstrate a high level of quality and consistency in the laboratory. GéoPointCom considers these results to be reliable.

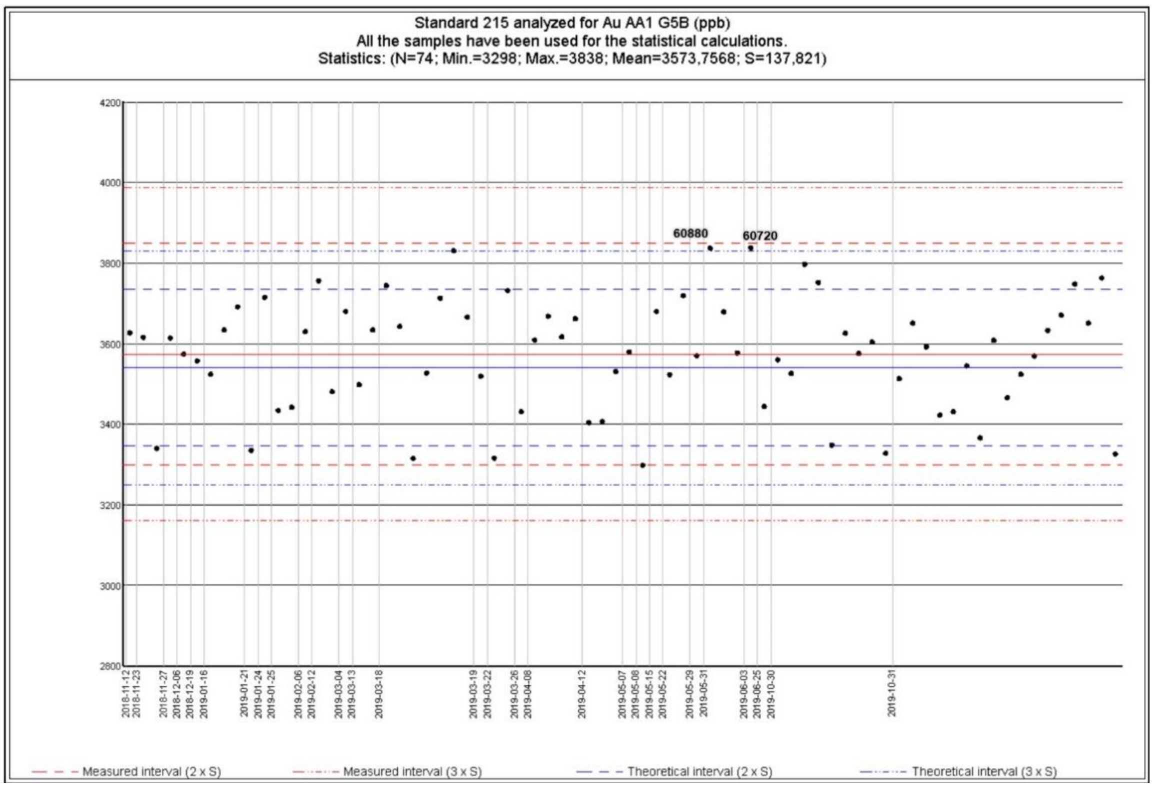


Figure 11-11: Shewart control chart showing gold content in standard 215 assayed at Techni-Lab.

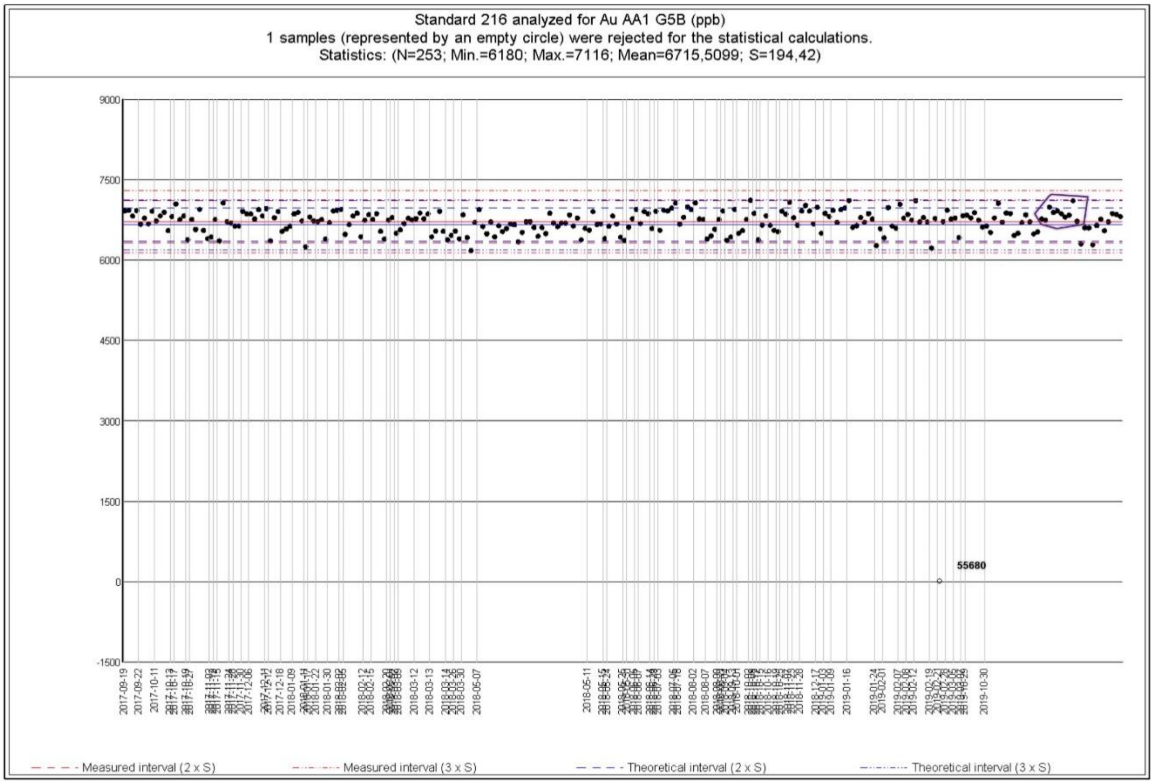


Figure 11-12: Shewart control chart showing gold content in standard 216 assayed at Techni-Lab.

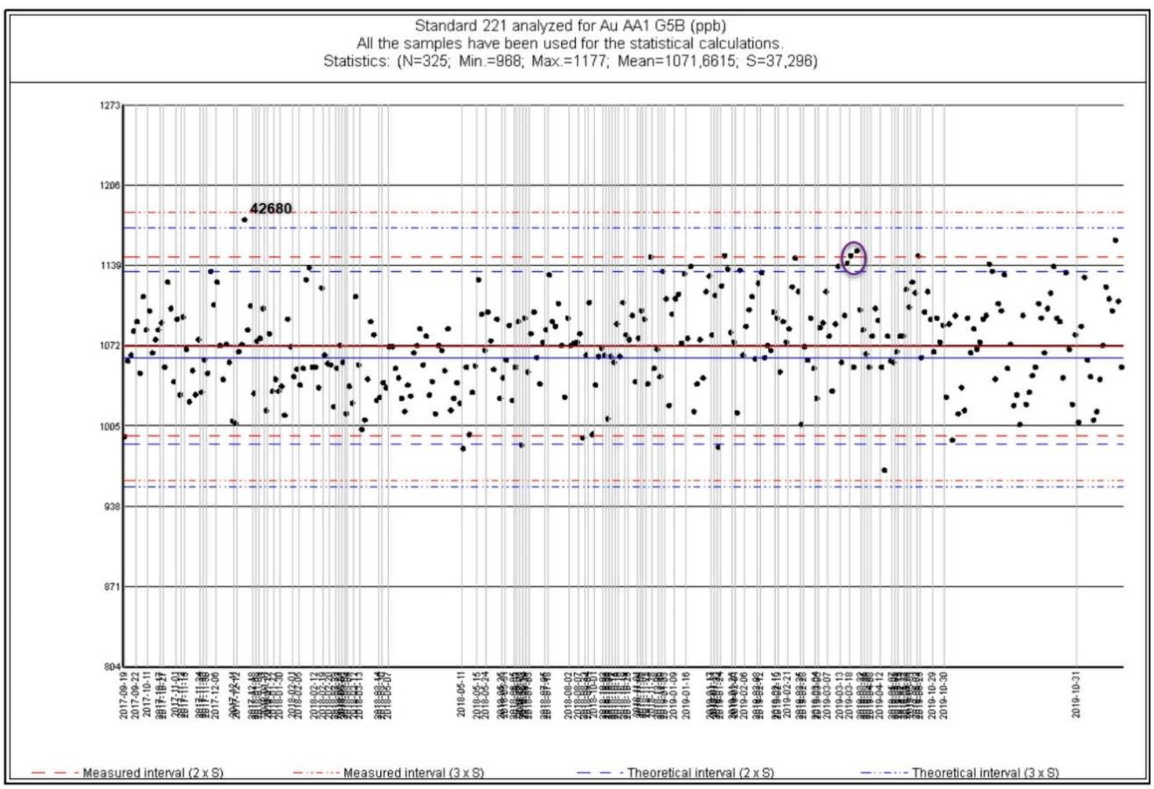


Figure 11-13: Shewart control chart showing gold content in standard 221 assayed at Techni-Lab.

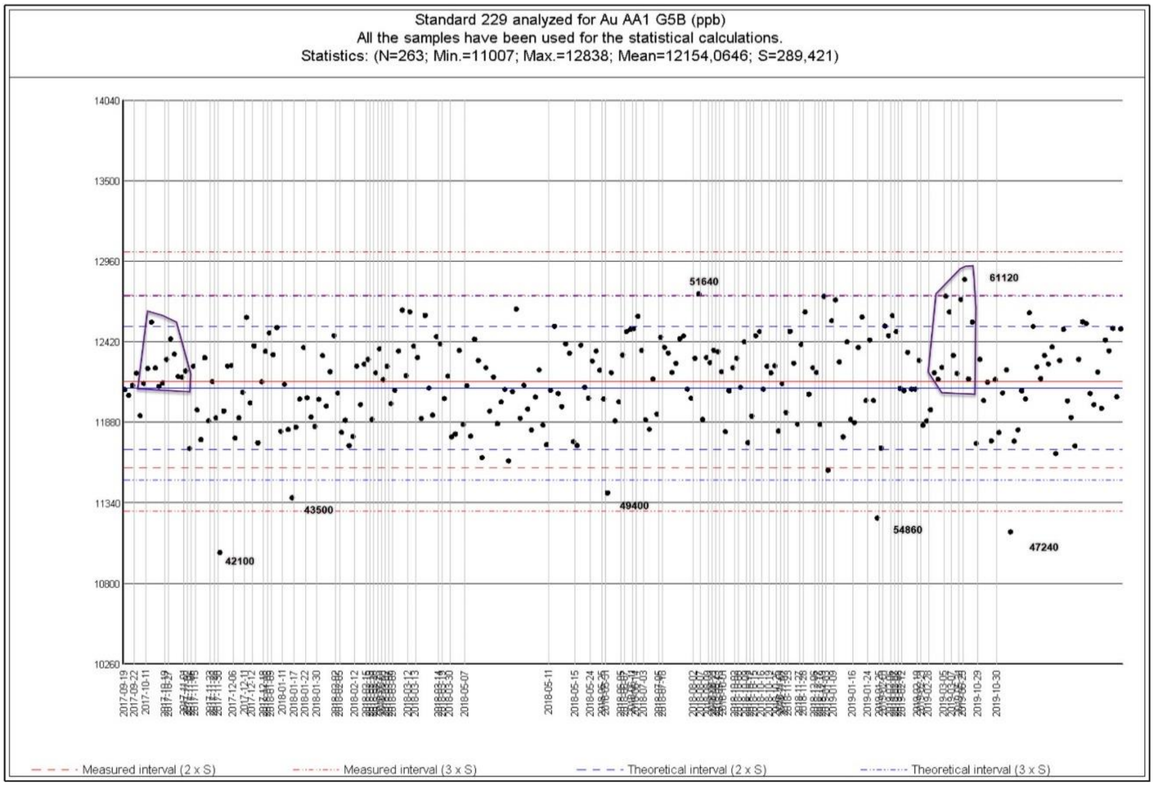


Figure 11-14: Shewart control chart showing gold content in standard 229 assayed at Techni-Lab.

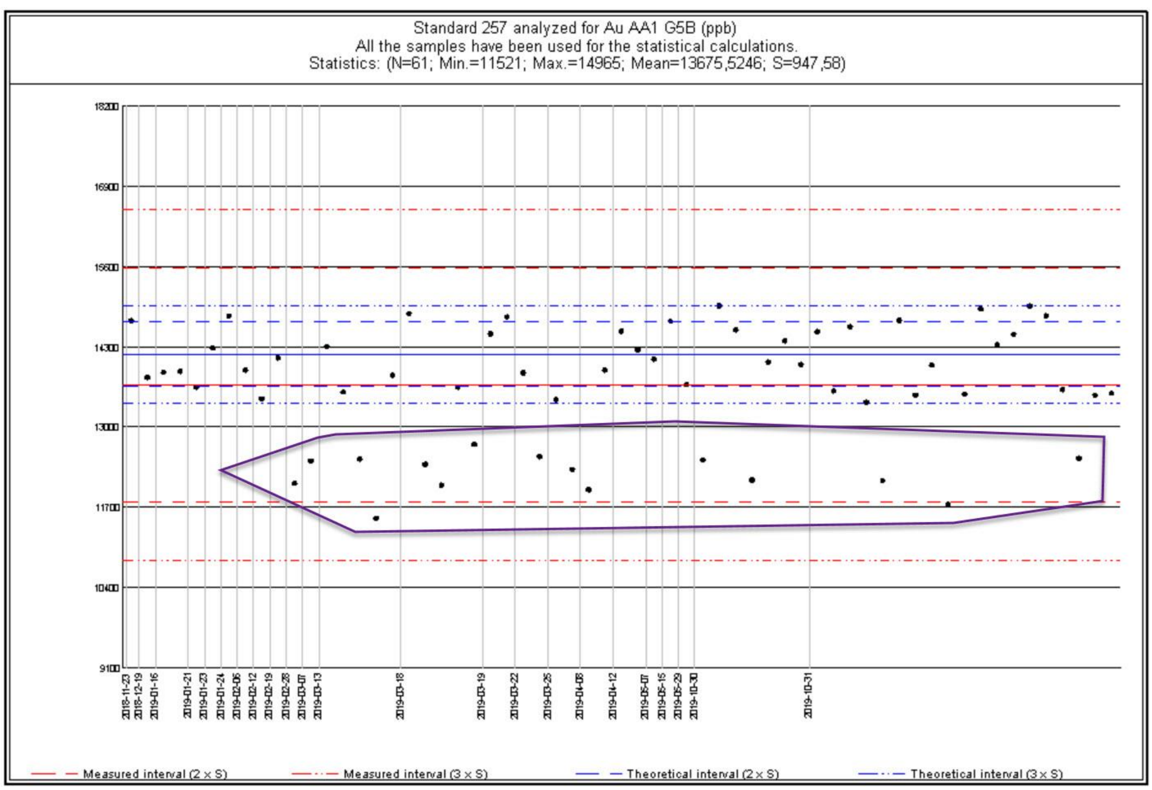


Figure 11-15: Shewart control chart showing gold content in standard 257 assayed at Techni-Lab.

#### 11.3.3 Duplicates

As mentioned above, Cartier's QA/QC procedure does not include systematic duplicate assays, although the analytical procedure does automatically create a set of duplicates (1,506 duplicate pairs). Some may criticize this procedure for not being sufficiently representative of low-grade duplicates. Although this is partly correct, it is not common practice to take low-grade samples into consideration when assessing the accuracy of duplicates because accuracy decreases rapidly as you approach the detection limit. There is no consensus on the threshold from which accuracy should be studied. In the literature, this threshold varies from 10 times the detection limit (which, in this case, corresponds to 0.08 g/t) to 5% of the cut-off grade (which, in this case, represents 0.125 g/t). Logically, the lower end of the range of values to be considered should be somewhere in between. In this case, 9% of the duplicate pairs have a grade of less than 1.0 g/t, and for at least one of the two samples, the lowest grade is 0.1 g/t. The author therefore considers this data to be a reliable source of information for this type of study.

There are several methods for comparing duplicate populations. One of the most common is the Howarth-Thompson method. Although quite popular, this method is often criticized for not being applicable to cases of non normal distributions. The author prefers a variant of this method to avoid forcing a linear regression on data that does not necessarily follow a normal distribution. The Howarth-Thompson method requires a fairly large amount of data (more than 100 duplicates). Figure 11-16 shows the estimated relative error associated with pulp duplicates using the variant of the Howarth-Thompson method. The estimated relative error associated with pulps is roughly 17%. An acceptable error for a vein-type gold deposit is generally between 10% and 20%.

A less common technique, but one that offers the advantage of being independent of distribution, was first proposed by Stanley and Lawie (2007) and subsequently used by several authors. The method calculates the mean coefficient of variation in duplicate pairs ($CV_{mean}$). This method also has the advantage of being applicable to smaller sample sets. Stanley and Lawie (2007) propose that for medium-lode gold systems with a moderate nugget effect, the $CV_{mean}$ of pulp duplicates is ideally below 10%, but up to 20% is acceptable. For core duplicates, these limits (ideal and acceptable) increase to 20% and 30%, respectively. For the 1,051 pulp duplicates, the author calculated a $CV_{mean}$ of 12.5%. The same calculation applied to the 31 reject duplicates (shipped to the AGAT laboratory) yielded a $CV_{mean}$ of 12.7%. Therefore, the calculated errors of the pulps and of rejects are similar and at an acceptable level for this type of mineralization. The similarity between the errors indicates that the crushing and pulverizing procedures are adequate for the processed material.

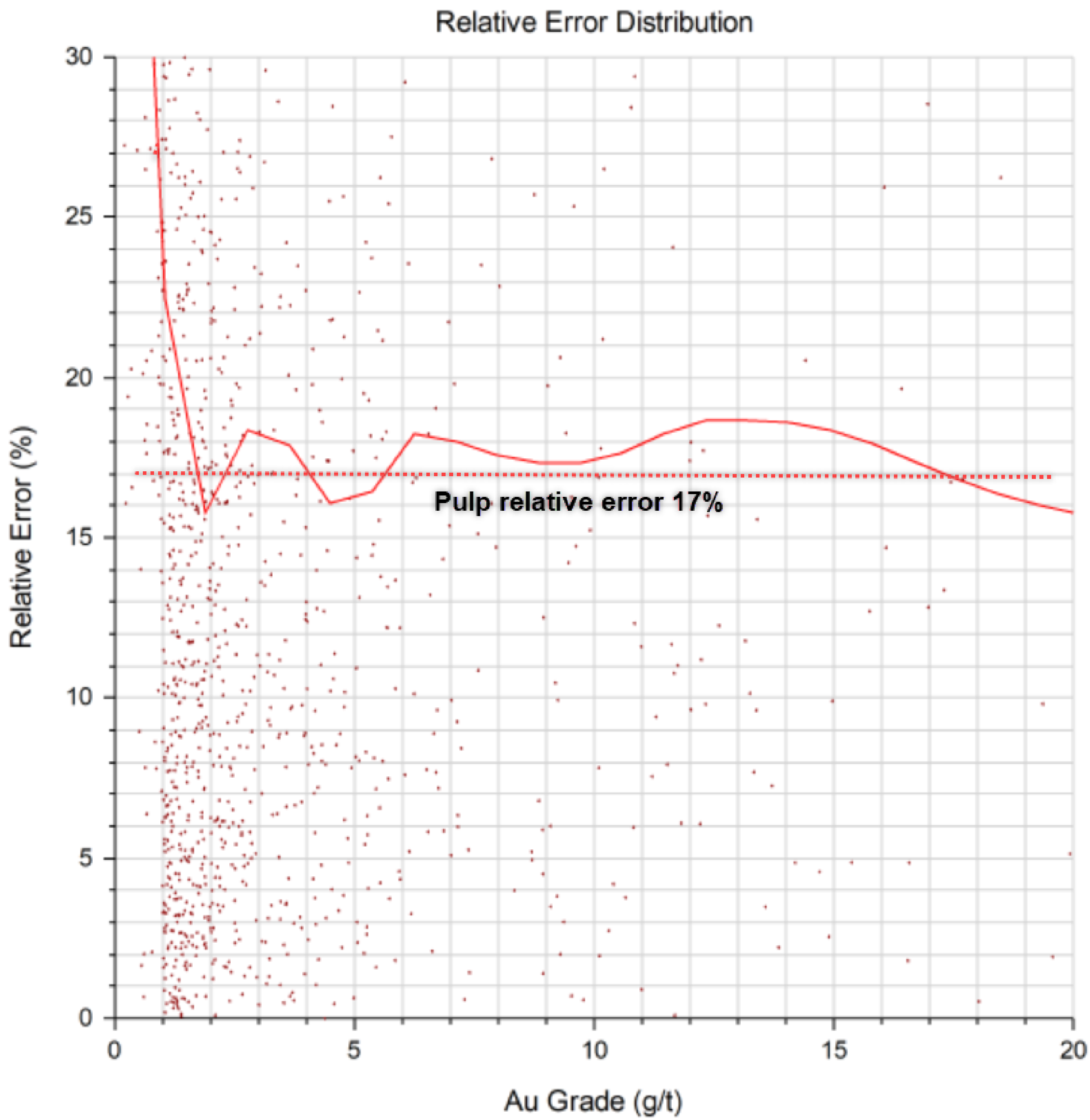


Figure 11-16: Modified Howarth-Thompson chart showing the relative error associated with pulp assaying.

## 11.4 Conclusions

After verifying in detail all of the procedures for sampling, sample preparation, storage, security, analytical methods and quality control, GéoPointCom believes that the methods employed have met the highest standards in the industry and that the results obtained are of sufficient quality for the purpose of this report.

## 12 DATA VERIFICATION

GéoPointCom assisted Ronan Déroff, Senior Geologist, Project Manager and GIS Specialist at Cartier in the geological interpretation and modelling of 3D solids for mineralized structures and mined-out stopes using GeoticMine software. The author, an independent QP, verified all available information (historical information on paper and 3D modelling carried out by InnovExplo in 2013). The QP also ensured the quality and representativeness of the built solids and either approved or modified, as appropriate, the interpretation.

### 12.1 Site Visit

The author visited the Chimo Mine Property on October 4, 2019 (Figure 12-1). The visit included a check on the location of the drill collars (casing) and some of the access roads. On October 7, he visited Cartier's core shack to examine the mineralization encountered in four (4) holes drilled between 2016 and 2019 that had been pre-selected by the QP a few days beforehand. During this visit, the QP collected 20 drill core samples and sent them to an independent laboratory to corroborate Cartier's results. He visited the exploration office several times to discuss and clarify geological interpretations and the geomatics procedures.

Figure 12-1: Inspection of drill collars on the Chimo Mine Property during the author's visit.

### 12.2 Drill Hole Database

The mineral resource estimate for the Property is based on a drilling database from several mining companies, including Quémartic Mines (1936-38), Chimo Gold Mines (1945-48 and 1963-67), SOQUEM (1978-80), LOUVEM Mines Inc. (1981-88), CAMBIOR Inc. (1990-96), X-Ore Resources (2010-11) and Cartier (2016-19).

GéoPointCom verified and validated the database for the Property. The database close-out date is July 2, 2019, which represents the approval date for the most recent drilling results considered in the resource estimate (CH18-52B, CH18-52BE, CH18-52C and CH18-52CE).

A total of 3,320 holes are considered historical (pre-Cartier), amounting to 230,429 m of drilling. The digital data for the majority of these holes (Figure 12-2) was derived from several sources (GM assessment reports, internal paper reports, and Excel or Access database files). However, a number of underground delineation holes drilled during production by LOUVEM and CAMBIOR were only found on plans, cross sections, longitudinal sections dating back to that time (i.e., this data was only available as images) (Figure 12-3). As a result, the information for 1,051 drill holes in the database was obtained manually, reported and/or calculated as true lengths (drill hole numbers, coordinates and hole traces, deviation measurements and analytical results) using cross sections and level plans that had been scanned and geo-referenced in GeoticMine. This information was incorporated into the final drilling database. The sources of the data are clearly indicated in the drilling database.

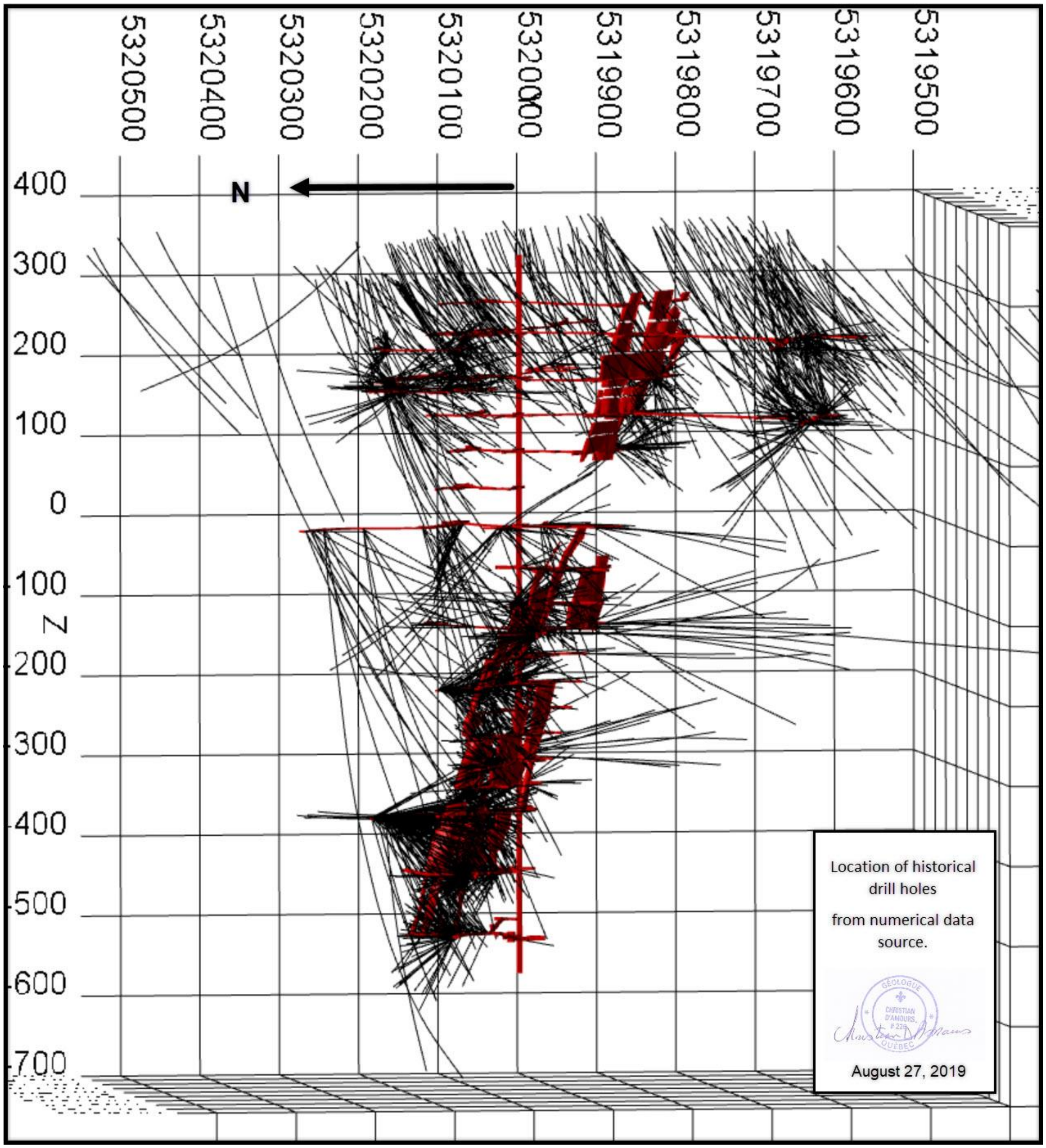


Figure 12-2: Location of historical drill holes obtained from digital data.

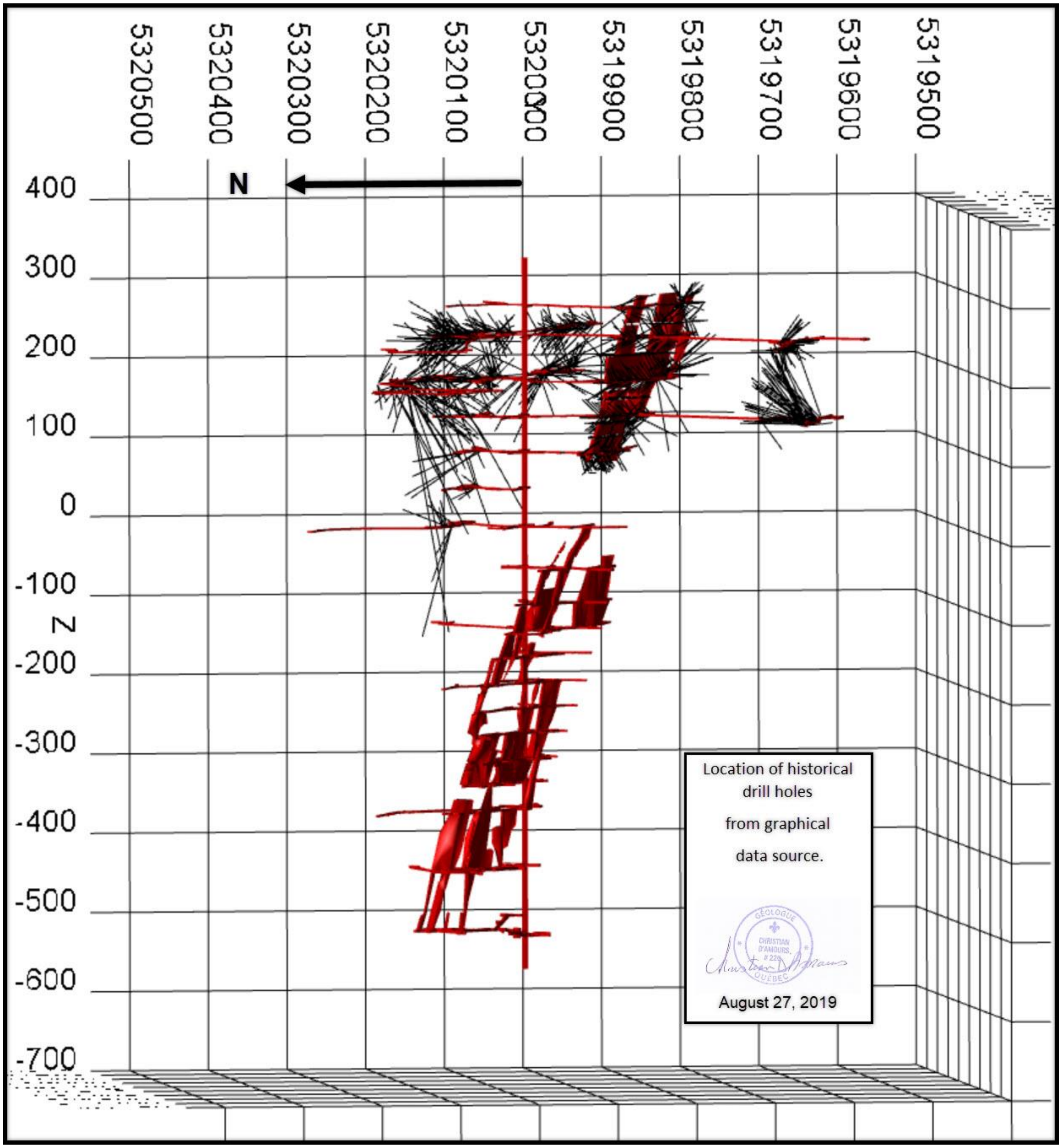


Figure 12-3: Location of historical drill holes obtained from graphical data.

Once the data is entered into the database, the final step is to generate a set of sections and plans from the Geotic database and compare them to the historical originals kept in Cartier's office. For the vast majority of drill holes, the match was perfect; exceptions included a few cases of obvious numerical errors (reversal of coordinates or the starting plunge of the hole, elevation problem between holes starting from the same location, and surveying issue for holes starting from drifts). In these cases, the boreholes were manually repositioned and corrected in the database.

During the 3D modelling step, the QP was able to visually verify information on lithology, structures and drill hole position. During this step, the location and/or deviation measurements of 11 boreholes (6 surface holes and 5 underground holes) were considered suspect. These drill holes are clearly identified in the database, but due to uncertainty, they have not been used to model mineralized bodies. However, composites from these drill holes did contribute to the estimate, even though some of the composites fell outside the mineralized envelopes.

In addition to geometric information (location and deviation), the QP was unable to fully verify the results of historical drilling analyses. However, since the density of information is very high in mined areas, a good reconciliation between historical production and the current estimate can be seen as an indirect validation of the quality and accuracy of drilling data and the volumes involved. Unfortunately, the source of information on historical production is not detailed enough to allow for stope reconciliation. The validation therefore covered the entire production. For example, from 1990 to 1996, the Chimo mine processed 1,175,658 tonnes of ore at a grade of 3.87 g/t Au. Using the procedure described in item 14, the mined tonnage is estimated at 1,117,826 tonnes at a grade of 3.99 g/t Au. The historical data thus represents an underestimation by about 5% in tonnage and 3% in grade. The author concludes that the historical information is accurate enough to produce a fair estimate of the Project's resources.

Detailed verification of the recent assay results (2016 to 2019 drilling programs; Figure 12-4) revealed some errors or irregularities when calculating the "Final Au" value. To correct this inaccuracy, GéoPointCom re-imported all 2016-2019 assay results directly from the original certificates and recalculated the "Final" value, giving precedence to metallic sieve analyses above gold assays by AA or gravimetric finish.

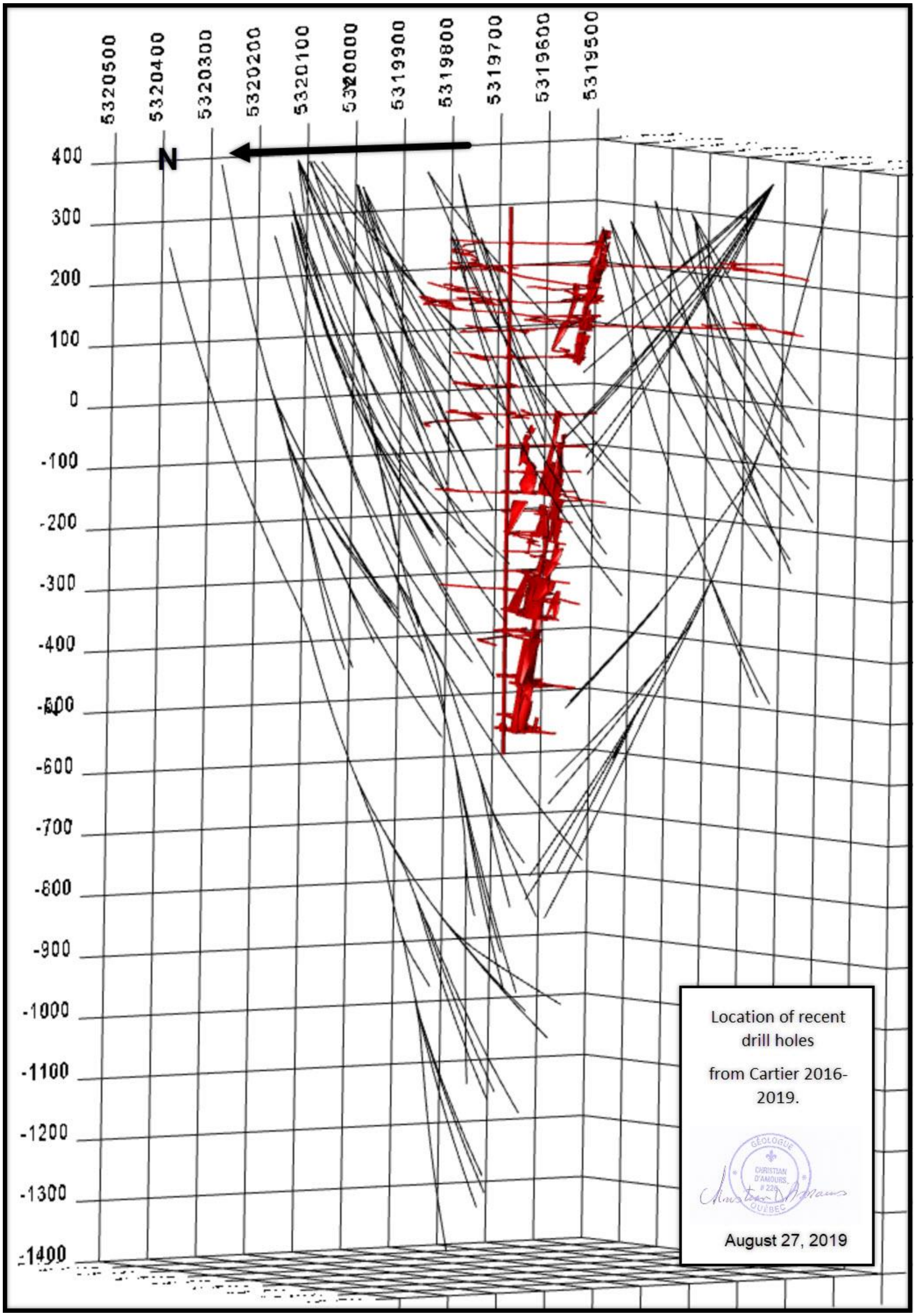

Figure 12-4: Location of Cartier's drill holes from 2016 to 2019.

#### 12.2.1.1 Sampling verification

A series of 20 samples (Table 12-1) was collected from the remaining half core for corroboration sampling. These samples are from four Cartier holes (CH16-06, CH17-27, CH18-20 and CH18-52E1), selected by the QP for their location on the Property and their distribution within the drilled areas. The samples were sent to the ALS Chemex laboratory in Val-d'Or for re-analysis to compare to the original results obtained by Cartier. The same analysis protocol as Cartier was used for the re-analysis. Of the 20 samples submitted, 4 were also analyzed by the metallic sieve method.

| Drill Hole | Original sample number | Average grade from Cartier (g/t) | Average Corroboration Grade (g/t) |
|---|---|---|---|
| CH16-06 | 36483 | 2.09 | 1.39 |
| CH16-06 | 36491 | 1.68 | 0.662 |
| CH16-06 | 36494 | 25.52 | 8.02 |
| CH17-27 | 44426 | 17.69 | 3.25 |
| CH17-27 | 44432 | 9.57 | 0.322 |
| CH18-20 | 51314 | 9.41 | 6.79 |
| CH18-20 | 51324 | 1.87 | 1.535 |
| CH18-20 | 51328 | 7.01 | 19.15 |
| CH18-52E1 | 57267 | 1.74 | 0.991 |
| CH18-52E1 | 57269 | 1.26 | 1.68 |
| CH18-52E1 | 57278 | 4.38 | 0.651 |
| CH18-52E1 | 57281 | 19.93 | 4.51 |
| CH18-52E1 | 57284 | 2.16 | 2.47 |
| CH18-52E1 | 57321 | 0.61 | 0.582 |
| CH18-52E1 | 57322 | 3.28 | 2.7 |
| CH18-52E1 | 57323 | 7.37 | 6.41 |
| CH18-52E1 | 57338 | 14 | 2.28 |
| CH18-52E1 | 57342 | 4.21 | 2.86 |
| CH18-52E1 | 57343 | 1.12 | 0.413 |
| CH18-52E1 | 57345 | 0.74 | 0.779 |

Table 12-1: The 20 corroboration samples.

The $CV_{mean}$ for the two half-cores is 39%. According to Stanley and Lawie (2007), this value is representative of a vein environment containing a lot of coarse gold.

On closer inspection, 4 of the 5 samples with a $CV_{mean}$ greater than 30% contain visible gold (identified in the logs) and were therefore analyzed by the metallic sieve method. The link between high $CV_{mean}$ and the presence of visible gold is undeniable. The question, then, is whether melting the entire coarse fraction (metallic sieve) reduces this error significantly. To answer this question, the author compared the results of the fine fraction to the final result (fine fraction + coarse fraction) for all the metallic sieve analyses in the database. For the 30 samples analyzed by metallic sieve, the $CV_{mean}$ between the fine fraction and the final result is 24%. This is double that of the pulp and reject duplicates analyzed by more standard methods (FA-AA and FA-GRAVIMETRY). Therefore, using the metallic sieve method when visible gold is observed actually reduces the analytical error.

### 12.3 Conclusion

A comparison of the $CV_{mean}$ values for the pulps, rejects, half-cores and metallic sieve fractions clearly shows that the bulk of the error is at the initial sampling stage, as is often the case for this type of environment. The most economical way to significantly reduce this type of error would be to analyze whole-core samples; that is, without keeping the half-core as a witness. At the current stage of exploration, this solution has more drawbacks than advantages. Fortunately, the sampling error tends to cancel out as the sample number increases. For this reason, when a significant analytical variance is present, it is essential to use a large number of samples in the cell estimation process. It should be kept in mind, however, that increasing the minimum number of samples often diminishes the correlation to nearby samples.

The verifications carried out by the author confirms the adequacy of the crushing and pulverizing procedures for this Project. In busy times, there is often strong pressure at laboratories to speed up crushing and pulverizing procedures. Under the current conditions, the author strongly recommends that Cartier not give in, and maintain the same standards even if this results in longer turnaround times.

According to the author, the quality and accuracy of the analyses, as well as the geological information, meets industry standards and allows a fair and accurate estimate of the project.

## 13 MINERAL PROCESSING AND METALLURGICAL TESTING

The Property was in production from 1966 to 1967 under Chimo Gold Mines Ltd, from 1984 to 1988 under LOUVEM Mines Inc., and from December 1989 to January 1997 under CAMBIOR Inc. Between December 1989 and July 1993, CAMBIOR processed the Chimo ore using the concentrator at the Lucien-Béliveau mine at a rate of 220 tonnes per day (Figure 13-1). The information presented in this item is an accurate portrait of Chimo ore processing between December 1989 and July 1993 (Vachon *et al.*, 1993).

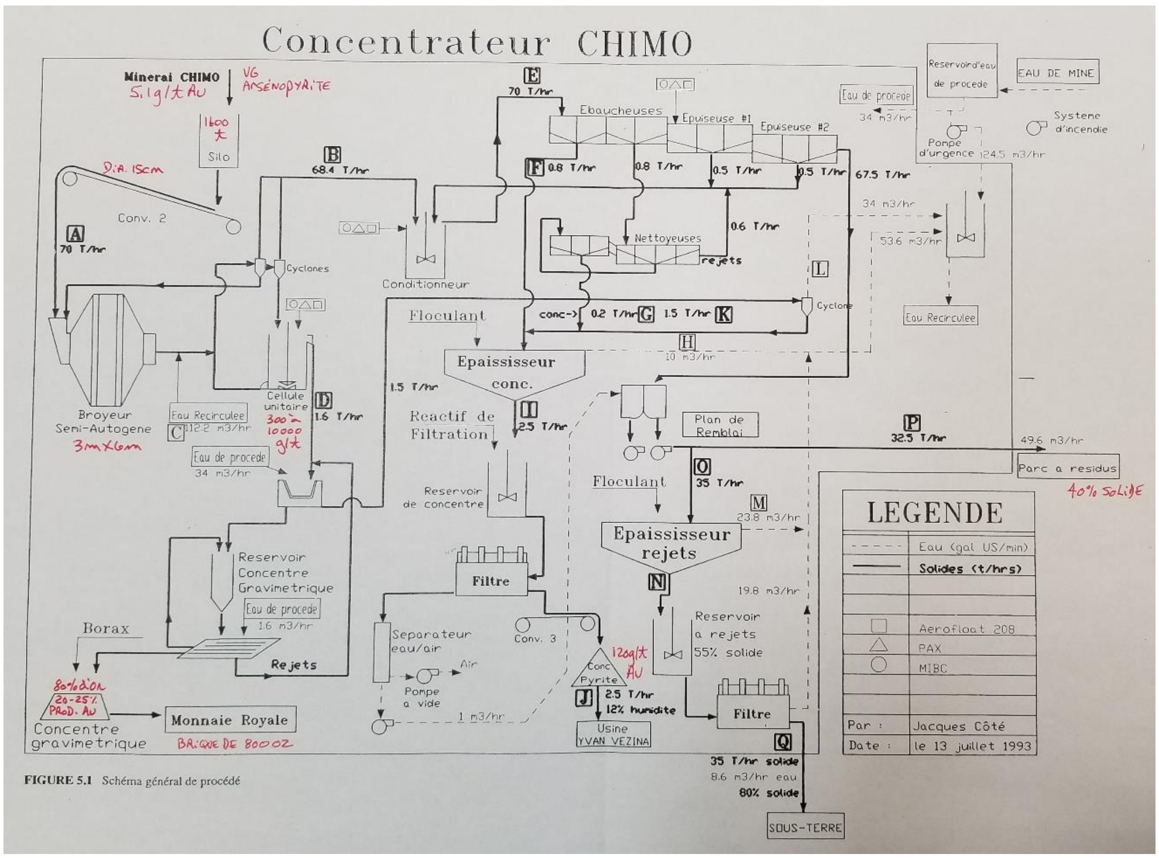


Figure 13-1: General ore processing flow sheet for the Chimo mine (July 1993)

Upon entering the mill, the average diameter of the ore was 15 cm. Gold was observed as visible gold in veins of smokey to milky quartz. Gold was also present as fine grains associated with arsenopyrite and quartz. The ore was composed of an average 25% quartz and silica and 4% arsenopyrite (Table 13-1).

Chemical and mineralogical composition of Chimo Mine Ore

| Paramètres | | Paramètres | |
|---|---|---|---|
| $SiO_2$ | : 55,1 % | Sphalérite | : 0,0 % |
| $Al_2O_3$ | : 13,1 % | Pyrite-pyrrho | : 4,1 % |
| $Fe_2O_3$ | : 10,6 % | | |
| MgO | : 2,9 % | | |
| CaO | : 6,3 % | Magnétite | : 7,0 % |
| $Na_2O$ | : 5,1 % | | |
| $K_2O$ | : 0,5 % | | |
| $TiO_2$ | : 1,1 % | Hornblende | : 13,2 % |
| MnO | : 0,2 % | Mica | : 4,5 % |
| $P_2O_5$ | : 0,2 % | | |
| PAF | : 4,0 % | | |
| | | Quartz | : 25,4 % |
| | | Fl. Plagioclase | : 34,1 % |
| Ag | : 1 ppm | F. Potassique | : 3,2 % |
| Co | : 38,0 ppm | | |
| Cu | : 211 ppm | | |
| Ni | : 65 ppm | Apatite | : 0,4 % |
| Pb | : 3 ppm | Calcite-dolomite | : 5,9 % |
| Zn | : 321 ppm | | |
| C total ($CO_2$) | : 3,5 % | | |
| S total | : 2,2 % | | |
| TOTAL | : 99,0 % | | : 97,7 % |

Table 13-1: Chemical and mineralogical compositions of the Chimo mine ore.

The gravity circuit recovered 20-25% of the mine's gold production. After it passed through the semi-autogenous grinder (SAG) mill circuit, the ore was transported to cyclones to produce a 300 g/t Au concentrate, which was then transported to the Knelson concentrator to produce a 5,000 to 10,000 g/t Au concentrate. This concentrate was processed on shaking tables to produce a final concentrate composed of 80% gold, which was then melted in the refinery furnace to produce 800-ounce gold bricks.

The flotation system recovered the portion not collected by the gravity circuit, producing an arsenopyrite concentrate of 100 to 120 g/t Au. Approximately 25 tonnes of ore was required to produce one tonne of concentrate, which was shipped at the rate of two trucks per day over a distance of 220 km to the Yvan Vézina mine in Destor to complete the treatment. At this stage, the concentrate, with a moisture content of 12%, was composed of 23% arsenopyrite and 14% quartz and silica (Table 13-2). The tailings, which consisted of 27% quartz and silica and 0.9% arsenopyrite (Table 13-3), were transported to the tailings pond (46%), and the other 50% was sent to the paste backfill plant where it was mixed with cement to backfill underground stopes. The residual portion, representing 4% of the initial ore, consisted of gravity concentrate and arsenopyrite concentrate.

Chemical and mineralogical composition of the Chimo Mine Concentrate

| Paramètres | | Paramètres | |
|---|---|---|---|
| $SiO_2$ | : 32,0 % | Sphalérite | : 0,1 % |
| $Al_2O_3$ | : 8,2 % | Pyrite-pyrrho | : 22,5 % |
| $Fe_2O_3$ | : 31,5 % | | |
| MgO | : 1,8 % | | |
| CaO | : 5,5 % | Magnétite | : 23,2 % |
| $Na_2O$ | : 3,2 % | | |
| $K_2O$ | : 0,3 % | | |
| $TiO_2$ | : 0,8 % | Hornblende | : 5,1 % |
| MnO | : 0,1 % | Mica | : 4,8 % |
| $P_2O_5$ | : 0,2 % | | |
| PAF | : 12,5 % | | |
| | | Quartz | : 14,4 % |
| | | Fl. Plagioclase | : 21,1 % |
| Ag | : 6 ppm | F. Potassique | : 1,9 % |
| Co | : 177,0 ppm | | |
| Cu | : 593 ppm | | |
| Ni | : 285 ppm | Apatite | : 0,5 % |
| Pb | : 17 ppm | Calcite-dolomite | : 8,2 % |
| Zn | : 1 300 ppm | | |
| C total ($CO_2$) | : 4,7 % | | |
| S total | : 12,0 % | | |
| TOTAL | : 95,8 % | | : 101,9 % |

Table 13-2: Chemical and mineralogical composition of the Chimo mine concentrate.

Chemical and mineralogical composition of the Chimo Mine tailings

| Paramètres | | Paramètres | |
|---|---|---|---|
| $SiO_2$ | : 59,0 % | Sphalérite | : 0,0 % |
| $Al_2O_3$ | : 13,8 % | Pyrite-pyrrho | : 0,9 % |
| $Fe_2O_3$ | : 7,0 % | | |
| MgO | : 3,2 % | | |
| CaO | : 6,3 % | Magnétite | : 4,1 % |
| $Na_2O$ | : 5,6 % | | |
| $K_2O$ | : 0,5 % | | |
| $TiO_2$ | : 1,1 % | Hornblende | : 15,2 % |
| MnO | : 0,2 % | Mica | : 2,5 % |
| $P_2O_5$ | : 0,1 % | | |
| PAF | : 3,8 % | | |
| | | Quartz | : 27,3 % |
| | | Fl. Plagioclase | : 37,0 % |
| Ag | : 0 ppm | F. Potassique | : 3,4 % |
| Co | : 8,0 ppm | | |
| Cu | : 33 ppm | | |
| Ni | : 21 ppm | Apatite | : 3,0 % |
| Pb | : 4 ppm | Calcite-dolomite | : 5,8 % |
| Zn | : 147 ppm | | |
| C total ($CO_2$) | : 3,4 % | | |
| S total | : 0,5 % | | |
| TOTAL | : 100,6 % | | : 96,6 % |

Table 13-3: Chemical and mineralogical composition of the Chimo mine tailings.

Chimo mine ore processing statistics for the period from December 1989 to January 1997 show a gold recovery rate at the mill ranging from 85.8% to 91.4%, for an average of 89.2% over 80 months of production (Table 13-4).

| Mill statistics | | |
|---|---|---|
| **Period** | **Grade (g/t)** Mill Entrance | **Recovery (%)** Mill Exit |
| December 1989 | 4.00 | 85.8 |
| 1990 (12 months) | 4.79 | 87.2 |
| 1991 (12 months) | 4.21 | 89.5 |
| 1992 (12 months) | 4.55 | 90.8 |
| 1993 (6 months) | 4.64 | 91.3 |
| 1994 (12 months) | 2.89 | 84.3 |
| 1995 (12 months) | 3.53 | 90.6 |
| 1996 (12 months) | 3.34 | 91.8 |
| January 1997 | 3.71 | 91.4 |

Table 13-4: Mill statistics at the Chimo mine from 1989 to 1997.

Acid generation predictive tests on the ore yielded concentrations ranging from 1.68 to 2.35% sulphur, demonstrating that it was non-acid generating material.

Although gold is associated with concentrations of arsenopyrite (Table 13-5), at least for some of the ore, the cumulative annual concentration of 0.04 mg arsenic per litre in the final effluent from the tailings pond is very low and below the maximum limits of current requirements (Table 13-6).

**Metal analysis results from Chimo Mine**

| | Concentrations (ppm) | | |
|---|---|---|---|
| Paramètres | Minerai | Concentré | Rejet |
| Argent | < 1 | 3 | < 1 |
| Aluminium | 0,91% | 0,43% | 0,71% |
| Arsenic | 8 800 | > 9 999 | 530 |
| Bore | < 10 | < 10 | < 10 |
| Barium | 23 | 18 | 66 |
| Beryllium | < 1 | < 1 | < 1 |
| Bismuth | 5 | < 5 | 15 |
| Calcium | 2,40% | 2,50% | 2,40% |
| Cadmium | < 1 | < 1 | < 1 |
| Cobalt | < 1 | < 1 | 3 |
| Chrome | 62 | 33 | 36 |
| Cuivre | 190 | 310 | 31 |
| Fer | 4,30% | 12% | 2,50% |
| Magnésium | 0,82% | 0,55% | 0,82% |
| Manganèse | 460 | 370 | 440 |
| Molybdène | 10 | < 2 | < 2 |
| Sodium | 0,14% | 0,02% | 0,02% |
| Nickel | 59 | 180 | 16 |
| Phosphore | 400 | 520 | 370 |
| Plomb | < 1 | 22 | < 1 |
| Antimoine | < 5 | < 5 | 15 |
| Scandium | 7 | 3 | 6 |
| Étain | < 10 | 10 | < 10 |
| Strontium | 22 | 20 | 19 |
| Thallium | 870 | 240 | 760 |
| Vanadium | 74 | 30 | 64 |
| Tungstène | < 10 | < 10 | < 10 |
| Yttrium | 15 | 8 | 10 |
| Zinc | 210 | 950 | 80 |
| Zirconium | 13 | 10 | 9 |

Table 13-5: Metal analysis results of the ore, concentrate and tailings from the Chimo mine.

| PARAMÈTRE | COLONNE I CONCENTRATION MOYENNE MENSUELLE ACCEPTABLE | COLONNE II CONCENTRATION MAXIMALE ACCEPTABLE |
|---|---|---|
| Arsenic extractible | 0,2 mg/l | 0,4 mg/l |
| Cuivre extractible | 0,3 mg/l | 0,6 mg/l |
| Fer extractible | 3 mg/l | 6 mg/l |
| Nickel extractible | 0,5 mg/l | 1 mg/l |
| Plomb extractible | 0,2 mg/l | 0,4 mg/l |
| Zinc extractible | 0,5 mg/l | 1 mg/l |
| Cyanures totaux | 1 mg/l | 2 mg/l |
| Hydrocarbures ($C_{10}$-$C_{50}$) | ----------- | 2 mg/l |
| Matières en suspension | 15 mg/l | 30 mg/l |

1 Selon la nature du minerai, du procédé, des résidus miniers ou selon le calcul des objectifs environnementaux de rejet (voir section 1.4.2), d'autres exigences au point de rejet de l'effluent final pourraient s'ajouter en vertu de l'article 20 de la Loi lors de la délivrance du certificat d'autorisation.

Column I: Monthly average of tested samples.
Column II: Individual samples.

Table 13-6: Final effluent discharge requirements (Directive 019 pertaining to the Mining Industry, March 2012, MDDEPQ).

## 14 MINERAL RESOURCE ESTIMATES

In late February 2019, Mr. Gaétan Lavallière, Vice-President for Cartier Resources, commissioned GéoPointCom to assist in the construction of solids representing the structures and voids of the Property. Under the mandate, Christian D'Amours, Geologist and President of GéoPointCom, was to assist Ronan Déroff, Senior Geologist and Geomatician at Cartier Resources, in modelling the solids in GeoticMine, and was tasked with ensuring their quality and representativeness. In late September 2019, the original mandate was changed to resource estimation. GéoPointCom was commissioned to prepare a mineral resource estimate for the Central Corridor on the Property in accordance with Canadian Securities Administrators' National Instrument 43-101 Respecting Standards of Disclosure for Mineral Project ("43-101") and Form 43-101F1.

The mineral resources presented in this Technical Report are not mineral reserves as economic viability has not been demonstrated. The selection of reasonable prospective parameters, which assume that some or all of the estimated resources could potentially be extracted, is based on an underground bulk mining scenario combined with material sorting at surface.

This study presents the current knowledge as of July 2, 2019, the close-out date of the most recent drill holes results included in the mineral resource estimate (CH18-52B, CH18-52BE, CH18-52C and CH18-52CE).

### 14.1 METHODOLOGY

This estimate is based on the geological interpretation of Mr. Déroff, who used historical and recent drilling information as well as historical mining data from the former Chimo mine. The author has verified in detail the available information and fully approves the interpretation made by the issuer.

The drilling database, in Geotic format (v. 8.0.10) and GeoticMine software (v. 1.2.14), was used to generate 3D envelopes representing the mineralized bodies as well as the major structures controlling the distribution of gold. Isatis software (v. 2018.3) was used to generate geostatistics and for the resource estimation on a percent block model. Basic statistics and some of the graphs were generated using NCSS software (v. 12).

The main steps in this study were:

- Validate basic information, client interpretation and 3D modelling;
- Generate intersections and composites from mineralized body envelopes;
- Study the distribution of composite grades specific to each structure to determine whether or not it will be necessary to cap high values;
- Variography;
- Select the estimator;
- Select neighbourhood settings;
- Estimate resources; and
- Validate results.

## 14.2 Database

At the time of this study, the database contained 3,429 drill holes totalling 279,670 m, 13,477 deviation (hole orientation) measurements and 79,236 samples analyzed for gold from 85,647 m of core, representing 35% of the total drilled core. The database contains 2,107 blank and standard samples, added by Cartier between November 1, 2016, and July 2, 2019. This database was validated before starting the resource estimate. The estimate was carried out on seven mineralized structures intersected by 51,029 m of drilling, producing 5,364 gold intersections.

The author considers the location data for 13 drill holes to be suspect. These drill holes are clearly identified in the database and were not used to model the mineralized envelopes due to the uncertainty. However, composites from these holes were used in the resource estimate even though it is possible that the composites fall outside the envelopes.

## 14.3 3D Model

The geological model, representing seven (7) mineralized structures as well as the topography and the bedrock surface below the overburden, was generated using a semi-automated procedure available in GeoticMine. This unique method creates sets of Voronoi-type triangles representing the two walls of a mineralized body, then links them to form a volume that fully respects the drilling intersections. This method is performed without having to interpret lines on a set of sections. Unlike the traditional method of lines on sections and tie lines, this technique does not produce the inevitable distortion caused by the orientation of the projection.

Drill hole intersections in the seven (7) mineralized structures of the Central Corridor represents 51,029 m of core in 5,364 different intersections. The average downhole core length of these intersections is 9.51 m, and the average true thickness is 7.42 m.

Between 1990 and 1996, CAMBIOR extracted 1,175,658 tonnes of ore from five (5) of the seven (7) structures covered in this Technical Report; the other two, 5B2 and 6N1, have not been mined. Stopes and drifts in the areas of interest were modelled in order to subtract them from the remaining resources. The estimated stope volumes are used to carry out the overall estimation process. Figure 14-1 shows the gold structures and underground workings on the Property.

Table 14-1 provides some information on the geometry of each mineralized structure. The average width of the structure corresponds to the volume of the structure divided by the surface; this geometric estimate does not take into account the density of information. The thickness of drill hole intersections varies greatly because structural modelling was not restricted to a minimum width. This is mainly due to the multiple intersecting relationships between structures. The selected intersections can be very narrow at the junction points between structures that intersect each other at very low angles or in areas away from mineralized zones (structural marker). Figure 14-2 shows an example where structure 5M is cut by structure 5B, making structure 5B very narrow at the intersection point. Composites were flagged with the name of each structure to ensure that no composite can exert influence over another structure. The grid in Figure 14-2 measures 3 x 3 m. Modelling constraints were based more on lithological markers and geometric considerations than assay grades.

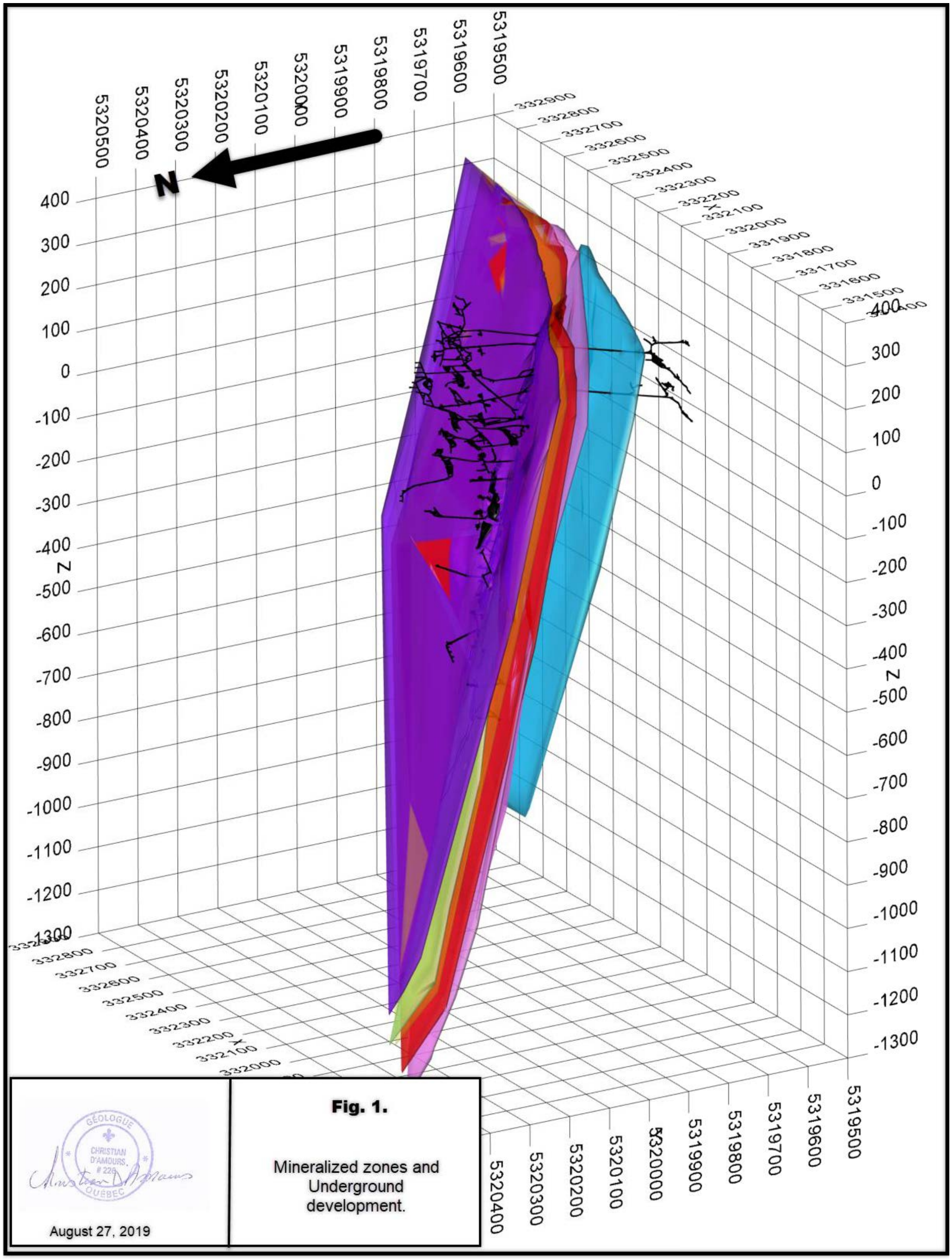


Figure 14-1: Gold structures and underground workings on the Chimo Mine Property.

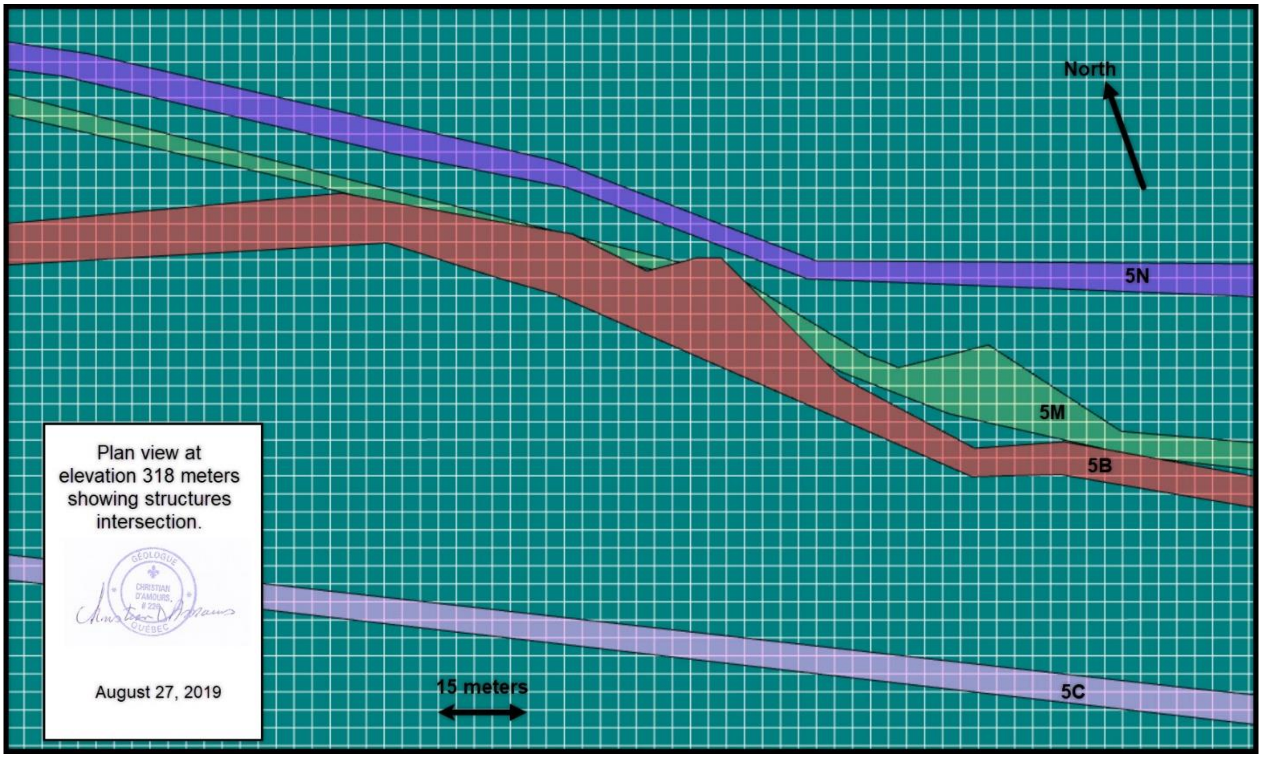


Figure 14-2: Modelling of intersections between structures.

| Structure | | | | DDH Intersection |
|---|---|---|---|---|
| | Azimut (°) | Dip (°) | Average True Thickness (m) | Average True Thickness (m) |
| **5B** | 294 | -76 | 6.4 | 11.1 |
| **5B2** | 297 | -81 | 4.0 | 4.5 |
| **5C** | 292 | -76 | 4.6 | 4.6 |
| **5M** | 293 | -74 | 4.5 | 5.0 |
| **5M2** | 290 | -77 | 3.9 | 4.3 |
| **5N** | 291 | -73 | 6.3 | 6.4 |
| **6N1** | 288 | -77 | 7.4 | 8.6 |

Table 14-1: Geometric data for mineralized structures.

## 14.4 Composites

The estimation method requires that all samples represent the same volume of rock. Since a large majority of the samples are 1 metre long, the length of selected composites is also 1 metre. Compositing the drill hole intersections used all samples in each intersection and generated composites of equal length as close to 1 metre as possible. This approach ensures that all composites in the same intersection represent the same volume of rock. Table 14-2 shows the basic statistics for the composites of each structure.

| Structure | Number of composits | Average grade (Au g/t) | Maximum Grade (Au g/t) | Standard Deviation (Au g/t) | Coefficient of Deviation |
|---|---|---|---|---|---|
| **5B** | 27672 | 2.79 | 438.80 | 6.44 | 2.31 |
| **5B2** | 2188 | 0.67 | 43.52 | 1.78 | 2.67 |
| **5C** | 2940 | 0.85 | 38.42 | 2.66 | 3.12 |
| **5M** | 7678 | 1.75 | 223.70 | 4.90 | 2.81 |
| **5M2** | 1842 | 1.83 | 93.70 | 6.76 | 3.70 |
| **5N** | 7917 | 1.01 | 175.70 | 3.85 | 3.80 |
| **6N1** | 1088 | 0.99 | 50.20 | 3.10 | 3.12 |

Table 14-2: Basic statistics for the composites of each structure.

## 14.5 High-Grade Processing

It is common practice in the industry to cap high gold values when estimating resources. This practice is not related to the accuracy of the analyses, but rather to local representativeness. For example, considering a population of 27,000 analyses with a log-normal distribution, an average of 2.79 g/t and a standard deviation of 6.44 g/t (similar to structure 5B), it would be quite normal to have a dozen samples with more than 100 g/t, or even 2 or 3 samples above 400 g/t. If a subset of a dozen individual samples is extracted from this population, the chances are slim that it will contain 1 sample above 100 g/t. However, if the dozen local samples do contain an exceptional value, this sample carries a disproportionate influence (weight) given its rarity and this will lead to an erroneous assessment of the average grade. For this reason, it is important to limit the influence of extreme values. Simply capping all high values to a certain threshold, as is commonly done, is tantamount to saying that high values are errors, which is not true. For this reason, the author prefers to limit the distance over which a high value can be used. Beyond this distance, the value will be capped to a certain threshold. Ideally, the distance of influence will be equal to 1.5 times the size of the cells. This way, only adjacent cells will use the high values without any limitation.

There are several ways to select the threshold at which values are considered exceptional. All methods are subjective. Professionals will use several methods and, if necessary, apply a conservative capping grade.

The most common method is to look for a positive slope change on the probability curve using a logarithmic scale. A more arbitrary method is to identify the limit on a simple or logarithmic histogram beyond which values are exceptional. This point represents the threshold at which high values are less supported.

When the distribution is log-normal, the Sichel average is very effective. This method is applicable only in the case of log-normal distribution and absolutely useless in other cases. When the distribution is not log-normal, it is possible to estimate the average using a Monte Carlo-type simulation, and then limit the high values so that the average of capped values is equal to the Monte Carlo average.

A method known as Parrish Decile Analysis compares the total amount of metal present in the upper deciles and percentiles. If any one of the following conditions are met, then it may be necessary to cap the high values: 1) the top decile (90-100) contains more than 40% of the total metal; 2) the metal contained in the top decile (90-100) is more than twice that of the previous decile (80-90); or 3) the upper percentile (99-100) contains more than 10% of the total metal.

A less common method is based on changes in the coefficient of variation by gradually discarding the highest values. The capping grade is the point of inflection where this curve becomes much steeper.

Finally, some estimation methods involve a high-grade capping procedure. When such methods are used, further capping of high values is never desirable. Among the best known are indicator and disjunctive kriging, Monte Carlo-type simulations, and a hybrid method developed by Rivoirard in 2009 consisting of co-kriging the truncated high-grade value and the indicator of the high value.

Figure 14-2 below shows the probability curve, density, box plot and selected capping grade for the composites in each structure.

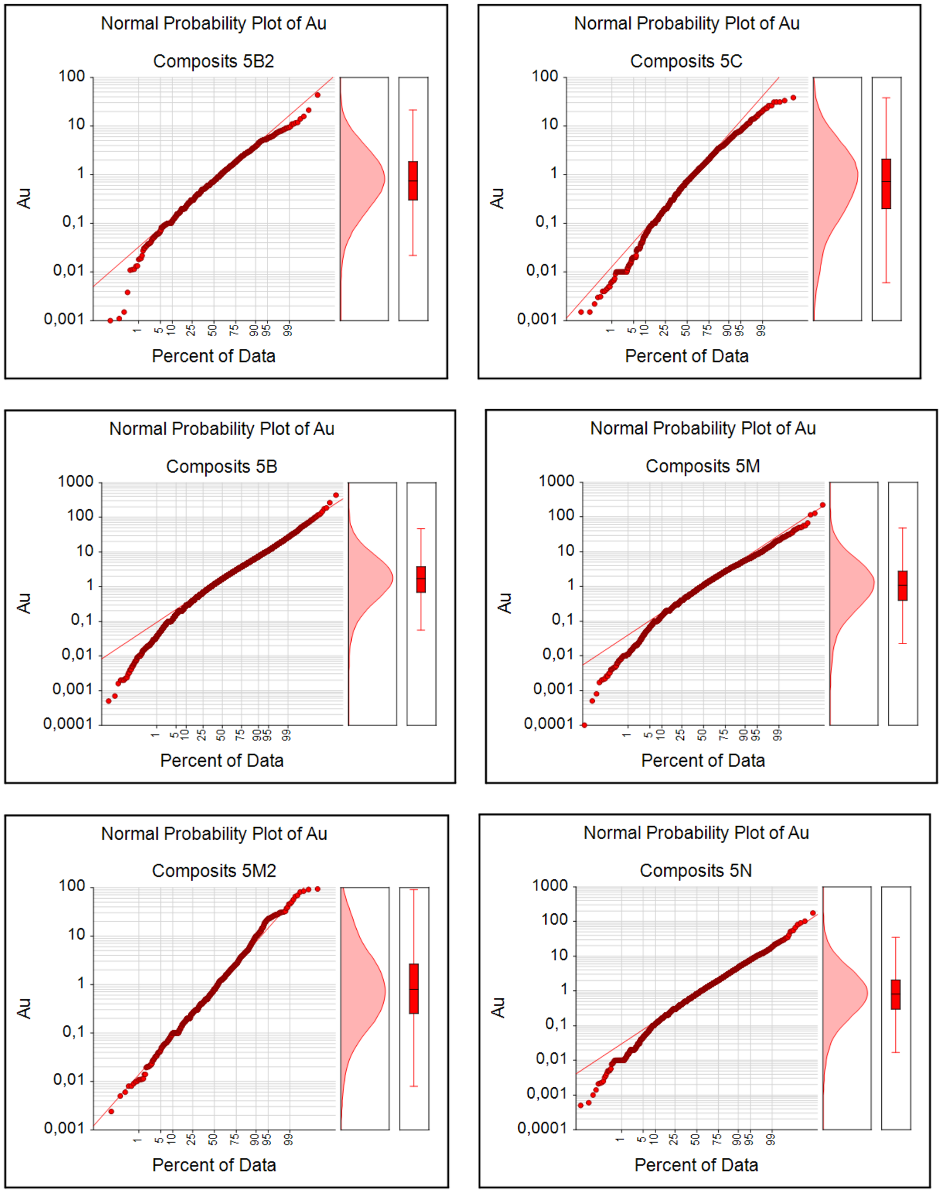


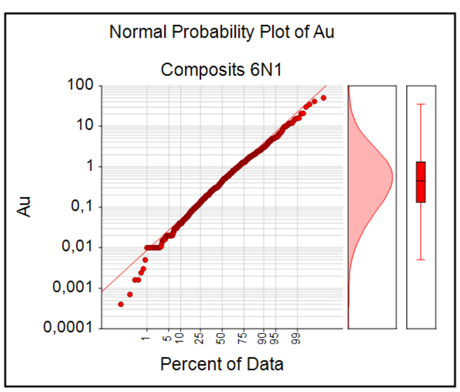


| Structure | Selected capping grade (g/t) | Main criteria for capping selection |
|---|---|---|
| **5B** | 110 | Bootstrapped average and Normal Probability Polt |
| **5B2** | --- | Normal Probability Plot |
| **5C** | --- | Normal Probability Plot |
| **5M** | 40 | Normal Probability Plot |
| **5M2** | 30 | CV vs Top Cut plot, Bootstrapped average and Normal Probability Polt |
| **5N** | 40 | Normal Probability Plot |
| **6N1** | 30 | Bootstrapped average and Normal Probability Polt |

Figure 14-2: High-grade capping.

Since most extreme grades are found in the upper third of the mine, the positive bias they create will be much less important than if they were widespread. In other words, their area of influence is very limited.

Five sectors were defined for the purpose of this study: Mine, Extension (Ext; the sector below the Mine area), East, 6N1 and Other; the latter includes residual resources not included in the other sectors. Figures 14-3 and 14-4 show these sectors.

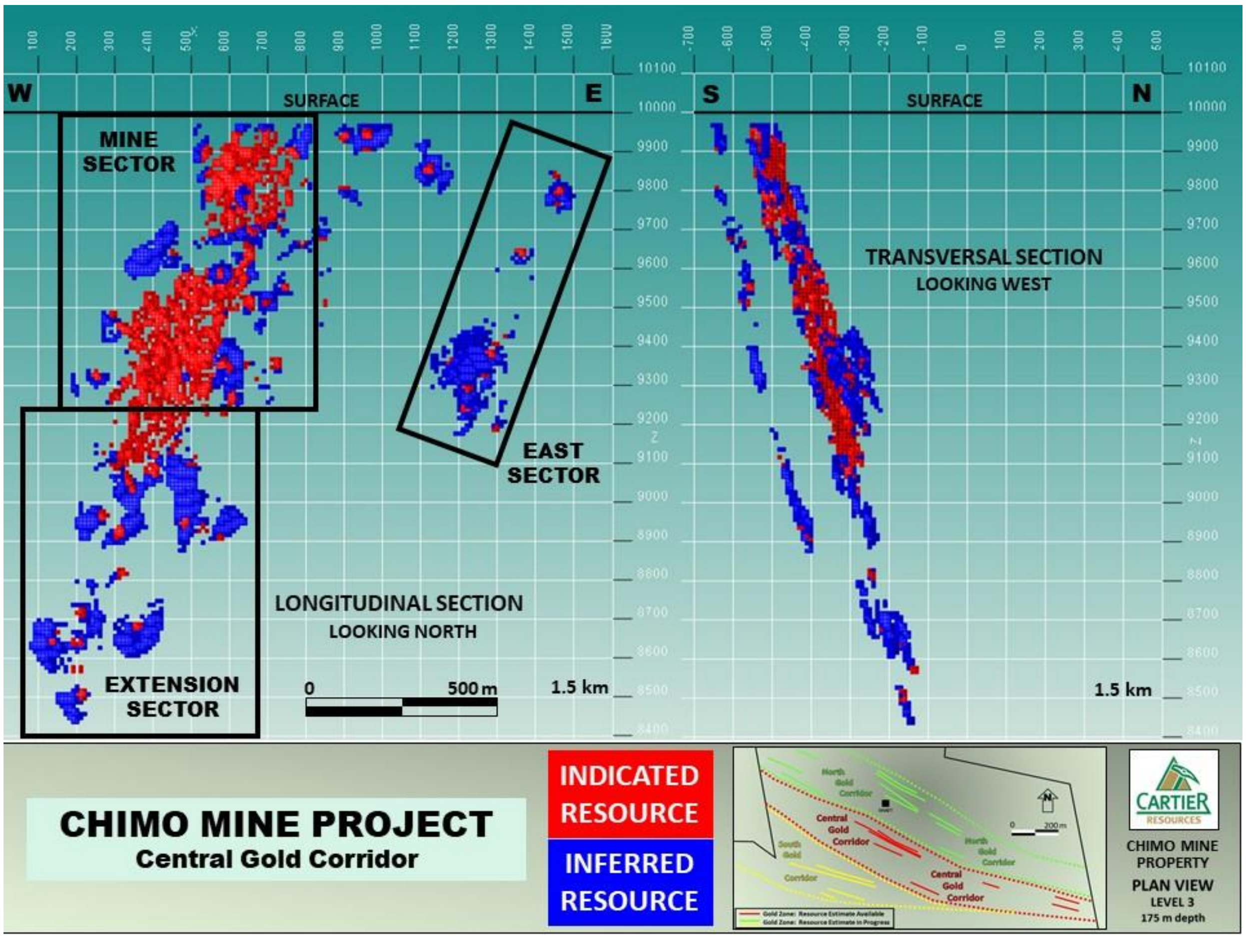


Figure 14-3: Longitudinal section and cross section showing the sectors considered in this study.

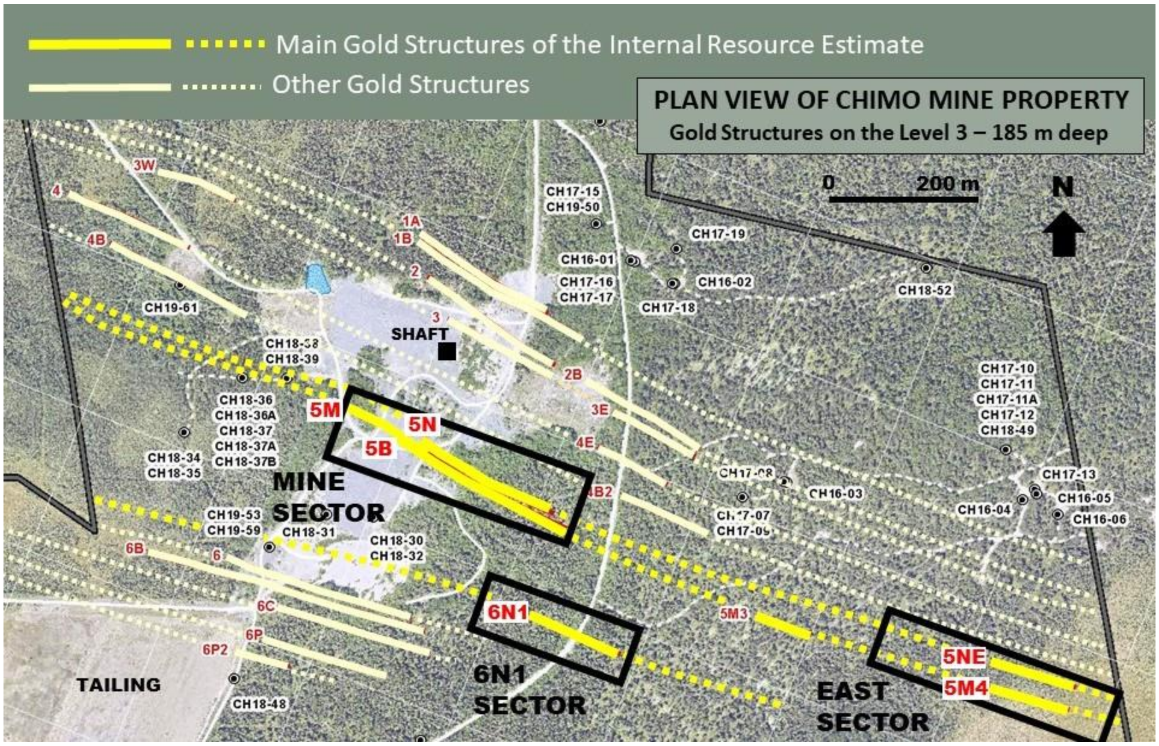


Figure 14-4: Map view of the Chimo Mine Property showing the areas of interest.

## 14.6 Variography

The important statistical differences between each structure require different modelling approaches for each. In addition, significant differences were noted between the different sectors, even within a single structure. The variography was therefore modelled independently for each structure and subsector. Pairwise relative variograms were preferred mainly due to their resistance to exceptionally high samples. Table 14-3 shows the models retained for each subsector. Variogram examples are presented in Figure 14-5.

| Subsector | Contribution | | | Range (m) | | Rotation (°clockwise) | | |
|---|---|---|---|---|---|---|---|---|
| | Nugget | Spherical 1 | Spherical 2 | Portée 1 | Portée 2 | Z-1 | X | Z-2 |
| **5B Extension** | 0.7 | 0.22 | 0.07 | 15 | 80 | -20 | 100 | 70 |
| **5B Regional** | 0.74 | 0.22 | 0.04 | 15 | 88 | -30 | 100 | 0 |
| **5B Mine** | 0.86 | 0.26 | 0.08 | 12 | 60 | -40 | 100 | 70 |
| **5B2** | 0.69 | 0.36 | 0.14 | 12 | 60 | -30 | 100 | 0 |
| **5C Extension** | 0.39 | 0.57 | 0.1 | 14 | 56 | -30 | 100 | 0 |
| **5C Regional** | 0.49 | 0.49 | 0.05 | 22 | 70 | -30 | 100 | 0 |
| **5C Mine** | 0.61 | 0.32 | 0.28 | 6.5 | 70 | -30 | 100 | 0 |
| **5M Extension** | 0.73 | 0.32 | 0.11 | 14 | 125 | -20 | 100 | 60 |
| **5M Regional** | 0.73 | 0.34 | 0.15 | 15 | 176 | -20 | 100 | 60 |
| **5M Mine** | 0.76 | 0.36 | 0.23 | 10 | 100 | -30 | 100 | 80 |
| **5M2 Extension** | 0.49 | 0.46 | 0.24 | 8.6 | 80 | -20 | 100 | 0 |
| **5M2 Regional** | 0.54 | 0.44 | 0.23 | 10 | 110 | -20 | 100 | 0 |
| **5N** | 0.52 | 0.46 | 0.11 | 10 | 50 | -20 | 100 | 0 |
| **6N1** | 0.76 | 0.32 | 0.13 | 30 | 120 | -20 | 100 | 0 |

Table 14-3: Selected models for each subsector.

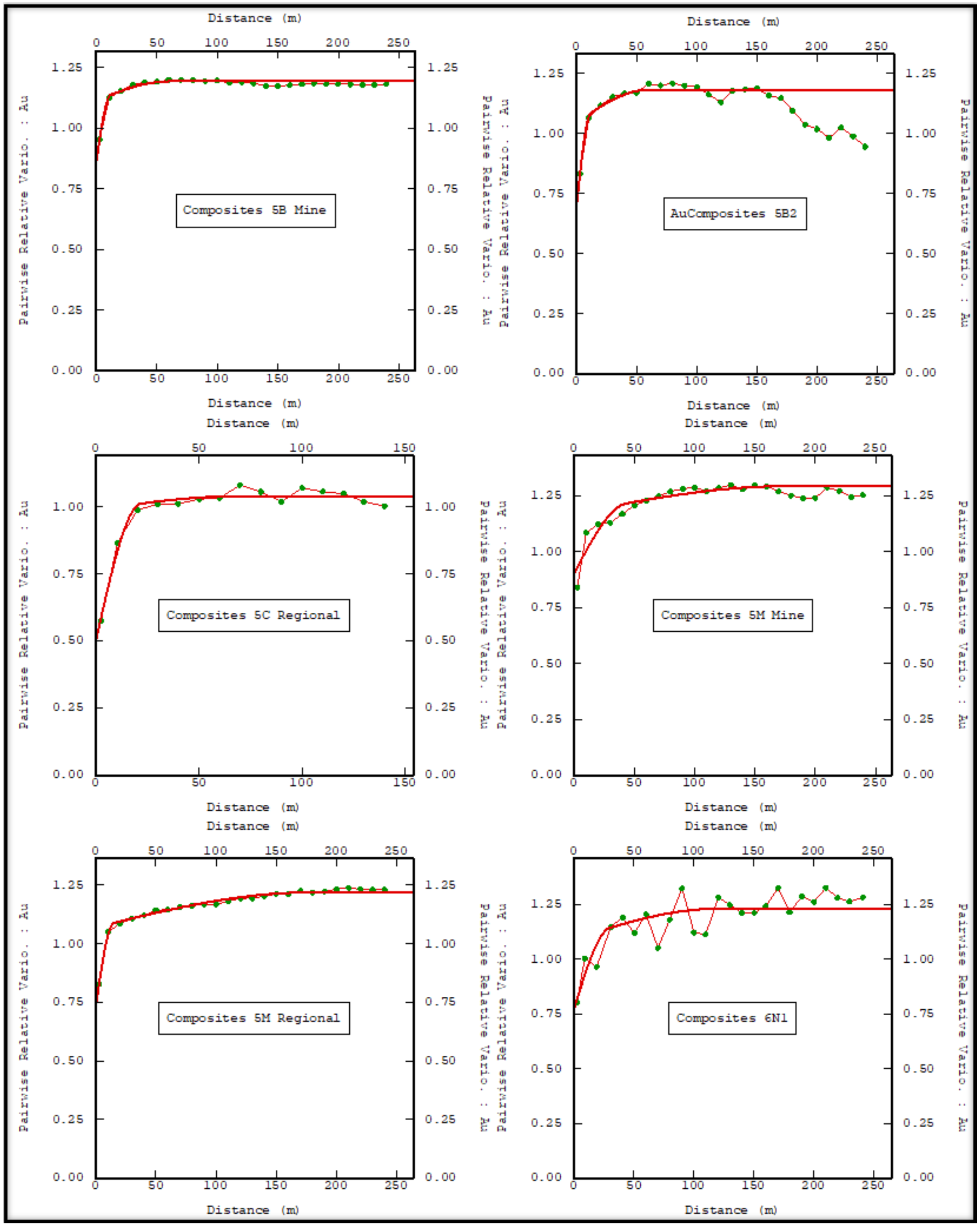


Figure 14-5: Example of variograms.

In general, the nugget effect accounts for 50 to 70%, followed by a spherical structure about 15 m across accounting for 20 to 50% of the total variance. The final structure measures between 80 and 100 m across and accounts for 10 to 20% of the variance. These parameters will largely control the dimensions of the search ellipsoids.

For all cases, the variography was modelled in an isotropic system. The rose diagram of the 5B and 5M structures (except in the 5B regional subsector) clearly shows a strong geometric anisotropy. The author was unable to build a reliable variogram representing this anisotropy. Thus, the geometry of the search ellipsoid used for the 5B and 5M will be built accordingly.

## 14.7 Estimator Selection

Using a linear estimator requires at least second-order stationarity. To test this hypothesis, the author calculated the average, the variance and the coefficient of variation on a grid 30 m by 30 m projected on the longitudinal section. This exercise was repeated for each mineralized structure without taking into account the sector in which it is located. Only cells containing a minimum of 20 composites were selected. Figure 14-6 shows the results of this test for the two most promising structures, 5B and 5M. Even if the second-order stationarity is not perfect, the charts do not show overly large trends or variations. The 5N structure is slightly more problematic. Linear estimators based on variograms should yield satisfactory estimates.

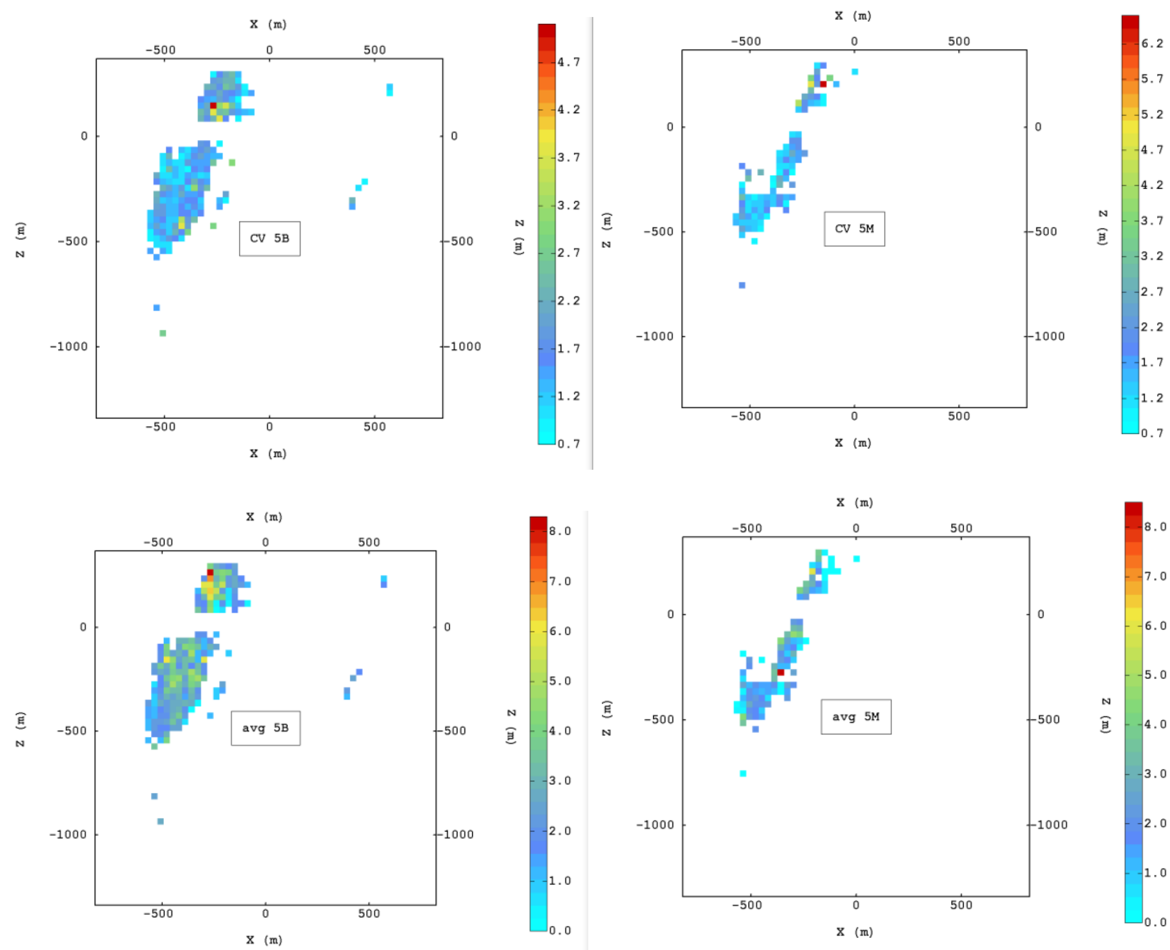

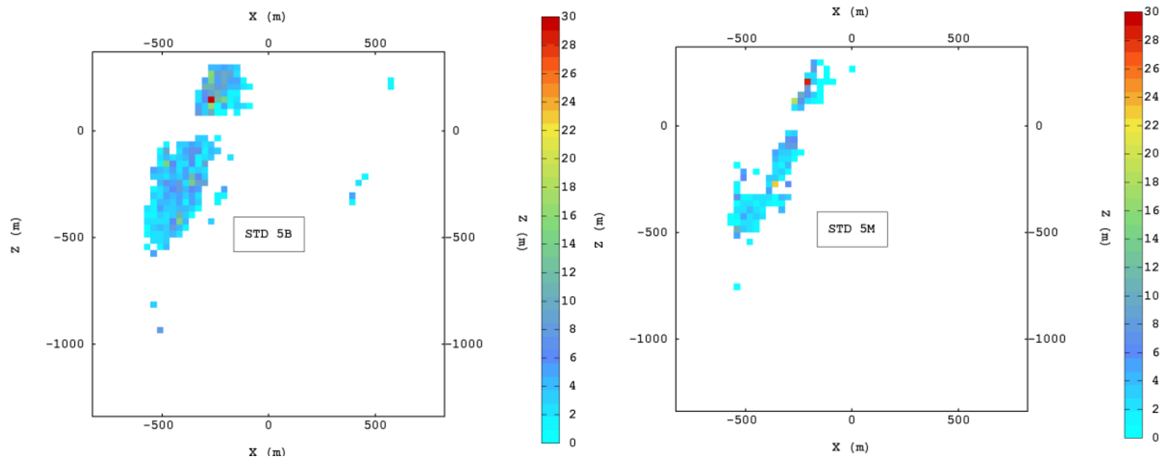

Figure 14-6: Second-order stationarity.

To select the best linear estimator, the author estimated the resources of the 5B structure using six methods or variations thereof and compared the results of this estimate with the average of the intersections of each cell. The methods compared are inverse distance square (ID2), indicator kriging (IK), ordinary kriging (OK), and three variants of ordinary kriging with capping of high values to 30, 70 and 110 g/t. Figure 14-7 shows the differences between each of these estimates and the average of the intersections in the concerned cells. Of these methods, OK without high-grade capping performed the best. The differences are well centred without systematic bias. This method will therefore be used to estimate the resources of the project. However, considering the low contribution of variograms for distances greater than 15 m (section 1.6) and the presence of extreme values associated with certain structures (section 1.5), the author considers it wiser to limit the range of high values (as identified in section 1.6) to a maximum distance of 15 m. This is therefore a limitation of the estimation and not the capping of composites. In this way, the high values will only influence the cell(s) whose centre is 15 m or less.

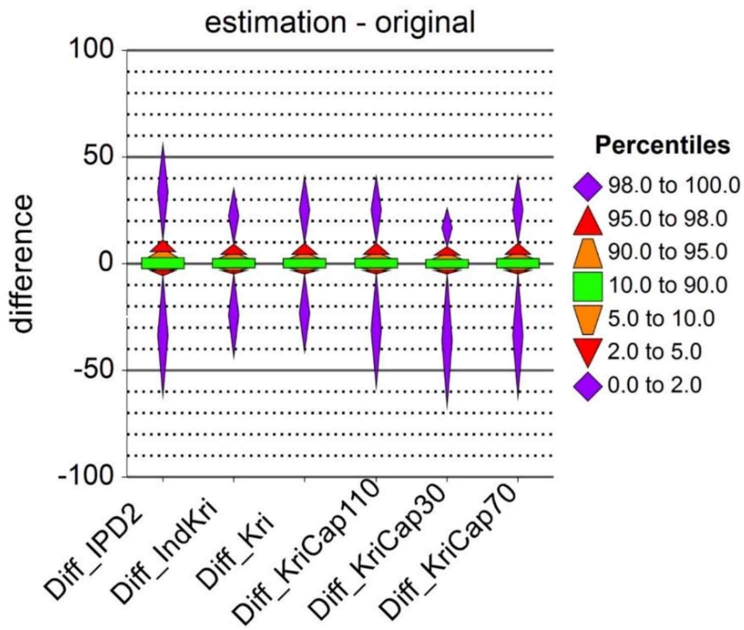


Figure 14-7: Cross-validation.

### 14.8 Neighbourhood Optimization

The optimization of neighbourhood parameters is done in two stages. First, it is important to decide on the maximum number of composites to use (the minimum having been set at 5 to fit with the geometry of the structures). The maximum number of samples to retain was determined by using, in turn, a maximum of 8, 10, 15, 20 and 25 composites for the estimation of each structure. The result for each cell was compared to the average of the intersections in the same cell. The final choice of the maximum number of composites is thus based on local error, absolute error, kriging efficiency (KE) and regression slope. Once this parameter is set, comparison tests are then carried out with and without octants.

The search strategy is carried out in three successive passes. A cell that does not meet the minimum conditions of the first pass will be estimated in the second pass. If it still does not meet the minimum conditions, it will be estimated in the third pass. If the cell still does not meet the minimum conditions of the third pass, it will not be estimated.

During each pass, if the grade of a composite is greater or equal to the capping grade (as described in Figure 14-2), the grade will be used as-is when the distance of the composite to the centre of the cell is less than 15 m. Otherwise, the grade will be capped (as shown in Figure 14-2).

In the case of anisotropic search ellipsoids (Table 14-4), the weighting is done according to ellipsoid distances.

The geometry of the third pass is optimized to reduce any lateral extrapolation at the edge of the structure while favouring vertical extension since the latter is recognized as more consistent over the Project. This compensates for not using the octants feature and results in far fewer geometric problems related to edges.

The geometry of the search ellipsoids is used for resource classification. The cells estimated by the first pass will be classified as indicated, whereas those estimated by the second and third passes will be classified as inferred.

| Subsector | Rotation (°clockwise) | | | First search ellipsoid (m) | | | Second search ellipsoid (m) | | | Third search ellipsoid (m) | | | N. Composites | | ellipsoidal | Higy grade |
|---|---|---|---|---|---|---|---|---|---|---|---|---|---|---|---|---|
| | Z-1 | X | Z-2 | X | Y | Z | X | Y | Z | X | Y | Z | Minimum | Maximum | distance | capping (g/t) |
| **5B Extension** | -20 | 100 | 70 | 22.5 | 15 | 15 | 45 | 30 | 30 | 90 | 65 | 65 | 5 | 12 | oui | 110 |
| **5B Regional** | -30 | 100 | 0 | 15 | 15 | 15 | 30 | 30 | 30 | 90 | 65 | 65 | 5 | 12 | non | 110 |
| **5B Mine** | -40 | 100 | 70 | 22.5 | 15 | 15 | 45 | 30 | 30 | 90 | 65 | 65 | 5 | 12 | oui | 110 |
| **5B2** | -30 | 100 | 0 | 15 | 15 | 15 | 30 | 30 | 30 | 90 | 65 | 65 | 5 | 12 | non | --- |
| **5C Extension** | -30 | 100 | 0 | 15 | 15 | 15 | 30 | 30 | 30 | 90 | 65 | 65 | 5 | 17 | non | --- |
| **5C Regional** | -30 | 100 | 0 | 15 | 15 | 15 | 30 | 30 | 30 | 90 | 65 | 65 | 5 | 17 | non | --- |
| **5C Mine** | -30 | 100 | 0 | 15 | 15 | 15 | 30 | 30 | 30 | 90 | 65 | 65 | 5 | 17 | non | --- |
| **5M Extension** | -20 | 100 | 60 | 22.5 | 15 | 15 | 45 | 30 | 30 | 90 | 65 | 65 | 5 | 17 | oui | 50 |
| **5M Regional** | -20 | 100 | 60 | 22.5 | 15 | 15 | 45 | 30 | 30 | 90 | 65 | 65 | 5 | 17 | oui | 50 |
| **5M Mine** | -30 | 100 | 80 | 22.5 | 15 | 15 | 45 | 30 | 30 | 90 | 65 | 65 | 5 | 17 | oui | 50 |
| **5M2 Extension** | -20 | 100 | 0 | 15 | 15 | 15 | 30 | 30 | 30 | 90 | 65 | 65 | 5 | 17 | non | 30 |
| **5M2 Regional** | -20 | 100 | 0 | 15 | 15 | 15 | 30 | 30 | 30 | 90 | 65 | 65 | 5 | 17 | non | 30 |
| **5N** | -20 | 100 | 0 | 15 | 15 | 15 | 30 | 30 | 30 | 90 | 65 | 65 | 5 | 10 | non | 50 |
| **6N1** | -20 | 100 | 0 | 15 | 15 | 15 | 30 | 30 | 30 | 90 | 65 | 65 | 5 | 10 | non | 30 |

Table 14-4: Neighbourhood parameters.

## 14.9 Block Model

The block model consists of cells 10 x 10 x 10 m, with the X-axis oriented N112. The centre of the lower-left cell is located at coordinate UTM 331355 East, 5319980 North and an elevation of 1335 m. The block model consists of 163 cells along the X-axis, 60 cells along Y and 169 along Z.

## 14.10 Resource Estimate

Cell grades were estimated by OK using the parameters described in sections 1.6 and 1.8. A code matches each composite to a mineralized structure. All composites of a mineralized structure (5B, 5B2, 5C, etc.) can be used, regardless of the sector in question. In other words, sectors represent permeable boundaries for the composites, whereas mineralized structures are hard boundaries.

The volume of each structure in a cell is estimated using a 10 x 10 m needle matrix parallel to the Y-axis (N022) of the block model.

The density used for this estimate is 2.8 g/cm$^3$, regardless of the structure or sector considered.

## 14.11 Cut-off Estimate

By definition, the cut-off is the grade at which the production costs equal the revenue. Table 14-5 shows the parameters used to estimate the cut-off grade.

| "Cut off" estimate | |
|---|---|
| Averaged gold value within the last 3 years. | 1 680.00 CAN$/oz |
| environmental cost | 1.50 CAN$/t (metric) |
| Mining cost (long hole) | 90.00 CAN$/t (metric) |
| Custom milling | 25.00 CAN$ /t (metric) |
| Transportation | 20.00 CAN$/t (metric) |
| Recovery | 90.00% |
| | |
| **Calculated "CutOff"** | **2.81 g/t** |

Table 14-5: Parameters used to determine the cut-off grade.

The exchange rate used is USD1.30/CAD per ounce giving a gold price of US $ 1,292 / oz.

Given the physical properties of the mineralized rock (colour and arsenopyrite), it is reasonable to anticipate a 35% reduction in milling and transportation fees if rock sorting takes place on-site. This will push the cut-off to 2.48 g/t. It is important to note that these costs are dynamic and can vary significantly over time. Therefore, they must be reviewed regularly. The author believes that a cut-off of 2.50 g/t represents the fair value of the potential of the Project. This is the reference value for this study.

The selection of reasonable prospective parameters, which assume that some or all of the estimated resources could potentially be extracted, is based on an underground bulk mining scenario (2,000 – 3,000 tonnes per day) combined with material sorting at surface on mining site.

### 14.12 Resource Tables

The mineral resources presented in this Technical Report are not mineral reserves as economic viability has not been demonstrated. The selection of reasonable prospective parameters, which assume that some or all of the estimated resources could eventually be extracted, is based on an underground bulk mining scenario. So far, there is no guarantee that any or all of the presumed resources will ever be converted to the indicated resource category.

Resources are presented in situ for an undiluted underground operation and are considered to have a reasonable outlook for economic extraction.

Using a cut-off grade of 2.50 g/t, the Indicated Resources amount to 3,263,300 tonnes at a grade of 4.40 g/t, for a total of 461,280 troy ounces. The Inferred Resources amount to 3,681,600 tonnes at a grade of 3.53 g/t, for a total of 417,250 troy ounces. Table 14-6 assesses the sensitivity of the mineral resource estimate to market fluctuations. According to the author, this mineral resource estimate reflects the current state of knowledge for the Project.

| Indicated Resource | | | | | Inferred Resource | | | |
|---|---|---|---|---|---|---|---|---|
| Cut Off Grade (g/t Au) | Metric Ton (t) | Grade (g/t Au) | Troy Ounce (oz) | | Cut Off Grade (g/t Au) | Metric Ton (t) | Grade (g/t Au) | Troy Ounce (oz) |
| 1.5 | 6 157 300 | 3.24 | 642 060 | | 1.5 | 8 520 400 | 2.62 | 716 570 |
| 2.0 | 4 479 300 | 3.81 | 548 380 | | 2.0 | 5 591 300 | 3.09 | 555 530 |
| **2.5** | **3 263 300** | **4.40** | **461 280** | | **2.5** | **3 681 600** | **3.53** | **417 250** |
| 3.0 | 2 389 100 | 5.01 | 384 540 | | 3.0 | 2 347 800 | 3.97 | 299 800 |
| 3.5 | 1 759 400 | 5.63 | 318 680 | | 3.5 | 1 199 000 | 4.66 | 179 470 |
| 4.0 | 1 255 900 | 6.40 | 258 410 | | 4.0 | 728 300 | 5.25 | 122 950 |

Table 14-6: Results of the mineral resource estimate at different cut-off grades.

The mineral resources are contained in several different structures, which are subdivided into several sectors and subsectors. The Mine sector is adjacent to existing mine workings. Figures 14-3, 14-4 and 14-8 illustrate the location of the different sectors considered in this study. The Ext sector represents the deep extension below the Mine sector. The East sector is located 450 m east of the Mine sector. The Muck sector lies within the Mine sector and represents a block of rock affected by a collapse.

Table 14-7 presents the breakdown of ounces by sector at a 2.50 g/t cut-off and Figures 14-3 and 14-8 provide a 3D representation of the distribution.

| Indicated Resource | | | | |
|---|---|---|---|---|
| **Sector** | **Structure** | **Metric Ton (t)** | **Grade (g/t Au)** | **Troy ounce (oz)** |
| Mine | 5B | 1 766 200 | 4.54 | 257 800 |
| | 5B2 | 8 600 | 3.01 | 840 |
| | 5C | 91 700 | 4.07 | 12 000 |
| | 5M | 387 900 | 4.22 | 52 630 |
| | 5M2 | 34 200 | 5.58 | 6 140 |
| | 5N | 203 900 | 4.78 | 31 340 |
| | **Sub Total** | 2 492 500 | 4.50 | 360 740 |
| Ext | 5B | 101 500 | 3.76 | 12 270 |
| | 5B2 | 0 | 0 | 0 |
| | 5C | 14 900 | 3.64 | 1 740 |
| | 5M | 49 100 | 3.95 | 6 230 |
| | 5M2 | 62 500 | 5.84 | 11 740 |
| | 5N | 0 | 0 | 0 |
| | **Sub Total** | 228 000 | 4.36 | 31 990 |
| East | 5B | 100 800 | 3.49 | 11 310 |
| | 5B2 | 0 | 0 | 0 |
| | 5C | 0 | 0 | 0 |
| | 5M | 23 800 | 3.90 | 2 990 |
| | 5M2 | 0 | 0 | 0 |
| | 5N | 109 100 | 4.02 | 14 110 |
| | **Sub Total** | 233 700 | 3.78 | 28 400 |
| Other | 5B | 46 400 | 3.56 | 5 310 |
| | 5B2 | 0 | 0 | 0 |
| | 5C | 7 900 | 4.32 | 1 100 |
| | 5M | 12 600 | 3.94 | 1 600 |
| | 5M2 | 0 | 0 | 0 |
| | 5N | 24 700 | 3.03 | 2 410 |
| | **Sub Total** | 91 600 | 3.53 | 10 420 |
| Muck | 5B | 87 700 | 4.55 | 12 830 |
| | 5M | 100 | 2.61 | 10 |
| | 5M2 | 0 | 0 | 0 |
| | 5N | 0 | 0 | 0 |
| | **Sub Total** | 87 800 | 4.55 | 12 840 |
| 6N1 | Upper | 113 300 | 4.00 | 14 570 |
| | Lower | 16 300 | 4.44 | 2 330 |
| | **Sout Total** | 129 600 | 4.06 | 16 900 |
| **TOTAL** | | **3 263 300** | **4.40** | **461 280** |

| Inferred Resource | | | | |
|---|---|---|---|---|
| **Sector** | **Structure** | **Metric Ton (t)** | **Grade (g/t Au)** | **Troy ounce (oz)** |
| Mine | 5B | 114 400 | 3.48 | 12 800 |
| | 5B2 | 0 | 0 | 0 |
| | 5C | 80 000 | 3.24 | 8 330 |
| | 5M | 55 200 | 3.56 | 6 320 |
| | 5M2 | 1 200 | 3.66 | 140 |
| | 5N | 141 800 | 3.18 | 14 500 |
| | **Sub Total** | 392 600 | 3.33 | 42 090 |
| Ext | 5B | 520 100 | 3.63 | 60 700 |
| | 5B2 | 0 | 0 | 0 |
| | 5C | 107 500 | 3.30 | 11 400 |
| | 5M | 118 700 | 3.27 | 12 480 |
| | 5M2 | 219 700 | 3.11 | 21 970 |
| | 5N | 0 | 0 | 0 |
| | **Sub Total** | 966 000 | 3.43 | 106 550 |
| East | 5B | 620 500 | 3.26 | 65 030 |
| | 5B2 | 0 | 0 | 0 |
| | 5C | 0 | 0 | 0 |
| | 5M | 88 900 | 3.29 | 9 400 |
| | 5M2 | 0 | 0 | 0 |
| | 5N | 458 900 | 4.25 | 62 700 |
| | **Sub Total** | 1 168 200 | 3.65 | 137 140 |
| Other | 5B | 311 800 | 3.29 | 32 980 |
| | 5B2 | 0 | 0 | 0 |
| | 5C | 23 900 | 3.70 | 2 840 |
| | 5M | 94 200 | 3.59 | 10 870 |
| | 5M2 | 0 | 0 | 0 |
| | 5N | 39 000 | 3.40 | 4 260 |
| | **Sub Total** | 468 900 | 3.38 | 50 960 |
| Muck | 5B | 0 | 0 | 0 |
| | 5M | 0 | 0 | 0 |
| | 5M2 | 0 | 0 | 0 |
| | 5N | 0 | 0 | 0 |
| | **Sub Total** | 0 | 0 | 0 |
| 6N1 | Upper | 435 000 | 3.49 | 48 810 |
| | Lower | 250 900 | 3.93 | 31 700 |
| | **Sub Total** | 685 900 | 3.65 | 80 520 |
| **TOTAL** | | **3 681 600** | **3.53** | **417 250** |

Table 14-7: Mineral resource estimate by area.

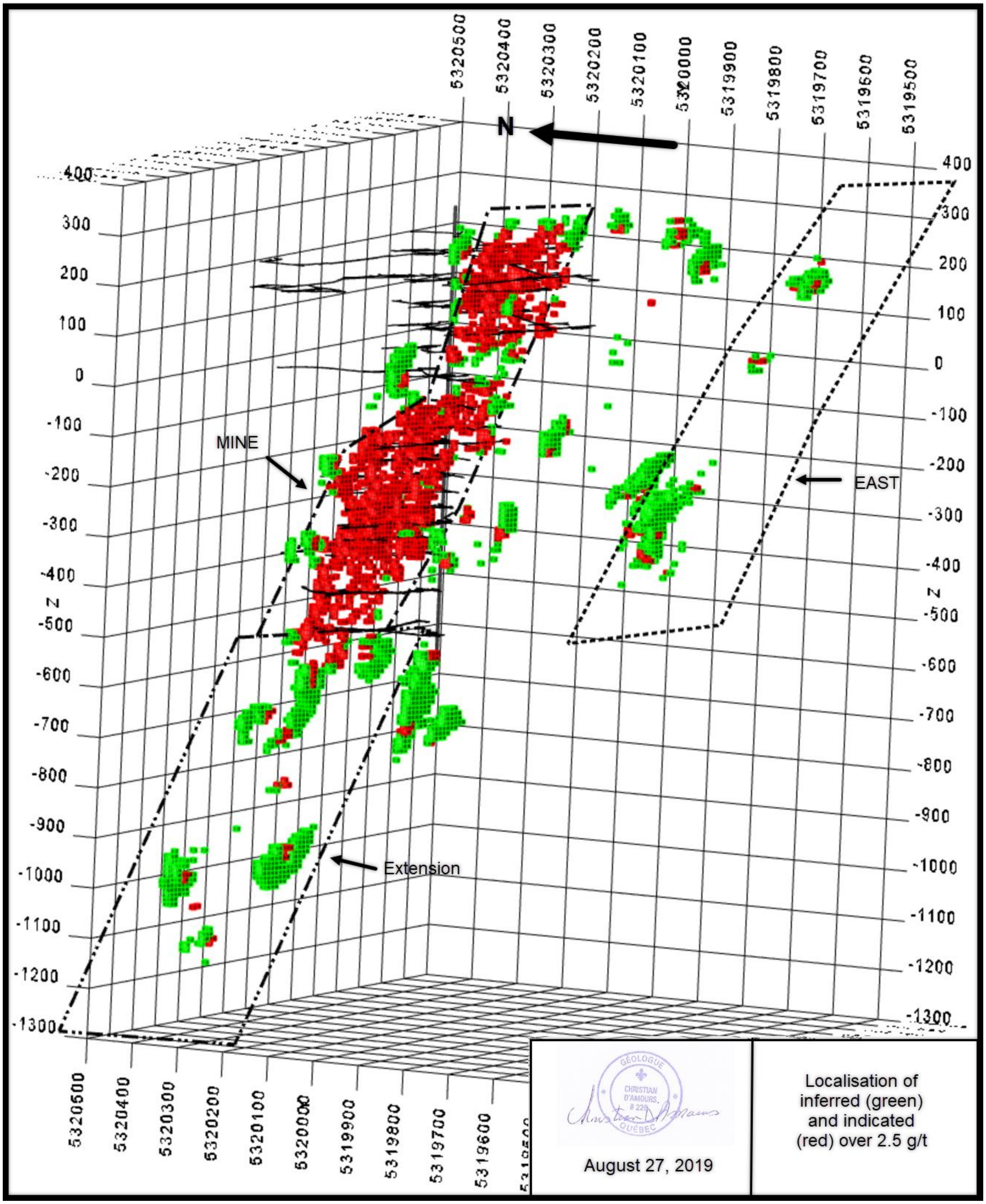


Figure 14-8: Location of inferred (green) and indicated (red) resources at a cut-off of 2.5 g/t Au.

### 14.13 Validation

To validate these results, the author estimated the production from stopes mined out by CAMBIOR between 1990 and 1996. Since some stopes may overlap more than one structure (according to the current model), the stope envelopes were initially separated by taking into account the current structural boundaries. The same estimation procedures outlined above were then applied to the calculated volumes. The cut-off grade and resource classification do not apply. Table 14-8 shows that this estimate reconciles very well (less than 5% difference) with mill feed data. This audit increases the level of confidence for sectors with a high density of information.

For less densely drilled sectors, the only possible validation was by visual inspection on cross sections and longitudinal sections. Again, the agreement between results seems very good. The author is convinced that this estimate provides a fair portrait of the resources currently known on the Project.

| Stope estimation | | | |
|---|---|---|---|
| **Structure** | **Metric Ton (t)** | **Grade (g/t Au)** | **Troy Ounce (oz)** |
| 5B | 922 322 | 4.13 | 122 508 |
| 5C | 21 810 | 3.32 | 2 329 |
| 5M | 104 917 | 3.10 | 10 452 |
| 5M2 | 14 349 | 5.12 | 2 362 |
| 5N | 54 427 | 3.19 | 5 577 |
| **TOTAL** | **1 117 826** | **3.99** | **143 228** |
| **Mill feed (Cambior 1990-1996)** | | | |
| **TOTAL** | **1 175 658** | **3.87** | **146 378** |
| difference | (57 832) | | (3 150) |
| difference % | -4.92% | | -2.15% |

Table 14-8: Reconciliation of stope estimates in this study and mill feed data from 1990 to 1996.

## 15 MINERAL RESERVE ESTIMATES

This item is not required for this technical report and mineral resource estimate.

## 16 MINING METHODS

This item is not required for this technical report and mineral resource estimate.

# 17 RECOVERY METHODS

This item is not required for this technical report and mineral resource estimate.

## 18 PROJECT INFRASTRUCTURE

This item is not required for this technical report and mineral resource estimate.

# 19 MARKET STUDIES AND CONTRACTS

This item is not required for this technical report and mineral resource estimate.

# 20 ENVIRONMENTAL STUDIES, PERMITTING AND SOCIAL OR COMMUNITY IMPACT

This item is not required for this technical report and mineral resource estimate.

## 21 CAPITAL AND OPERATING COSTS

This item is not required for this technical report and mineral resource estimate.

## 22 ECONOMIC ANALYSIS

This item is not required for this technical report and mineral resource estimate.

## 23 ADJACENT PROPERTIES

The Property is located in the Val-d'Or mining camp. It is surrounded on all sides by properties belonging to O3 Mining Inc. (O3). The East Cadillac Property owned by O3 contains the Nordeau West deposit, for which the latest 43-101 technical report was prepared by Langton *et al.*, 2019 (MRB & Associates). The report presents the following mineral resource estimate:

- Indicated resources of 226,000 t at 4.19 g/t Au for 30,400 ounces of gold, and inferred resources 1,271,900 t at 4.14 g/t Au for 169,400 ounces of gold.

The Nordeau West deposit is located immediately east of the Property (Figure 7-4). The author has been unable to verify the information regarding the Nordeau deposit. The information presented here is not necessarily indicative of the mineralization of the Property that is the subject of this report.

## 24 OTHER RELEVANT DATA AND INFORMATION

GéoPointCom is not aware of any other relevant data and information that could have a significant impact on the interpretation and conclusions presented in this report.

## 25 INTERPRETATION AND CONCLUSIONS

GéoPointCom has verified all available data as well as the procedures and processing methods. GéoPointCom believes that the information presented in this report provides a fair and accurate picture of the Property's potential.

The Property is located in the Val-d'Or mining camp, a 50-km drive east of the city of Val-d'Or. Mining infrastructure is still present at the site and could facilitate the transition to a more advanced stage of exploration.

This Technical Report presents the maiden mineral resource estimate for the Central Corridor since CAMBIOR closed the mine in 1997. Using a cut-off of 2.50 g/t, the Indicated Resources amount to 3,263,300 tonnes at a grade of 4.40 g/t Au, for a total of 461,280 troy ounces. The Inferred Resources amount to 3,681,600 tonnes at a grade of 3.53 g/t Au, for a total of 417,250 troy ounces. Table 1-2 assesses the sensitivity of the mineral resource estimate to market fluctuations. According to the author, this mineral resource estimate reflects the current state of knowledge on the Project. The mineral resources presented in this Technical Report are not mineral reserves as economic viability has not been demonstrated.

| Indicated Resource | | | | | Inferred Resource | | | |
|---|---|---|---|---|---|---|---|---|
| Cut Off Grade (g/t Au) | Metric Ton (t) | Grade (g/t Au) | Troy Ounce (oz) | | Cut Off Grade (g/t Au) | Metric Ton (t) | Grade (g/t Au) | Troy Ounce (oz) |
| 1.5 | 6 157 300 | 3.24 | 642 060 | | 1.5 | 8 520 400 | 2.62 | 716 570 |
| 2.0 | 4 479 300 | 3.81 | 548 380 | | 2.0 | 5 591 300 | 3.09 | 555 530 |
| **2.5** | **3 263 300** | **4.40** | **461 280** | | **2.5** | **3 681 600** | **3.53** | **417 250** |
| 3.0 | 2 389 100 | 5.01 | 384 540 | | 3.0 | 2 347 800 | 3.97 | 299 800 |
| 3.5 | 1 759 400 | 5.63 | 318 680 | | 3.5 | 1 199 000 | 4.66 | 179 470 |
| 4.0 | 1 255 900 | 6.40 | 258 410 | | 4.0 | 728 300 | 5.25 | 122 950 |

Table 25-1: Sensitivity of the mineral resource estimate to market fluctuations.

These mineral resources are not mineral reserves as their economic viability has not been demonstrated. The tonnage and grade of the inferred resources reported in this mineral resource estimate is uncertain and there can be no assurance that some or all of the inferred mineral resources may be converted to the indicated category with further exploration drilling.

The mineral resource estimate is in accordance with the current standards and guidelines of the Canadian Institute of Mining, Metallurgy and Petroleum (CIM) and NI 43-101 for the publication of mineral resources.

Resources are presented in situ for an undiluted underground scenario and considered to have a reasonable outlook for economic extraction.

The mineral resources were estimated at a cut-off grade of 2.5 g/t Au and calculations used the following key parameters:

Gold price of US $1,292 per ounce;

Exchange rate of USD1.30/CAD per ounce;

Mining and hoisting cost of $90 per tonne;

Transportation cost of $20 per tonne;

Milling cost of $25 per tonne;

Recovery percentage of 90%;

Given the physical properties of the minerals (quartz and arsenopyrite) associated with gold, it is reasonable to expect a 35% reduction in transportation and milling costs if material sorting takes place at surface on the Chimo mine site. This cost reduction produces a calculation of 2.5 g/t Au for the cut-off grade. It is important to note that these costs are dynamic and may vary over time. Therefore, they must be re-evaluated regularly according to market conditions. The author estimates that the threshold of 2.5 g/t Au for the cut-off grade represents the fair value of the potential of this project and that this value constitutes the reference value for this study. The selection of reasonable prospective parameters, which assume that some or all of the estimated resources could potentially be extracted, is based on a bulk underground mining scenario involving a daily extraction rate of approximately 2,000 to 3,000 tonnes.

A density of 2.8 g/cm$^3$ was used.

The estimate was made from a database as at July 2$^{nd}$, 2019, of 3,429 drill holes totalling 279,670 m drilled, 13,477 deviation (hole orientation) measurements and 79,236 samples analyzed for gold and collected over a core length of 85,647 m representing 35% of the drilled core length. This database contains 2,107 blank and standard samples, inserted by Cartier between November 1, 2016, and July 2, 2019. This database validated before starting the resource estimate. The estimate was carried out on seven (7) mineralized structures intersected by 51,029 m of drilling, producing 5,364 different gold intersections.

A high-grade cap of 30 g/t Au (5M2 and 6N1 structures), 50 g/t Au (5M and 5N structures) and 110 g/t Au (5B structure) was applied for the interpolation on composites located more than 15 m from the centre of the estimated cell.

Underground openings (open and backfill-cemented stopes, drifts, raises and shafts) were modelled from cross-sectional and longitudinal sections as well as detailed historical geological maps and mining plans. Historical underground production has been subtracted from the resource estimate. The reconciliation of the resource estimate to the detailed feed information at the plant between 1990 and 1996 shows a difference of only 4.92% in the tonnage extracted and 2.15% in ounces produced.

This mineral resource estimate has been prepared using GeoticMine (v.1.2.14) and Isatis (v.1208.3) software. GeoticMine was used for 3D modelling of topographic and bedrock surfaces, mined sites and various underground openings as well as the interpretation of gold structures. Each structure has been defined by individual meshes. Isatis was used for geostatistics and resource estimation on a percent block model. Statistical studies were performed with NCSS (v. 12) and Microsoft Excel software. The grade interpolation was performed using the OK method, based on 1.0 m composites and 10 m x 10 m x 10 m blocks.

The mineral resource estimate presented here is classified as inferred and indicated. The indicated category is defined by interpolation using a research ellipsoid with an average radius of 20 m for Pass 1. The inferred category is defined by interpolation using a research ellipsoid having an average radius of 40 m for pass 2 and 80 m for Pass 3. Cells that were not estimated during one pass were estimated in the next pass, except for Pass 3.

## 26 RECOMMENDATIONS

GéoPointCom recommends continuing the current resource estimation to include the North and South corridors in order to provide a complete estimate of the current state of resources for the three known gold corridors on the Property. The resource estimation for the North and South gold corridors should begin as soon as possible. This work is expected to take approximately 10 to 12 weeks at a total cost of approximately $60,000.

Concurrently, drilling should continue in order to expand resources at depth in the extensions of zones 5B4-5M4-5NE at a distance of 450 m to the east of the underground workings, as well as around the periphery of Zone 6N1, which is located 125 m from the underground infrastructure. The objective of this program would be to add gold mineralization over a vertical distance of 600 m below zones 5B4-5M4-5NE between depths of 700 m and 1,300 m and to increase the width of zone 6N1 over a vertical distance of 500 m between depths of 600 m and 1,100 m. Drilling began on November 19, 2019, and is expected to be completed in July 2020. To achieve this goal, 11 km of controlled directional precision drilling will be required at an estimated cost of $2.5 million.

## 27 REFERENCES


Ayer, J., Amelin, Y., Corfu, F., Kamo, S., Ketchum, J. F., Kwok, K., Trowell, N. F. (2002): Evolution of the Abitibi greenstone belt based on U-Pb geochronology: Autochthonous volcanic construction followed by plutonism, regional deformation and sedimentation. Precambrian Research, v. 115, p. 63–95.

Bateman, R., Ayer, J. A., Dubé, B. (2008): The Timmins-Porcupine gold camp, Ontario: Anatomy of an Archean greenstone belt and ontogeny of gold mineralizations. Economic Geology, v. 103, p. 1285–1308.

Beauregard, A. J., Gaudreault, D., D'Amours, C. (2012): NI 43-101 Technical Report on the Akasaba property, province of Québec, Canada as of May 1, 2012. Prepared by Geological Groupe – Conseil for Alexandria Minerals Corporation, 161 p. Sedar website.

Beauregard, A. J., Gaudreault, D. (2014): NI 43-101 Technical Report on the Sleepy Lake Property, Province of Québec, Canada. Prepared by Geological Groupe – Conseil for Alexandria Minerals Corporation, 76 p. Sedar website.

Beausoleil, C., Pelletier, C., Faure, S., Noël, G. (2019): NI 43-101 Technical Report and Mineral Resource Estimate for the Kiena Mine Complex, Québec. Prepared for Wesdome, 183 p.

Benn, K., Miles, W., Ghassemi, M. R., Gillet, J. (1994): Crustal structure and kinematic framework of the north-western Pontiac Subprovince, Québec: an integrated structural and geophysical study. Canadian Journal; of Earth Sciences, Vol. 31, p. 271-281.

Benn, K., Peschler, A. P. (2005): A detachment fold model for fault zones in the Late Archean Abitibi greenstone belt. Tectonophysics, v. 400, p. 85–104.

Berclaz, A. (1993): Étude métamorphique de la région du Front de Grenville à l'est de Louvicourt, Abitibi, Québec. Thèse de Maîtrise, Université Laval, 244 p.

Buchan, K. L.; Ernst, R. E. (2004): Essaims de dykes de diabase et unités apparentées au Canada et dans les régions avoisinantes. Geological Survey of Canada, "A" Series Map no. 2022A.

Campiglio, C. (1977): Batholite de Bourlamaque, ES-26, Ministère des Richesses Naturelles du Québec, 211 p.

Card, K. D., Ciesielski, A. (1986): DNAG No.1 – Subdivisions of the Superior Province of the Canadian Shield. Geoscience Canada, v13, p.5-13.

Colvine, A.C., Fyon, J. A., Heather, K. B., Marmont, S., Smith, P. M., Troop, D. G. (1988): Archean lode gold deposits in Ontario. Ontario Geological Survey, miscellaneous paper 139, 136 p.

Daigneault, R., Mueller, W. U., Chown, E. H. (2004): Abitibi greenstone belt plate tectonics: the diachronous history of arc development, accretion and collision. In Eriksson, P. G., Altermann, W., Nelson, D. R., Mueller, W. U., Catuneanu, O. (Eds.). The Precambrian Earth: Tempos and Events, Series: Developments in Precambrian geology, vol. 12, Elsevier, p. 88-103. Couture, J. P., Pilote, P., Machado, N., and Desrochers, J., P. (1994): Timing of gold mineralization in the Val-d'Or district, Southern Abitibi belt: Evidence for two distinct mineralizing events. Economic Geology, v. 89, p. 1542-1551.

Davis, D. W. (2000): Report on U-Pb geochronology of rocks from Québec, march 11 2000. Ministère des Ressources naturelles, Québec. Rapport interne 5 p., 12 figures.

Dimroth, E, Imrech, L., Rocheleau, M., Goulet, N. (1983): Evolution of the southcentral part of the Archean Abitibi Belt, Québec. Part III: plutonic and metamorphic evolution and geotectonic model. Canadian Journal of Earth Sciences, Vol. 20, pages 1374-1388.

Dubé, B., Gosselin, P. (2007): Greenstone-hosted quartz–carbonate vein deposits. In Goodfellow, W. D. (ed). Mineral deposits of Canada: a synthesis of major deposit-types, district metallogeny, the evolution of geological provinces, and exploration methods.

Eisenlohr, B. N., Groves, D. I., Partington, G. A. (1989): Crustal-scale shear zones and their significance to Archean gold mineralization in Western Australia. Mineralium Deposita, v. 24(1), pp.1–8.

Faure, S. (2015): Le segment volcanique Taschereau-Amos-Senneterre (Abitibi) et son potentiel métallogénique pour l'or et les métaux de base. Projet 2015-01, Consorem, 58 p.

Gaudreau, R., Lacoste, P and Rocheleau, M. (1986): Géologie et gitologie du secteur de Louvicourt-Vauquelin, Abitibi. Ministère de l'Énergie et des Ressources du Québec, Report MB 86-67.

Goutier, J., Melançon, M. (2007): Compilation géologique de la Sous-province de l'Abitibi (version préliminaire): Ministère des Ressources naturelles et de la Faune du Québec.

Groves, D.I., Goldfarb, R.J., Gebre-Mariam, M., Hagemann, S.G. and Robert, F. (1998): Orogenic gold deposits - a proposed classification in the context of their crustal distribution and relationship to other gold deposit types. Ore Geology Reviews 13, 7-27.

Hagemann, S.G. and Cassidy, K.F. (2000): Archean orogenic lode gold deposits: Society of Economic Geologists Reviews, v. 13, p. 9-68.

Houle, N. (1995): Projet Chimo, Campagne de sondage 1995, Canton Vauquelin, SNRC 32C03, 303 p.

Jolly, W.T. (1978): Metamorphic history of the Archean Abitibi belt, *in* Fraser, J.A. and Heywood, W.W., *eds.*, Metamorphism in the Canadian Shield, Geological Survey of Canada, Paper 78-10.

Langton, J., Jourdain, V. (2019): NI 43-101 Technical Report and Mineral Resource Estimate for the East Cadillac Gold Project, Québec. Prepared for Chalice Gold Mines Ltd, 204 p.

Monecke, T., Mercier-Langevin, P., Dubé, B. (2017): Chapter 1. Geology of the Abitibi Greenstone Belt: Reviews in Economic Geology, vol. 19.

Moorhead, J., Vorobiev, L., Tremblay, A. (2000): Caractéristiques lithogéochimiques et corrélations lithostratigraphiques des roches volcaniques du secteur du canton Vauquelin, Sous-province de l'Abitibi, Québec, MB 2000-16, 60 p.

Mueller, W. U., Donaldson, J. A. (1992): Development of sedimentary basins in the Archean Abitibi belt, Canada: an overview. Can. J. Earth Sci. 29, 2249–2265.

Powell, W. D., Carmichael, D. M., Hodgon, C. J. (1993): Thermobarometry in a subgreenschist to greenschist transition in metabasite of the Abitibi greenstone belt, Superior Province, Canada. Journal of Metamorphic Geology, Vol. 11, p. 165-178.

Plouffe, C. (1990): Analyse structural et contrôles de la minéralisation aurifère de la Mine Chimo, Canton de Vauquelin, Abitibi, Québec. Mémoire de maîtrise, Université du Québec à Montréal, Montréal, 152 p.

Racine, M. (1989): La Zone Tectonique de Cadillac à l'est de Val-d'Or: Exemple du complexe structural de Trivio, Canton Vauquelin. Thèse de maîtrise non publiée, Université Laval, 79 p.

Rafini, S. (2015): Assurance et contrôle de la qualité (QA/QC) en exploration minérale: synthèse et évaluation des usages. Projet 2013-05, Consorem, 52 p.

Richard, P. L., Athurion, C. (2019): NI 43-101 Technical Report and Mineral Resource Estimate for the Bonnefond South Intrusive Project, Québec. Prepared for QMX Gold Corp., 172 p.

Robert, F. (1990): Structural setting and control of gold-quartz veins of the Val-d'Or area southeastern Abitibi subprovince, in Ho, S. E., Robert, F., Groves, D. I., eds., Gold and Base-Metal Mineralization in the Abitibi Subprovince, Canada, with Emphasis on the Québec Segment. University of Western Australia, Short Course Notes, v. 24, p.167-210.

Robert F., Brommecker R., Bourne B. T., Dobak P. J., McEwan C. J., Rowe R. R., Zhou X. (2007): Models and Exploration methods for Major Gold Deposit Types; *in*, Proceedings of Exploration 2007: Fifth Decennial International Conference on Mineral Exploration, *ed*. B. Milkereit (Vol. 7, pp. 691-711).

Rocheleau, M., Gaudreau, R., Sauvé, P., Perrier, B. (1988): Géologie des gisements aurifères de Chimo et de Nordeau, Région de Val-d'Or; Université Laval IREM-MERI, MRN QC, MB 88-14, 53 p.

Rocheleau, M., Hébert, R., Lacoste, P., Racine, M., Gaudreau, R., St-Julien, P. (1997): Synthèse stratigraphique, paléogéographique et gitologique: cantons Vauquelin, Pershing, Haig et parties des cantons de Louvicourt, Pascalis et Denain. Gouvernement du Québec, Ministère des Ressources naturelles, Secteur des mines, MB97-11, 224 p., 6 maps.

Sauvé, P., Blanchet, P., Blouin, J. Y., Champage, M., Leclerc, A. (1987): Géologie de la mine d'or Chimo – Région de Val-d'Or; Gouvernement du Québec, Ministère des Ressources naturelles, Secteur des mines, MB 87-05, 75 p.

Savard, C., Carrier, A., Durieux, G. (2018): NI 43-101 Technical Report and Updated Mineral Resource Estimate for the Orenada zones 2 and 4 project, Orenada Group Porperties, Québec. Prepared for Alexandria Minerals Corporation, 176 p.

Stanley, C.R., and Lawie, D 2007, Average relative error in geochemical determination: Classification, calculationand plea for concistency¨Exploration and Mining Geology, V16, P.267-275.

Taner, M. F. (1996): The East Sullivan Stock and its Gold-Copper Potential, Val-d'Or, Québec, Canada. Exploration Mining Geology, Vol. 5, No.1, pp. 45-60.

Thurston, P. C., Chivers, K. M. (1990): Secular variation in greenstone sequence development emphasizing Superior province, Canada: Precambrian Research, v. 46, p. 21–58.

Vachon, A., Aubé, F., Casault, N., Cyr, R., Marchand, S. and Rood, M. (1993): Déménagement du concentrateur Lucien C. Béliveau à la mine Chimo et disposition des résidus minier. Demande de certificat d'autorisation, ROCHE Ltée, No. de projet: 15193, préparé pour CAMBIOR, 73 p.

Vallières, D., (1996): Rapport annuel 1996 de la mine Chimo (CAMBIOR), 52 p.